# SYSTEMATIC APPROACHES FOR DESIGN OF IONIC LIQUIDS AND THEIR MIXTURES FOR ENHANCED CARBON CAPTURE PURPOSE

**CHONG FAH KEEN, MEng.**

**Thesis submitted to the University of Nottingham**

**for the degree of Doctor of Philosophy**

**OCTOBER 2016**

# ABSTRACT

Post-combustion capture using amine-based solvents has been considered as the most viable technology for carbon capture, to mitigate industrial carbon dioxide ($CO_2$) emissions; but the solvents show a number of shortcomings. Recently, ionic liquids (ILs) are suggested as possible alternative to amine-based solvents, for they can be molecularly engineered to match various target thermophysical properties. This work focused on the development of systematic approaches to design IL-based solvents for carbon capture purpose. The first focus of this work is to develop an insight-based based visual approach to determine potential IL solvents as substitute to conventional carbon capture solvents. This approach allows visualisation of high-dimensional problem to be visualised in two or three dimensions, and assist designers without mathematical programming background in IL design. Following that, a mathematical optimisation approach to design optimal IL solvent for $CO_2$ capture purpose was developed as second focus of this thesis. This has been done by formulating the IL solvent design problem as mixed integer non-linear programming (MINLP) optimisation problem. The abovementioned approaches were developed to design task-specific ILs with high $CO_2$ absorption capacity as substitute to common carbon capture solvents. However, studies show that such ILs are relatively more expensive and have higher viscosities. To reduce the cost and viscosity of solvent, task-specific IL can be mixed with conventional IL, ensuring $CO_2$ solubility remains high, while viscosity and cost are acceptable. Hence, the previously

developed visual approach was extended to design pure ILs and IL mixtures, specifically to capture $CO_2$.

In order to ensure the designed IL is performing at its optimum (highest $CO_2$ solubility in this case), the operating conditions of the carbon capture process shall be considered because they will affect the thermophysical properties and $CO_2$ solubility of ILs. Therefore, the forth focus of this work will be incorporation of operating temperature and pressure into design of IL solvents. Similarly, the design problem was formulated as MINLP problem and solved using mathematical optimisation approach, where operating temperature and pressure were defined as variables through disjunctive programming. Replacing solvent for carbon capture system to IL-based solvent or installing carbon capture system will affect the overall process, as this will affect the utilities consumption of carbon capture system. Therefore, process design has been integrated with IL design in this thesis, to study how the solvent substitution affects the entire process, and followed by retrofitting of the entire process including carbon capture system accordingly. The design problem was formulated and solved as MINLP problem. Finally, this thesis concludes with possible extensions and future works in this area of research work.

# ACKNOWLEDGEMENTS

I would like to express the deepest appreciation to my principal supervisor, Dr. Nishanth Chemmangattuvalappil for his constant support, guidance and patience. The good advice and support of my co-supervisors, Prof. Dominic Foo and Dr. Fadwa Eljack, have been helpful and invaluable, for which I am thankful. I would like to acknowledge the financial, academic, and also technical support of the University of Nottingham, Malaysia Campus and its staff, especially in the award of Faculty of Engineering Dean's Scholarship that provided the necessary financial support for this research. Furthermore, I would like to thank Prof. Denny Ng for advice and encouragement he has provided throughout the research. I am most grateful to Prof. Mert Atilhan at Qatar University for providing me with his experimental support, to make this research possible. I would like to thank my friends and co-workers, Viknesh Andiappan A/L Murugappan, Liew Yuh Xiu, Kalaimani A/P Markandan, Feven Mattews Michael, and Goh Wui Seng for promoting a stimulating and welcoming research environment. Last but not least, I thank my parents, grandmother, and sisters for giving me their support and encouragement throughout, for which I will be grateful forever.

# PUBLICATION

## Referred Journals

**Chong, F.K.**, Foo, D.C.Y., Eljack, F.T., Atilhan, M., Chemmangattuvalappil, N.G. (2015) Ionic liquid design for enhanced carbon dioxide capture by computer-aided molecular design approach. Clean Technologies and Environmental Policy, 17(5), 1301-1312, DOI: 10.1007/s10098-015-0938-5

**Chong, F.K.**, Foo, D.C.Y., Eljack, F.T., Atilhan, M., Chemmangattuvalappil, N.G. (2016) A systematic approach to design task-specific ionic liquids and their optimal operating conditions. Molecular Systems Design & Engineering, 1, 109-121, DOI: 10.1039/C5ME00013K

**Chong, F.K.**, Chemmangattuvalappil, N.G., Eljack, F.T., Atilhan, M., Foo, D.C.Y. (2016) Designing ionic liquid solvents for carbon capture using property-based visual approach. Clean Technologies and Environmental Policy, 18(4), 1177-1188, DOI: 10.1007/s10098-016-1111-5

**Chong, F.K.**, Eljack, F.T., Atilhan, M., Foo, D.C.Y., Chemmangattuvalappil, N.G. (2016) A systematic visual methodology to design ionic liquids and ionic liquid mixtures: Green solvent alternative for carbon capture. Computers &

Chemical Engineering, 91, 219-232, DOI: 10.1016/j.compchemeng.2016.04.006

Ng, L.Y., **Chong, F.K.**, Chemmangattuvalappil, N.G. (2015) Challenges and Opportunities in Computer-Aided Molecular Design. Computers & Chemical Engineering, 81, 115-129

## Keynote Lecture

Ng, L.Y., **Chong, F.K.**, Chemmangattuvalappil, N.G. (2014) Challenges and Opportunities in Computer Aided Molecular Design. IN: Eden, M., Siirola, J.D., Towler, G.P. (Eds.) *8th International Conference on Foundations of Computer-Aided Process Design 2014*

## Conference Proceedings

**Chong, F.K.**, Eljack, F.T., Atilhan, M., Foo, D.C.Y., Chemmangattuvalappil, N.G. (2014) Ionic Liquid Design for Enhanced Carbon Dioxide Capture – A Computer Aided Molecular Design Approach. Chemical Engineering Transactions, 39, 253-258.

**Chong, F.K.**, Chemmangattuvalappil, N.G., Foo, D.C.Y., Atilhan, M., Eljack, F.T. (2014) A Systematic Approach to Determine Optimal Ionic Liquid and

Operating Conditions for Carbon Capture Purpose. IN: *27th Symposium of Malaysian Chemical Engineers 2014*, Paper no.: EE007

**Chong, F.K.**, Chemmangattuvalappil, N.G., Foo, D.C.Y., Atilhan, M., Eljack, F.T. (2014) Disjunctive Optimisation for Ionic Liquid Design for Carbon Dioxide Capture. IN: *4th International Gas Processing Symposium*, Doha, Qatar

**Chong, F.K**., Chemmangattuvalappil, N.G., Foo, D.C.Y., Atilhan, M., Eljack, F.T. (2015) A Systematic Visual Approach to Ionic Liquid Design for Carbon Dioxide Capture, Computer Aided Chemical Engineering, Computer Aided Chemical Engineering, 37, 1211-1216.

**Chong, F.K.**, Chemmangattuvalappil, N.G., Foo, D.C.Y., Atilhan, M., Eljack, F.T. (2015) Ionic liquid mixture design for carbon capture using a systematic visual approach. IN: Asia Pacific Confederation of Chemical Engineering Congress 2015: APCChE 2015, incorporating CHEMECA 2015, 384-389.

**Chong, F.K.**, Chemmangattuvalappil, N.G., Foo, D.C.Y., Atilhan, M., Eljack, F.T. (2015) Ionic liquid mixture design for carbon capture using property clustering technique. Chemical Engineering Transactions, 45, 1567–1572.

# Table of Contents

# LIST OF TABLES

# LIST OF FIGURES

# NOMENCLATURE

*Abbreviations*

| | |
|---|---|
| AD | Anaerobic digester |
| ANN | Artificial neural networks |
| AUP | Augmented property index |
| BECC | Bio-energy with carbon capture |
| BTS | Biomass tri-generation system |
| CAFD | Computer-aided flowsheet design |
| CAMD | Computer-aided molecular design |
| $CAM^bD$ | Computer-aided mixture/blend design |
| CCS | Carbon capture and storage |
| $CH_4$ | methane |
| $CO_2$ | Carbon dioxide |
| CoMT-CAMD | Comtinous-molecular-targeting computer-aided molecular design |
| COSMO-RS | Conductor-like screening model for real solvents |
| CT | Cooling tower |
| DEA | Diethanolamine |
| DEPG | Dimethylether polyethylene glycol |
| DoE | Design of experiments |
| DR | Dryer |
| EoS | Equation of state |
| EDS | Exhaustive direct search |
| EFB | Empty fruit bunches |
| FBN | Free bond number |
| GA | Genetic algorithm |
| GC | Group contribution |
| GHG | Greenhouse gas |
| GT | Gas Turbine |

| | |
|---|---|
| $H_2S$ | Hydrogen sulphide |
| HPS | High pressure steam |
| HRSG | Heat recovery steam generator |
| HST | High pressure steam turbine |
| IL | Ionic liquid |
| IO | Input-output |
| IPCC | Intergovernmental Panel on Climate Change |
| LPS | Low pressure steam |
| MCH | Mechanical chiller |
| MDEA | Methyl-diethanolamine |
| MEA | Monoethanolamine |
| MHI | Mitsubishi Heavy Industries |
| MILP | Mixed integer linear programming |
| MINLP | Mixed integer non-linear programming |
| MM | Membrane separator |
| MPS | Medium pressure steam |
| MST | Medium steam turbine |
| NMP | N-methyl-2-pyrrolidone |
| $N_2O$ | Nitrous oxide |
| $NO_x$ | Nitrogen oxides |
| $O_3$ | Ozone |
| PC | Propylene carbonate |
| PMF | Palm mesocarp fibre |
| POME | Palm oil mill effluent |
| QSAR | Quantitative structure activity relationships |
| QSPR | Quantitative structure property relationships |
| RCN | Resource conservation network |
| RST | Regular solution theory |
| SA | Simulated annealing |
| SAFT | Statistical associating fluid theory |
| $SO_x$ | Sulphur oxides |
| TI | Topological index |

| | |
|---|---|
| UNIQUAC | Universal-quasi-chemical theory |
| VBI | Viscosity blending index |
| VOC | Volatile organic compounds |
| WTB | Water tube boiler |

*Ionic liquids*

| | |
|---|---|
| $[MIm]^+$ | Methylimidazolium cation |
| $[Im]^+$ | Imidazolium cation |
| $[Py]^+$ | Pyridinium cation |
| $[MPyr]^+$ | Methylpyrrolidinium cation |
| $[N4111]^+$ | Butyltrimethylammonium cation |
| $[N1888]^+$ | Methyltrioctylammonium cation |
| $[DEMA]^+$ | Diethylmethylammonium cation |
| $[BF_4]^-$ | Tetrafluoroborate anion |
| $[PF_6]^-$ | Hexafluorophosphate anion |
| $[Cl]^-$ | Chloride anion |
| $[Tf_2N]^-$ | Bis(trifluoromethylsulfonyl)imide anion |
| $[OTf]^-$ | Trifluoromethanesulfonate anion |
| $[OMs]^-$ | Methanesulfonate anion |

*Indices*

| | |
|---|---|
| $d$ | Property ($d$ = 1, 2, …, $N_p$) |
| $g$ | Temperature range ($g$ = 1, 2, …, $u$) |
| $h$ | Pressure range ($h$ = 1, 2, …, $v$) |
| $i$ | Component ($i$ = 1, 2, …, $p$) |
| $j$ | Organic functional groups ($j$ = 1, 2, …, $r$) |
| $k$ | Groups ($k$ = 1, 2, …, $q$) |
| $m$ | Cation groups ($m$ = 1, 2, …, $s$) |
| $n$ | Anion groups ($n$ = 1, 2, …, $t$) |

*Parameters*

| | |
|---|---|
| $a$ | Coefficient in the model equation for the density |
| $a_{mn}$ | UNIFAC group interaction parameter between group $m$ and $n$ |
| $A_i$ | Constant for group $I$ in Antoine equation |
| $A_{k,\mu}$ | Contribution of group $k$ to parameter $A$ |
| $b$ | Coefficient in the model equation for the density |
| $B_i$ | Constant for group $i$ in Antoine equation |
| $B_{k,\mu}$ | Contribution of group $k$ to parameter $B$ |
| $c$ | Coefficient in the model equation for the density |
| $C_i$ | Constant for group $i$ in Antoine equation |
| $c_{p,k}$ | Specific heat capacity contribution of group $k$ (J $mol^{-1}$ $K^{-1}$) |
| $G_{CH3,m}$ | Number of $CH_3$ groups in cation $m$ |
| $\Delta H_{vap,k}$ | Heat of vaporisation contribution of group $k$ (kJ $mol^{-1}$) |
| $N$ | Avogadro constant |
| $n_k$ | Free bond number of group $k$ |
| $P$ | System pressure (MPa) |
| $P_h$ | Pressure range $h$ |
| $P_h^{\text{switch}}$ | Boundary pressure between pressure ranges (MPa) |
| $P^{\text{L}}$ | Lower bound for system pressure (MPa) |
| $P^{\text{U}}$ | Upper bound for system pressure (MPa) |
| $Q_k$, $Q_m$, $Q_n$ | Group surface area parameter in the UNIFAC model |
| $R$ | Universal gas constant (J $mol^{-1}$ $K^{-1}$) |
| $R_k$ | Group volume parameter in the UNIFAC model |
| $T$ | System temperature (K) |
| $T_g$ | Temperature range $g$ |
| $T_g^{\text{switch}}$ | Boundary pressure between temperature ranges (K) |
| $T^{\text{L}}$ | Upper bound for system temperature (K) |
| $T^{\text{U}}$ | Upper bound for system temperature (K) |
| $V_k$ | Molecular volume of group $k$ ($Å^3$) |

*Variables*

| | |
|---|---|
| $A$ | Coefficient in the model equation for the viscosity |
| $AUP_i$ | Augmented property index for component $i$ |
| $AUP_k$ | Augmented property index for group $k$ |
| $B$ | Coefficient in the model equation for the viscosity |
| $C$ | Cost of solvent (USD $mol^{-1}$) |
| $C_{di}$ | Property cluster for property $d$ of component $i$ |
| $C_{dk}$ | Property cluster for property $d$ of group $k$ |
| $c_p$ | Specific heat capacity (J $mol^{-1}$ $K^{-1}$) |
| $f$ | Design objective function |
| $F_i$ | Auxiliary property for component $i$ (surface fraction / mole fraction) |
| $g_{CH_3}$ | Number of $CH_3$ groups in the selected cation |
| $\Delta H_{vap}$ | Heat of vaporisation (kJ $mol^{-1}$) |
| $I_g$ | Binary variable for temperature range selection |
| $I_h$ | Binary variable for pressure range selection |
| $K$ | Solvent cost (USD $mol^{-1}$) |
| $M$ | Molecular weight (g $mol^{-1}$) |
| $m_i$ | Mass flowrate of component $i$ (kg $h^{-1}$) |
| $P_h^{\text{chosen}}$ | Chosen system pressure in range $h$ (MPa) |
| $P_i^S$ | Saturated vapour pressure of component $i$ (MPa) |
| $Q^{\text{C}}$ | Cooling power (kW) |
| $Q^{\text{H}}$ | Heating power (kW) |
| $q_i$ | Parameter relative to the molecular van der Waals surface areas of pure component $i$ |
| $r_i$ | Parameter relative to the molecular van der Waals volumes of pure component $i$ |
| $S$ | Solubility of $CO_2$ in mixture (mol $CO_2$/mol solvent) |
| $S_i$ | Solubility of $CO_2$ in component $i$ within mixture (mol $CO_2$/mol solvent) |
| $T_g^{\text{chosen}}$ | Chosen system temperature in range $g$ (K) |

| | |
|---|---|
| $V$ | Molecular volume (Å$^3$) |
| $VF_i$ | Volumetric flowrate of component *i* (m$^3$ h$^{-1}$) |
| $V_i$ | Auxiliary property of component *i* |
| $VBI_i$ | Viscosity blending index of component *i* |
| $v_k$, $v_m$ | Number of group *k* or *m* |
| $v_k^{(i)}$, $v_m^{(i)}$ | Number of group *k* or *m* in component *i* |
| $W$ | Pumping power (kW) |
| $x_i$ | Mole fraction of component *i* in liquid phase |
| $x_j$ | Mole fraction of group *j* in the mixture |
| $X_m$, $X_n$ | Fraction of group *m* or *n* in the mixture |
| $y_i$ | Mole fraction of component *i* in gas phase |

*Greek Symbols*

| | |
|---|---|
| $\alpha_m$ | Binary variable representing cation *m* |
| $\beta_n$ | Binary variable representing anion *n* |
| $\mu$ | Dynamic viscosity (Pa.s) |
| $\mu_i$ | Dynamic viscosity of component *i* (Pa.s) |
| $\rho$ | Density (g cm$^{-3}$) |
| $\rho_c$ | Critical density (g cm$^{-3}$) |
| $\rho_i$ | Density of component *i* (g cm$^{-3}$) |
| $\rho_k$ | Density contribution of group *k* (g cm$^{-3}$) |
| $\rho_0$ | Adjustable parameter for density (g cm$^{-3}$) |
| $\delta$ | Reduced density |
| $\phi^r$ | Reduced dimensionless Helmholtz function |
| $\phi_\delta^r$ | Derivative of reduced dimensionless Helmholtz function |
| $\varphi_i(T,P,y_i)$ | Gas-phase fugacity coefficient of component *i* |
| $\gamma_i$ | Activity coefficient of component *i* |
| $\gamma_i^C$ | Combinatorial contribution to the activity coefficient of component *i* |
| $\gamma_i^R$ | Residual contribution to the activity coefficient of |

| | |
|---|---|
| | component *i* |
| $\Gamma_K$ | Residual activity coefficient of group *k* |
| $\Gamma_K^{(i)}$ | Residual activity coefficient of group *k* in pure component *i* |
| $\theta_m$ | Fraction of group *m* in a mixture of the liquid phase |
| $\psi_{nm}$ | Group interaction parameter |
| $\tau_d$ | $d^{\text{th}}$ property |
| $\tau_d^{\min}$ | Lower bound of $d^{\text{th}}$ property |
| $\tau_d^{\max}$ | Upper bound of $d^{\text{th}}$ property |
| $\psi_d(\tau_{di})$ | Property operator of $d^{\text{th}}$ property of component *i* |
| $\psi_d(\tau_{dk})$ | Molecular property operator of $d^{\text{th}}$ property of functional group *k* |
| $\psi_d^{\text{ref}}(\tau_d)$ | Reference value for molecular property operator of $d^{\text{th}}$ property |
| $\psi_d(\tau_d)_M$ | Property operator of $d^{\text{th}}$ property of mixture *M* |
| $\Omega_{di}$ | Normalised property operator for $d^{th}$ property of component *i* |
| $\Omega_{dk}$ | Normalised molecular property operator for $d^{th}$ property of group *k* |
| $\nu_i$ | Kinematic viscosity of component *i* ($m^2\ s^{-1}$) |

# CHAPTER 1

# INTRODUCTION

Climate change is now regarded as a major issue to the society, mainly due to greenhouse gases (GHGs) emissions which include carbon dioxide ($CO_2$), methane ($CH_4$), nitrous oxide ($N_2O$) and ozone ($O_3$) (Hosseini et al., 2013). $CO_2$ makes up the vast majority of GHGs and it is claimed to be responsible for 60% of the global warming caused by GHGs (Houghton et al., 2001). In October of 2016, global atmospheric $CO_2$ concentration were reported to be at 402.31 ppm (Dlugokencky and Tans, 2016), which is higher than the upper safe limit of 350 ppm (Rockström et al., 2009). In fact, atmospheric $CO_2$ levels have been above 350 ppm since early 1988. On top of that, human activities are altering the carbon cycle, by adding $CO_2$ to the atmosphere continuously and removing natural $CO_2$ sinks, such as forests. According to Intergovernmental Panel on Climate Change (IPCC), the human activities contributing to $CO_2$ emissions include energy supply, transportation, industrial processes and forestry (IPCC, 2007). Study showed that most of the $CO_2$ released into the atmosphere originate from the combustion of fossil fuels, which is approximately 99% of global annual $CO_2$ emissions of close to 32 Gt (Hoeven, 2013). Despite this, fossil fuel is still projected to continue its supply to meet 77% of the world energy demand for year 2020, as shown in Figure 1-1 (U.S. Energy Information Administration, 2016). This is due to its availability, reliability, low cost, and energy density (Figueroa et al., 2008).

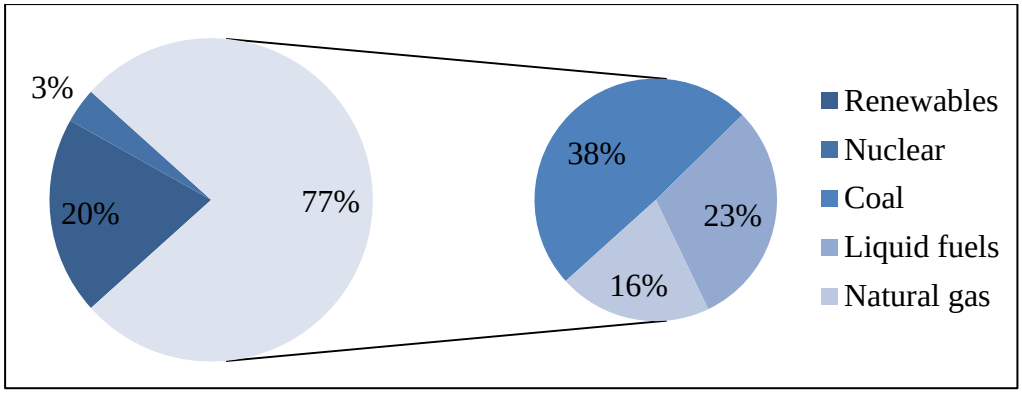


**Figure 1-1**: Estimated world net electricity generation by fuel in 2020

In order to reduce the environmental impacts, researchers have been working on improving efficiency of current technologies and searching for alternatives to fossil fuels (Varun et al., 2009; Weisser, 2007). The use of sustainable energy sources such as solar, tides, hydropower, geothermal and wind energy have the potential to meet the demands of modern society (Asif and Muneer, 2007). These options are very attractive due to their low carbon emissions, but they are often subject to significant geographical limitations, which hinder the implementation of renewable energy. Nuclear power is another prospective replacement to fossil fuels, with its mature technologies, high energy density, and low-carbon emissions. However, in the wake of the 2011 Fukushima disaster in Japan, nuclear power has raised public concerns (e.g. on safety, health, and long term environmental issues) over its use.

Due to the drawbacks of renewable energy and nuclear power, fossil fuels still remain as a major contributor to the world's energy supply in the

future (Quadrelli and Peterson, 2007), especially in developing countries characterised by growing economies and rising energy demands. Since the usage of fossil fuels is inevitable and fossil fuel based technologies are well established, there is a need to find an alternative to reduce $CO_2$ emission from power generation using fossil fuels. Recently, *carbon capture storage* (CCS) has gained the attention of the society for its possibility to mitigate climate change by reducing industrial $CO_2$ emissions (Pires et al., 2011). Studies presented by Cuéllar-Franca & Azapagic (2015) shows that the potential of causing global warming for a plant can be reduced by 63 – 82 % via CCS.

## 1.1 Carbon Capture and Storage

Carbon capture and storage (CCS) involves carbon capture (isolation of carbon dioxide, $CO_2$ from process gas streams) and carbon storage (captured $CO_2$ is sent for storage in an appropriate geological storage reservoir), as its name suggests. Currently, there are four CCS techniques as listed below:

1) Post-combustion: $CO_2$ is captured from flue gases released after fuel combustion.
2) Pre-combustion: $CO_2$ is captured from synthetic gas before fuel combustion.
3) Oxy-combustion: $CO_2$ is removed from air and captured prior to the fuel combustion.

4) Chemical looping combustion: $CO_2$ is captured by using metal oxide, during the fuel combustion with oxygen.

Using these techniques, typically up to 90 % of $CO_2$ released in power plants can be captured (Folger, 2013). The captured $CO_2$ is compressed for secure storage in various geological formations, such as depleted oil or gas reservoirs, inaccessible coal deposits, saline aquifers and other geological structures of sufficient integrity.

Among the four techniques, post-combustion and pre-combustion have been widely applied for gas purification in industrial processes. Some technologies that can be considered near-term have been tested at coal-fired power plants of 5 to 25 MWe (Global CCS Institute, 2012). On the other hand, oxy-fuel combustion and chemical looping combustion are still in the early stage of process development, where both are being tested in pilot-scale plant (D'Alessandro et al., 2010; Figueroa et al., 2008). While all these approaches are capable of capturing $CO_2$ at high efficiencies, they still possess some drawbacks such as high cost and high energy consumption, leading to the lack of full-scale applications of carbon capture on fossil fuel-fired power plants.

For CCS to succeed at reducing industrial $CO_2$ emissions, carbon capture technology would need to be deployed widely. This would depend on the cost and reliability of the capturing technology. Currently, post-combustion capture based on aqueous amine scrubbing is the most reliable

technology among all carbon capture technologies (Rochelle, 2009). However, amines possess some disadvantages such as solvent loss due to high vapour pressure, degradation of solvent in the presence of pollutants, and high equipment corrosion rate (Yu et al., 2012; Zaman and Lee, 2013). Besides, using amines as solvent is costly as large absorber volume is required and high amounts of energy is required during solvent regeneration (Olajire, 2010). To overcome these problems, much research has been devoted to synthesise new solvents and materials for carbon capture, such as absorption solvents, solid adsorbents, membranes, and even biomimetic approaches (Herzog et al., 2009). These materials are attractive with their own advantages, but still have some drawbacks such as low selectivity, require energy intensive regeneration, cause membrane fouling, and loss of solvents (Herzog et al., 2009; Spigarelli and Kawatra, 2013).

## 1.2 Background Problems

Recently, ionic liquids (ILs) have been proposed as a substitute to current commercial carbon dioxide ($CO_2$) capturing solvents (Maginn, 2007). ILs are organic salts that remain as liquid at close to ambient conditions, and consist of large organic cations and inorganic or organic anions of smaller size and asymmetrical shape. The ionic nature of ILs results in a distinctive combination of properties, which includes large liquid-phase range, non-flammability, high thermal stability, and most importantly, extremely low vapour pressure (Seddon, 1997). These means ILs can potentially be environmentally benign or “green” solvents, replacing the conventional

volatile organic compounds (VOCs). Furthermore, their physical and chemical properties can be finely customised by proper selection of cations and anions (Rogers and Seddon, 2003). However, it is estimated that at least $10^6$ unique combinations of cation and anion exist, and all can be prepared in laboratories (Plechkova and Seddon, 2008). It will be a challenging task to determine a suitable IL for carbon capture merely through experimental works.

Hasib-ur-Rahman et al. (2010) showed that pure ILs designed specifically to absorb $CO_2$ can have high $CO_2$ absorption rate and capacity, but they generally have relatively higher viscosities and are more expensive (Wang et al., 2013). To reduce the viscosity and cost of the designed solvent, a mixture of task specific ILs and conventional ILs can be used instead. This can ensure that the $CO_2$ solubility of solvent remains high, while its viscosity and cost are acceptable. However, if binary and tertiary mixtures of ILs are considered, Holbrey and Seddon (1999) estimated that there are about $10^{18}$ theoretically possible combinations. It will be more costly and time consuming, as compared to pure IL, to determine the optimal IL solvent (either pure IL or IL mixture) for carbon capture purpose through experimental works only.

On the other hand, ILs have different $CO_2$ solubility with respect to temperature and pressure, this will have different effects on the carbon capture process (Ali et al., 2013b). Designing IL solvents at fixed conditions (i.e.

temperature and pressure) may result in suboptimal or inefficient solvent, given the process can operate at a wide range of operating conditions. As such it is necessary to identify optimal carbon capture conditions of the chosen or synthesised ILs, during the solvent design stage itself.

In product design problems, the product is generally designed based on the components, without considering the process that the product is involved with. In this case, the product is identified by targeting relevant properties and fulfilling certain constraints, which gives desired functionalities. By doing so, the performance of designed product within the process is neglected, and may result in a product with good target properties but unfavourable for the process. For example, IL solvents designed to possess higher $CO_2$ solubility will reduce the amount of solvent required in the process, as well as the raw material cost. This might, however, increase the energy consumption during solvent regeneration that directly affects the operating cost, and increases the overall cost of the process. Hence, to avoid such problems, product design and process design problems should be integrated and solved together. The research development and gap will be discussed further in Chapter 2.

## 1.3 Research Objective and Scopes

The objective of this work is to address the abovementioned problems faced during the design stage of pure ionic liquids (ILs) or IL mixtures as

carbon capture solvents, also to connect solvent design problem with process design problem and solve these problems systematically.

Based on the problems discussed in Section 1.2, the scopes of this research can be summarised as follows and each will be further explained in Chapter 3:

1) To develop an insight-based visual approach to assist the process of pure IL design, with multi properties consideration, to provide insight to user regarding design problem and results.

2) To develop a systematic mathematical optimisation approach to aid the design of optimal pure IL for enhanced carbon capture process.

3) To develop a visual approach to assist the design of pure IL or IL mixture for carbon capture purpose with multi properties consideration by using experimental data and property prediction models.

4) To develop a systematic methodology to determine task-specific IL as carbon capture solvent and the corresponding optimal operating conditions of carbon capture process using designed IL solvent.

5) To develop an approach integrating process design and IL design to identify IL-based solvent for carbon capture purpose, considering the effect of this design on the entire process.

## 1.4 List of Achievements

The research objective and scopes presented in Section 1.3 has been achieved, where each is described in details in the following chapters. The achievements are summarised and listed as following:

1) Development of insight-based visual methodology to identify potential pure ionic liquids (ILs) to substitute conventional carbon capture solvent.

2) Development of mathematical optimisation approach to design optimal IL-based carbon capture solvent.

3) Extension of visual approach to determine pure IL and IL mixture solvents for carbon capture purpose.

4) Extension of mathematical optimisation approach to identify optimal IL solvent and its optimal operating conditions for carbon capture purpose.

5) Integration of IL design and process design by considering the effects of designed IL solvent on the overall process.

## 1.5 Thesis Outline

The outline of this thesis is presented in this section. Chapter 1 introduces carbon capture and storage (CCS) to readers and presents the background problems faced by designers during the design of ionic liquid (IL) solvents for carbon capture purpose. Research objective and scopes of this research work are also briefly presented in Chapter 1. Chapter 2 presents critical literature review on carbon capture solvents (both chemical and physical solvents) currently available, various applications of ILs, different computer-aided molecular design (CAMD) techniques, and the currently available property prediction models for ionic liquids (specifically on density, viscosity, and $CO_2$ solubility). Following these, research gap is discussed at the end of Chapter 2. This leads to detailed discussion of research scopes and research methodologies in Chapter 3.

Various novel approaches to design IL or IL mixture specifically for carbon capture purpose are presented in Chapter 4 to 8. Firstly, a visual approach for pure IL solvent design is introduced in Chapter 4, which is able to determine potential pure IL solvents according to multiple target properties. This approach enables users to solve IL design problem visually, and provides users useful insights about the problem. Following that, a mathematical

optimisation approach to design pure IL solvent as carbon capture solvent is presented in Chapter 5. This methodology is able to determine the optimal IL based on the main objective of the problem, through property estimation and consideration of all relevant constraints. The visual approach developed in Chapter 4 is further extended to solve pure IL and IL mixture design problem, which will be presented in Chapter 6. The proposed approach can utilise either the experimental data of relevant properties of ILs or predicted properties of ILs, or even both together, depending on the availability of data or prediction models.

As a first step to integrate process design with IL design, Chapter 7 presents an extension of the methodology in Chapter 5, by considering the effect of operating conditions on IL solvent design. This approach designs the optimal IL as carbon capture solvent, and determines the corresponding optimal operating conditions of carbon capture process. In chapter 8, a systematic approach to identify optimal IL-based carbon capture solvent, by considering the effects on overall process is presented. Information of the process that has carbon capture system installed is used to determine the optimal IL solvent and its optimal operating conditions, followed by retrofitting of the entire process to ensure the addition carbon capture system is favourable. Lastly, the summary of achievements and contributions of this research work up till now is included in Chapter 9. Potential future works and improvements for the developed approaches are also discussed in the same chapter.

# CHAPTER 2

# LITERATURE REVIEW

## 2.1 Ionic Liquids as Alternative Carbon Capture Solvents

There are various potential technologies and methods for carbon dioxide ($CO_2$) separation, as shown in Figure 2-1 (D'Alessandro et al., 2010). Among all, absorption by solvent scrubbing is the most established $CO_2$ separation approach, which is widely implemented in chemical and petroleum industries (Kenarsari et al., 2013). As mentioned in Section 1.1, the most popular solvent for $CO_2$ absorption is amine-based solvent. The use of amines to capture $CO_2$ was patented over eighty years ago, and since then they have been used to meet $CO_2$ product specifications in industries (Rochelle, 2009). Amines can absorb $CO_2$ at fast rates due to high enthalpy of reaction, and this also causes large amount of energy is required to remove dissolved $CO_2$, which will lead to energy intensive and costly process. On top of that, there are doubts about the rate of degradation in oxidising environment of flue gases and solvent losses of amine solvents (Abu-Zahra et al., 2013; Olajire, 2010). Gjernes et al. (2013) reported that amines based $CO_2$ capture plant is associated with minor release of amines and amines degradation products to the environment along with treated flue gas, due to high volatility of amines. A study done by Rohr et al. (2013) showed that inhalation exposure to amines at high concentration can cause lung inflammation under acute exposure conditions.

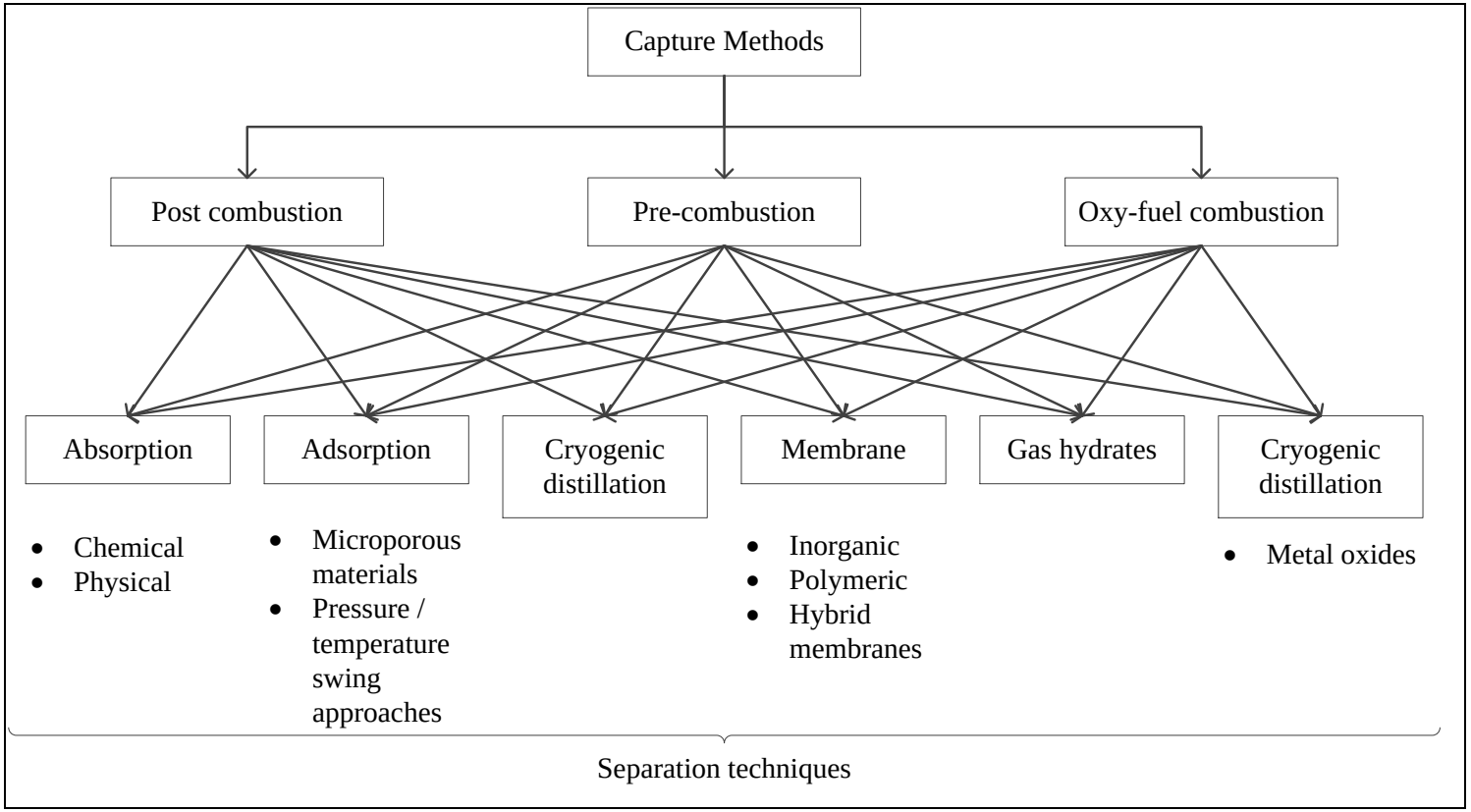


**Figure 2-1**: Materials for $CO_2$ capture in the context of post-combustion, pre-combustion, and oxy-fuel combustion processes

The problems discussed are due to high volatility of amine-based solvents, which can be reduced by using low volatility solvents. A new class of compounds, namely ionic liquids (ILs), has emerged recently and became a focal point of green chemistry. ILs become a key ally in achieving the target of becoming efficient and sustainable society, and thus have stimulated interest in both academia and industry (Seddon, 2003). ILs refer to organic salts that are liquids at close to ambient conditions, which consist of relatively large organic cations and inorganic or organic anions of smaller size and asymmetrical shape, an example of IL is shown in Figure 2-2 (Miyafuji, 2013). The group on the left of Figure 2-2, which is relatively large and denoted with a positive sign in the ring is an imidazolium ion (i.e. a cation); while the group on the right is chloride ion (i.e. an anion). The large size and unsymmetrical shape of organic cations depress the melting points of ILs to temperature at or below room temperature (Seddon, 1997).

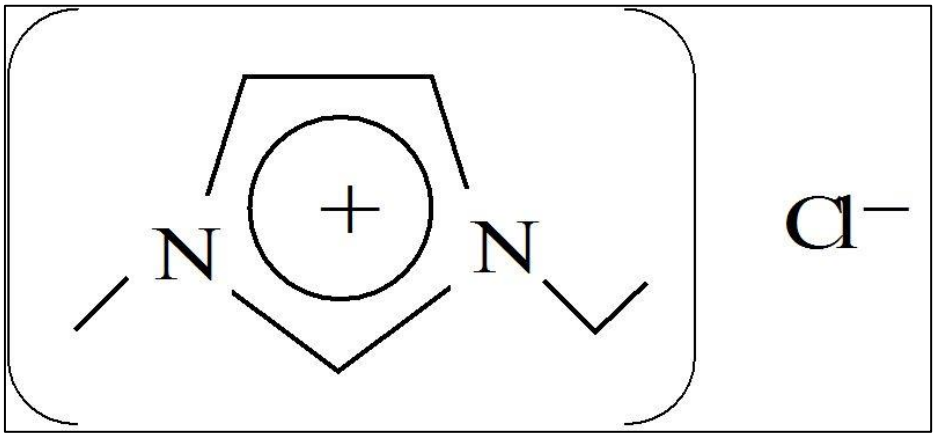


**Figure 2-2**: Chemical structure of 1-ethyl-3-methylimidazolium chloride

Due to the Coulombic attraction between ions of the liquids (Bates et al., 2002), ILs exhibit no measurable vapour pressure at room temperature and generally stable over their wide temperature range (Marsh et al., 2004). This suggests that ILs are “green” solvents as compared to traditional volatile organic compounds (VOCs). The strong ionic interaction between ions also makes ILs a non-flammable, chemically and thermally stable substance (Bates et al., 2002). In addition, ILs are reported to have properties such as good solvents for inorganic and organic components, high ionic conductivity, high heat capacity, and high thermal conductivity (Rogers and Seddon, 2003; Seddon, 1997; Welton, 1999). In short, ILs suppress conventional solvation and provide capability of dissolving a vast range of inorganic molecules to very high concentrations (Seddon, 1997). Furthermore, a key feature of ILs is that they offer a wide range of thermophysical properties, which means they can be fine-tuned to optimise the chemistry and also the system (Brennecke and Maginn, 2001). As a result, ILs can be designed for a particular end use, or to possess a particular set of properties. Therefore, ILs can be legitimately called “designer” solvents, and offer a freedom and flexibility for process design (Plechkova and Seddon, 2008). However, some of the ILs feature some undesirable properties, including high manufacturing cost, toxicity, and corrosive (Rogers and Seddon, 2003). While ILs can be designed to be environmentally benign, the manufacturing cost is a clear shortcoming (Chávez-Islas et al., 2011). Nevertheless, the other properties of ILs are important from industrial point of view, and thus ILs are reported for various industrial applications.

### 2.1.1 Applications of Ionic Liquids

Freemantle (1998) first alerted the scientific community on the existence and potential of ILs with his review. Few years later, BASF announced a new process by the company, called the BASIL (biphasic acid scavenging using ionic liquids) (Seddon, 2003). This is the first commercial publicly announced process using ILs (Plechkova and Seddon, 2008). Since then, applications of ILs have been reported in various fields, and these applications will be further discussed in this section.

Brennecke and Maginn (2001) reviewed a list of potential applications of ILs for which the unique properties of ILs may be advantageous. For example, ILs have been used for hydrogenations, hydroformylations, isomerisations, and alkylations, where generally reaction rates and selectivity are shown to be better in ILs compared to conventional VOCs. Brennecke and Maginn (2001) also reported that ILs are efficient in gas or liquid separations. Anthony et al. (2001) showed that ILs are hygroscopic and able to remove water vapour from gas mixtures efficiently. Fadeev and Meagher (2001) reported to use ILs to separate alcohols from fermentation broth, and hence Brennecke and Maginn (2001) suggested that ILs may be used for selective separation of liquids as well.

Much of the early development of ILs actually focused on their applications as electrochemical solvents (Zhao, 2006). This is mainly due to wide electrochemical window, high conductivity, wide operating temperature range, and low dielectric constant of ILs (Brennecke and Maginn, 2001). ILs have been used as electrolytes in batteries (Tobishima, 2002), actuators (Zhou et al., 2003), capacitors (Sato et al., 2004), fuel cells (de Souza et al., 2003), solar cells (Xue et al., 2004), membrane-free microelectrode sensors (Buzzeo et al., 2004), and electrosynthesis (Koo et al., 2004). MacFarlane et al. (2014) reviewed the energy applications of ILs comprehensively, and showed that ILs have been widely used for power generation purpose.

Apart from that, Brennecke and Maginn (2001) also found that ILs tend to wet metal, polymeric, and inorganic surfaces. The authors concluded that ILs are excellent candidates for lubricants in high temperature and/or low pressure applications, with their high thermal stability and large liquid-phase range. Ye et al. (2001) studied two ILs and found them to achieve excellent friction reduction and antiwear performance, as well as high load-carrying capacity when these ILs were used as lubricants.

Since ILs have wide liquid-phase range and good thermal stability, Brennecke and Maginn (2001) also suggested that ILs have the potential to be good heat transfer fluids. Zhao (2006) reported some important properties of

ILs such as liquid-phase range, thermal conductivity, heat capacity, and storage density. This data shows that ILs are suitable as heat transfer fluids for solar energy storage.

Besides, Jork et al. (2004) and Seiler et al. (2004) reported that ILs have high boiling point, thermally stable, high selectivity, and high capacities, which are advantageous in azeotrope separation as compared to the conventional entrainers. Choosing a suitable entrainer to separate azeotropic mixtures has been a challenge in process design, and now ILs are suggested as a potential option. The distillation process can be energy efficient by lowering reflux ratios when favourable entrainers (e.g. ILs) are used. Regeneration of entrainers (ILs) can be done by stripping, evaporation, drying, or even crystallisation.

Recently, ILs have been introduced for biomass applications, such as biotechnological process (Quijano et al., 2010), biomass fractioning (Liebmann et al., 2012) and pre-treatment of lignocellulosic biomass (Mood et al., 2013). Quijano et al. (2010) reviewed that the flexible nature of ILs is the most promising characteristics over traditional solvents in bioreactor technology. Liebmann et al. (2012) reported that a stepwise procedure to fraction cellulose, xylan, and lignin from mixtures can be done with IL. Apart from these, Zhao et al. (2009) reported that cellulose could be dissolved by ILs

containing chloride, formate, acetate or alkylphosphonate by formation of hydrogen bonds. This leads to degradation of the complex network of cellulose, hemicelluloses, and lignin (Alvira et al., 2010), and hence ILs are suitable to treat lignocellulosic waste. Besides, ILs pre-treatment is carried out under less dangerous condition and easily recycled (Mood et al., 2013).

Based on the wide applications of ILs, the concept of using ILs for carbon capture is gaining interest. Blanchard et al. (1999) first reported that carbon dioxide ($CO_2$) is highly soluble in imidazolium-based ILs, and the dissolution of $CO_2$ in ILs is completely reversible where pure ILs remain after the desorption process. This study has led to a rapid growth of scientific research on $CO_2$ capture using ILs. Bates et al. (2002) showed that the efficiency of a new task-specific ionic liquid is comparable to the commercial $CO_2$ capture solvents. It was shown that $CO_2$ has higher solubility in imidazolium-based ILs, as compared to nitrogen ($N_2$), oxygen ($O_2$), and methane ($CH_4$) (Anthony et al., 2004). Maginn (2007) reported that ILs is a viable technical option for post-combustion capture by properly tuning the ILs, which can overcome many of the problems associated with current $CO_2$ capture solvents. Hasib-ur-Rahman et al. (2010) reviewed on variety of techniques using ILs, such as task-specific ILs, supported IL membranes, and polymerised ILs, for $CO_2$ capture and showed that carbon capture using ILs is feasible, if there is inexpensive and diverse ILs. Wappel et al. (2010) made comparison between a large range of ILs with different purity and 30 wt% of

MEA solvent, with the results showing that energy demand of 60 wt% ILs is lower than that of MEA. Ramdin et al. (2012) also reviewed that $CO_2$ absorption capacity can be improved by functionalising conventional ILs with an amine functional group, with a better reaction stoichiometry compared to amine-based solvents. Lei et al. (2015) showed that IL can be mixed with zeolitic imidazolate framework, and used for carbon capture purpose through adsorptive absorption. These show that ILs are promising substitute to the conventional $CO_2$ capture solvents, through proper match of cations and anions. As mentioned in Section 1.2, there are about a million of simple IL systems, and approximately $10^{18}$ possible tertiary mixtures of ILs. Hence, identifying possible ILs candidates through trial-and-error based on experimental works will be nearly impossible. A systematic methodology can be followed to determine suitable IL solvent that is able to capture $CO_2$, environmental-friendly and consumes less energy for solvent regeneration. This is to avoid guessing the IL solvent blindly, and also save time and cost.

## 2.2 Computer-Aided Molecular Design

It is now identified that ionic liquids (ILs) are the potential substitute of conventional organic solvents in carbon capture, with some expected general behaviours or characteristics of ILs. However, the final molecular structure or identity of ILs is still unknown. This problem can now be defined in generic terms as follows: Given a set of desired needs, determine a suitable IL that satisfies these needs. This is the reverse of property prediction

problem, which is similar to the product design problem presented by Gani (2004a), where the needs are defined through properties. A general product design problem, considering the properties of product, can be described using the following set of generalised mathematical expressions:

$$F_{Obj} = \max\left\{C^T y + f(x)\right\} \tag{2.1}$$

$$h_1(x) = 0 \tag{2.2}$$

$$h_2(x) = 0 \tag{2.3}$$

$$h_3(x, y) = 0 \tag{2.4}$$

$$l_1 \le g_1(x) \le u_1 \tag{2.5}$$

$$l_2 \le g_2(x) \le u_2 \tag{2.6}$$

$$l_3 \le By + Cx \le u_3 \tag{2.7}$$

In the equations, $x$ represents the vector of continuous variables such as compositions and flowrates, $y$ is the vector of binary integer variables that represent the presence of a unit operation or group, $h_1(x)$ represents a set of process design specifications related equality constraints, $h_2(x)$ represents a set of process model related equality constraints, $h_3(x, y)$ represents a set of product structure related equality constraints, $g_1(x)$ represents a set of process design specifications related inequality constraints, while $g_2(x)$ represents a set of product design related inequality constraints.

Various mathematical formulations can be formed from the equations above, depending on the requirements and nature of the problem. Some examples are given as follows (Gani, 2004a):

1) Satisfy only Equation 2.6: This is generally a product design problem based on database search to generate a list of possible results. Since the product is identified from existing database, molecular structure generation and property models are not required.
2) Satisfy only Equations 2.4 and 2.6: This is a product design problem, where molecular structures are generated based on Equation 2.4, and screened on the basis of Equation 2.6.
3) Satisfy Equations 2.1, 2.4, and 2.6: This is optimal product design problem, where the molecular structures generated will be screened to match the objective function given in Equation 2.1.
4) Satisfy Equations 2.2 to 2.7: This is simultaneous product and process design problem. A set of feasible candidates will be generated, products along with respective processes.
5) Satisfy all equations: This is an integrated product and process design problem, where optimum product and its corresponding optimum process are targeted. However, the objective function and the property models, which are non-linear in nature, make this problem more complex.

There are few approaches that can be applied to solve the above-mentioned problems, including empirical trial-and-error approach, mathematical programming, and hybrid methods (Gani, 2004a). Among the three approaches, mathematical programming and hybrid methods both require property predictive models to estimate the behaviour of designed products. When the models are not available, experimental based trial-and-error method is the only option. In contrast, when models are available, mathematical programming and hybrid methods are preferable because they can reduce the time and expense required to carry out experiments. On top of that, mathematical programming and hybrid methods will be more convenient for ILs design, as they can provide systematic framework to transform the solution technique into computer-aided tools (Gani, 2004a). Computer-aided techniques can accelerate the molecular discovery and development process (Eslick et al., 2010), and improve the efficiency at the same time (Gani, 2004b). A computer-aided molecular design (CAMD) problem is defined as: *Given a set of building blocks and a specified set of target properties; determine the molecule or molecular structure that matches these properties* (Gani, 2004a). The CAMD technique was first introduced by Gani and Brignole (1983), and since then many works have been proposed and developed based on this technique. An overview of this approach is shown in Figure 2-3, and it can be applied on various levels of size and complexity of molecular structure representation (Gani, 2004a).

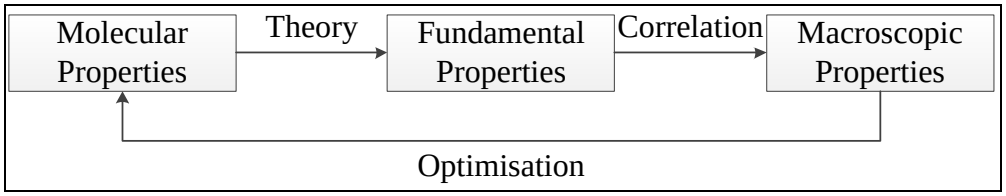


**Figure 2-3**: Overall methodology for CAMD

As described by Figure 2-3, there are two problems to be solved in CAMD approach, (1) the forward problem (top section), which requires the prediction of macroscopic properties for a given molecular structure, and (2) the inverse problem, which needs to identify the appropriate molecular structure based on targeted properties (Venkatasubramanian et al., 1994). The forward problem can include any properties, ranging from simple properties (e.g. density, viscosity, and boiling point) to highly complex properties (e.g. toxicity, solubility, and resistance to wearing) (Eslick et al., 2010). The main goal in CAMD is to solve the inverse problem, using optimisation techniques, as shown in the bottom section of Figure 2-3. In other words, the fundamental objective of CAMD is to identify a set of compounds that possess desired properties. The structures of the compounds are represented by using appropriate descriptors, and thus the properties should be predicted based on these descriptors (Gani et al., 2003).

Gani et al. (2003) presented the general approach in CAMD, which starts with generating compounds with chemically feasible molecular

structures from a set of descriptors (represented by fragments or building blocks). The most widely used feasibility criteria is the valency rule proposed by Macchietto et al. (1990) which states that fulfilment of octet rule is a must. The generated compounds will be tested, by predicting the specified properties of each compound. These properties are estimated by using fragment-based methodology, where the contributions of each fragment to the specific property is summed up as the property value of the compound. The optimal compound will be chosen among all feasible compounds, based on the selection criteria provided or objective function. The major differences between the CAMD methods are the type of descriptors, the way to perform all the steps, and the estimation of property values. The following sections will discuss about the methods selected and used in this thesis.

### 2.2.1 Group Contribution Methods

Most of the CAMD methods or tools work at the macroscopic level, which means the molecular structure is represented by descriptors such as groups (Gani et al., 1991). It was reported that most CAMD techniques are based on group contribution (GC) approaches (Gani et al., 2003). In GC approaches, the compound is broken down into various simple groups (Joback and Reid, 1987). The property of the compound is estimated by adding up contributions of all simple groups according to the occurrence of the groups. These contributions are estimated through regression of a huge amount of sample compounds. GC approaches are useful when the experimental data is

not available, because this approach is simple yet able to provide reasonably accurate results. Constantinou et al. (1993) reported that GC methods can estimate properties of compounds easily without much computational load and errors. GC methods can provide accurate estimation in the case of simple compounds, and help to generate molecular structure of a compound to meet a specific property from molecular groups systematically (Joback and Stephanopoulos, 1989). Most of the currently-used GC methods employ the same set of first-order groups (Constantinou and Gani, 1994). However, the accuracy of first order GC models is less reliable when the complexity of molecule structures increases, because these models do not consider the proximity effects between isomers (Wu and Sandler, 1989). First order GC methods are for large set of simple groups, allowing description of wide variety of organic compounds, but various concepts in organic chemistry and quantum mechanics, such as conjugation and interactions between groups, are ignored as well (Argoub et al., 2014).

Constantinou and Gani (1994) later introduced second order groups, and modified the estimation of properties into two stages approach. The first level uses data of first order groups; while the next level uses a set of second order groups with first-order groups as building blocks. The role of second-order groups is to provide more structural information about the portions of the molecular structure of the compound, which is not given by first-order groups. Implementing second-order groups enhances the accuracy, reliability,

and the range of applicability of GC methods. It can also overcome some of the disadvantages of first-order groups, by providing partial description of proximity effects and distinguish among isomers. Despite the advantages of second-order groups, their applicability is still restricted. The relatively small sets of data used in the development of second-order GC methods lead to break down of prediction capability when dealing with large, polycyclic or polyfunctional molecules.

Following that, Marrero and Gani (2001) further extended GC methods into three steps approach and included third-order groups. The first level of estimation has a large set of simple groups to describe a wide variety of organic compounds. The next level involves groups that allow better description of proximity effects and differentiation among isomers. The third level has groups to provide more structural information about molecular groups, which cannot be described using first- or second-order groups. The third-order groups deal with complex heterocyclic and large polyfunctional acyclic compounds.

### 2.2.2 Computer-Aided Molecular Design Techniques

Different approaches have been proposed for solving CAMD problems, and these can be grouped into three main categories, namely mathematical programming, stochastic optimisation, and enumeration

techniques (Gani et al., 2003). Common to all the solution approaches is that they are aiming to find a compound or compounds that fulfil the requirements set forth in the constraints and goals.

Mathematical programming solves the CAMD problem, which is represented mathematically, as an optimisation problem. In mathematical programming, the objective function is represented by the targeted performance; while the mathematical bounds are represented by the property constraints. The nature of this optimisation problem is normally mixed integer non-linear programming (MINLP) problem, and thus solved using MINLP solution methods. However, there is a major drawback for problem of such nature, where the solution methods suffer from a large computational load and there is no guarantee of obtaining global optimal solution (Vaidyanathan and El-Halwagi, 1994).

Stochastic optimisation techniques are heuristic search methods, which do not require any gradient information; discontinuous properties can be freely specified as design targets (Eljack, 2007). In stochastic optimisation, the mathematical representation of CAMD problem is solved using numerical stochastic methods, including simulated annealing (SA), genetic algorithm (GA), and Tabu search. SA is a combinatorial optimisation technique for solving unconstrained and bound-constrained optimisation problems based on

random estimates of the objective function, as well as evaluation of the constraints (Harini et al., 2013). In GA approach, populations of potential solutions are obtained from the previous populations based on their performance. It takes into account how attributes are passed from previous solution to the next solution (Eljack, 2007). In Tabu search, the random moves are performed to avoid already-visited solutions by keeping track of previous moves with incorporation of short-term memory function (Harini et al., 2013). The long term memory function helps in determine the new starting point and time to restart the whole procedure. A detailed review on the usage of these techniques, along with their respective advantages and disadvantages, has been reported by Fouskakis and Draper (2002). Among all three, SA and GA are more commonly techniques used in CAMD.

On the other hand, enumeration techniques refer to solving the combination of mathematical and qualitative representation of CAMD problem by hybrid solution approaches. Enumeration techniques aim to satisfy the feasibility and property constraints by first generating molecules using a combinatorial approach, followed by testing against targeted specifications. Therefore, generation and testing of compounds are done separately. An undesired effect of this technique is that solving a simple enumeration of a CAMD problem might lead to combinatorial explosion (Eljack, 2007).

In addition to the abovementioned approaches, visual approaches are also developed to solve product design problem (Eljack et al., 2005). Visualisation of the product design problem can be achieved through property clustering technique (Shelley and El-Halwagi, 2000). The formulation of property clusters ensures that they obey two fundamental conservation rules (intra-stream conservation and inter-stream conservation). Therefore, lever-arm analysis can be employed to study relationship between clusters, and allows visualisation of high-dimensional problem in two or three dimensions (Eden et al., 2004). For visualisation purpose, the number of clusters is limited to three (i.e. plotted on ternary diagram), but this does not imply that the number of properties describing each stream is also limited to three. Property operators can be reformulated as functions of several properties, when desired to visualise the problem and more than three properties are considered (Eden et al., 2004). When visualisation of the problem is not necessary, mathematical programming can be employed to solve the problem, and limitation of number of clusters is relieved (Eden et al., 2004). Following this, Sections 2.2.3 and 2.2.4 show the application examples for organic compounds design and mixture design using the techniques mentioned above.

### 2.2.3 Computer-Aided Molecular Design for Organic Compounds

There are many works done previously to design organic compounds by using CAMD. Cabezas et al. (2000) developed a database approach with interactive search for the appropriate solvent. The developed tool will need

properties databases, target property estimation systems and a knowledge-based system as guidance for the user through the solvent selection and screening steps. Since this is based on search of the database, there is no need to generate molecular structure (Gani, 2004a).

Harper and Gani (2000) proposed a multi-step, multi-level hybrid CAMD method that employs generate-and-test paradigm. In this proposed methodology, CAMD was expanded into a three steps procedure consisting of problem formulation (pre-design step), compound identification (design step), and result analysis (post-design step). This method combines GC approach at a lower level and molecular modelling approach at a higher level. GC method employed in this work includes the first-order groups and second-order groups, to differentiate the molecular structures of isomers (Gani, 2004a). Gani (2002) also developed ProCAMD tool based on this work, which can be used to design organic compounds.

Venkatasubramanian et al. (1994) proposed the use of GA combining GC approach for polymer design. GA can perform a guided stochastic search to identify improved solutions by sampling areas of the parameter space that have a higher possibility for good solutions. Due to heuristic nature of the search, there is no guarantee of finding the best solution using the proposed approach. Camarda and Maranas (1999) presented optimal polymer design via

mathematical programming technique, by using connectivity indices as descriptors. Nonlinearities due to the expressions for connectivity indices in this approach led to MINLP formulations, and hence the solution methodology is computationally expensive and no guarantee of global optimal solution. Sahinidis et al. (2003) employed GC methods and global optimisation algorithm developed previously (Sahinidis, 1996) in alternative refrigerants design using mathematical programming technique. The employed algorithm resolves the multiple local optima difficulty in the context of MINLP formulations and provides all feasible solutions to the problem.

Chavali et al. (2004) formulated a metal catalyst design problem as MINLP problem, and compared the performance of Tabu search and mathematical programming in solving this problem. This presented work extended and applied connectivity indices to predict physical properties of designed transition metal complexes. Tabu search was shown to consistently found near-optimal solutions, which had better objective function value than those found via mathematical programming. Karunanithi et al. (2006) also proposed a CAMD framework for crystallisation solvents design, using mathematical techniques combining with GC approach. Decomposition approach was employed to solve the formulated MINLP model and identify the optimal solvent molecular structure. Yang and Song (2006) presented a new algorithm, namely classified enumeration, which breaks down molecular structure generation into few steps and followed by property prediction using

GC methods. The proposed methodology targets to avoid combinatorial explosion and consider all molecules in the range at the same time. In this approach, the molecular structure was broken down into alkane, cycloalkane and arene as skeleton groups and the rest as function groups. Function groups will replace skeleton groups in the molecules to build different structure, and properties will then be calculated using GC methods.

Eljack and Eden (2008) proposed a property-based visual approach to solve molecular design problems, using the property clustering technique. Molecular synthesis problem is different from process design, descriptors are involved instead of molecule or process stream. Therefore, there is a need to include appropriate method to connect both the descriptors and properties, thus allow for prediction of physical properties from structural information. Eljack and Eden (2008) applied proven first order GC methods in property integration framework, introducing a property-based platform to facilitate visualisation of property performance requirements and design of new formulations.

Chemmangattuvalappil et al. (2009) proposed to combine second order estimation of GC methods with the approach presented by Eljack and Eden (2008) to increase the accuracy of the property predictions. An mathematical approach was developed using the second order groups built from first order

groups, subject to the constraints of overlapping. The proposed approach is able to capture proximity effects and differentiate between isomers, therefore increases the application range and reliability of in solving molecular design problem. Since the problem is solved using property clustering technique, the simple linear mixing rules are still valid even though second order GC methods are included in this approach.

Chemmangattuvalappil et al. (2010a) then developed an mathematical approach for molecular design by incorporating molecular signature descriptors in the framework. The proposed approach can include different quantitative structure property relationships (QSPR) or quantitative structure activity relationships (QSAR) expressions based on multiple TI. The advantage of this approach is that combination of property prediction models based on GC and topological index (TI) based QSPR/QSAR can be utilised to track different properties in the molecular design problem. This expands the application range of the framework as it is possible to consider biological, environmental, health, and safety related properties that cannot be predicted using GC methods.

### 2.2.4 Computer-Aided Mixture/Blend Design

In Section 2.2.3, the application of CAMD techniques for single component design is shown. The application of the same techniques on

mixture design will be discussed in this section. In general, the definition of a computer-aided mixture/blend design ($CAM^bD$) problem is as follows: *given a set of chemicals and a set of specified property constraints, determine the optimal mixture that satisfies the constraints* (Gani, 2004b). For this problem, the set of chemicals can be identified by solving the single component molecular design problem. Following that, prediction of mixture properties can be done by using properties of pure components and mixing rules (Karunanithi et al., 2005).

Klein et al. (1992) developed a two-loop optimisation algorithm, namely successive regression and linear programming, to solve a $CAM^bD$ problem. This algorithm consists of a local activity coefficient model which correlates the function of non-linear constraint using a regression parameter. This function is then used as part of an inner loop linear programming problem to obtain minimum cost of mixture. The value of regression parameter is iteratively regressed in an outer loop until it converges, and the value of inner loop will be the solution.

Duvedi and Achenie (1997) presented refrigerant mixtures design using mathematical programming model, which can be evaluated through experiment afterwards. Binary variables are added into model to specify type and number of single component that exist in the mixture. Sinha et al. (2003)

also presented a blanket wash solvent blend design problem as MINLP problem and solved using an interval-based global optimisation tool called LIBRA. The problem consists of a discrete problem which involve the selection of solvents from a set of pure-component solvents, and a continuous problem to determine the blend composition.

Karunanithi et al. (2005) proposed a new decomposition-based solution strategy to solve CAM$^{b}$D problems. In this methodology, the design problem is formulated as MINLP problem, and solved as a series of solvable sub-problems. All the necessary constraints, including pure component property constraints, mixture property constraints, process model constraints, and structural constraints, along with objective function are handled in separate sub-problems. This can reduced the complexity of optimisation problem, where some of the property models are handled in initial sub-problems.

Solvason et al. (2009) presented a systematic property-based visual approach for mixture design using property clustering technique. Design of experiments (DoE) tool was utilised in this work, and combined with property clustering. DoE tool can determine the optimum combination of chemical constituents with desired properties using minimum number of experimental runs, but it suffers combinatorial explosion and visualisation difficulties when

multicomponent mixtures involve. Property clustering technique was employed to avoid these problems and provide insights into the effectiveness of the design. The proposed approach offers the potential to solve process, molecular, and mixture design problems simultaneously.

Conte et al. (2011) presented a systematic model-based computer-aided methodology for liquid formulated product design, which involves active ingredients in the mixture. The methodology is part of an integrated 3-stages chemical based product design approach, where first stage is to identify promising candidates, while second and third stages are to experimentally validate the products. Similarly, Yunus et al. (2012) proposed a 3-stages computer-aided methodology for blended products design. The three stages include 1) product design, 2) process identification, and 3) experimental validation. The first stage is divided into four sub-problems and solved with decomposition-based approach presented by Karunanithi et al. (2005).

Kheireddine et al. (2013) adopted property clustering technique to develop systematic visual approach for solvents or solvent blends selection. The approach was demonstrated for solvent extraction process to recover spent lube oil. A combination of experiments and simulations were used to define the feasibility ranges for target properties. Experimental works were done afterwards to validate the results obtained using this proposed approach.

## 2.3 Ionic Liquid Design via Computer-Aided Molecular Design

Computer-aided molecular design (CAMD) approach is proven to be able to design or choose a list of potential substitutes to the commercial organic compounds and their mixtures. More recently, this approach is extended to design potential ionic liquids (ILs) for specific tasks. Matsuda et al. (2007) first presented the design of ILs, using property prediction models for ionic conductivities and viscosities, which are based on quantitative structure property coupled with descriptor of group contribution (GC). Firstly, the value of the target property needed for application is set, and followed by exhaustively searches by calculating ILs properties. These searches are performed by changing cation, anion, and length of side chains attached to cation. The structures of ILs that satisfy target properties value will be determined. Matsuda et al. (2007) also built a Java program specifically to reverse design ILs using the approach presented, but only ionic conductivity and viscosity were considered in this program.

McLeese et al. (2010) applied CAMD approach to design ILs for use within environmentally friendly refrigeration systems. The ILs design problem is formulated as a mixed integer linear programming (MILP) problem. Therefore, the presented approach was claimed to be able to provide optimal results using standard techniques. In the same work, McLeese et al. (2010) also compared the computational efficiency of different algorithms in solving the problem. The group concluded that Tabu Search algorithm is more

efficient compared to deterministic algorithm for the purpose of generating near-optimal solutions to this design formulation.

Billard et al. (2011) established a quantitative structure property relationship (QSPR) between chemical structure of ILs and their viscosity. The same QSPR model was used to reverse design ILs with targeted viscosity. Billard et al. (2011) also demonstrated in silico design of three new ILs by using the developed QSPR model, prior to synthesis and experimental test. These ILs were synthesised and tested afterwards, the predicted viscosities are in good qualitative agreement with the experimentally measured ones.

Chávez-Islas et al. (2011) then presented mixed integer non-linear programming (MINLP) formulation for optimal design of IL to recover high purity ethanol from ethanol-water system, where IL should feature water affinity to break ethanol-water azeotrope. The presented model considers the mole balances and equilibrium relationships using UNIFAC method. Process restrictions are considered in this work, which are not included by previous works. The results showed that higher purity of ethanol product, higher energy consumption of the distillation process, and hence trade-off between these two contradicting objectives should be included. Therefore, Valencia-marquez et al. (2012) then extended the work by Chávez-Islas et al. (2011) by considering IL design and extractive distillation column design simultaneously.

Roughton et al. (2012) also proposed to design ILs entrainers and azeotropic separation processes at once. Several of the existing GC models were used, along with a newly developed solubility parameter GC model and UNIFAC-IL model. The UNIFAC-IL model is used to screen design candidates based on minimum IL concentration required to break azeotrope. The extractive distillation column is designed once the IL is chosen, using the driving force method with a new proposed feed stage scaling to minimise energy inputs. This is followed by design of an IL regeneration stage.

Karunanithi and Mehrkesh (2013) presented a general framework that can be applied for computer-aided ILs design. This framework is similar to CAMD approach for organic chemical design; consist of a general mathematical framework of the proposed approach, a set of structural constraints that define feasibility and bonding rules for ILs design, physical properties constraints, and solution properties constraints. Both physical and solution properties of ILs are estimated using GC based approach. The presented framework is suitable for different applications, and few simple case studies were shown, including electrolytes, heat transfer fluids, and separation process. The problems are formulated as MINLP models and solved using decomposition methods and genetic algorithm (GA) based optimisation.

A computational scheme based on CAMD has been proposed by Harini et al. (2015) to design a task-specific IL for extraction of pharmaceutical immediate. Structural constraints and properties constraints have been defined for this design problem. In this proposed approach, UNIFAC-IL model and GC method were used to estimate properties of ILs. Exhaustive direct search (EDS) approach was employed in this approach to determine the suitable IL for the specific purpose. However, this approach is appropriate when there are only few groups for study, the computational time increases as the number of groups is increased. Any optimisation technique can be employed to replace EDS approach in this proposed methodology. Table 2-1 is included to summarise the work done on IL design using CAMD technique thus far.

**Table 2-1**: Work done for IL design using CAMD

| Year | Authors | Research work |
|---|---|---|
| 2007 | Matsuda et al. | • Designed ILs based on ionic conductivities and viscosities<br>• Built a Java program based on the same concept |
| 2010 | McLeese et al. | • Designed ILs to be used within environmental-friendly refrigeration system<br>• Formulated the problem as MILP problem and solved using standard techniques<br>• Compared computational efficiency of different solving algorithms |
| 2011 | Billard et al. | • Established QSPR between IL structure and viscosity<br>• Applied the same QSPR model to present design of IL |

**Table 2-1** Continued

| | | |
|---|---|---|
| | Chávez-Islas et al. | • Designed IL to recover high purity ethanol from ethanol-water system<br>• Formulated the problem as MINLP problem<br>• Considered mole balance, equilibrium relationship using UNIFAC method, and process restriction |
| 2012 | Valencia-marquez et al. | • Extended the work by Chávez-Islas et al. (2011)<br>• Considered IL design and extractive distillation column design simultaneously |
| | Roughton et al. | • Designed IL entrainers and azeotropic separation processes simultaneously<br>• Adapted newly developed solubility parameter for IL and UNIFAC-IL model |
| 2013 | Karunanithi and Mehrkesh | • Presented a general framework for computer-aided IL design<br>• Formulated the problem as MINLP problem and solved using decomposition methods and GA based optimisation |
| 2015 | Harini et al. | • Proposed computational scheme to design task-specific IL for extraction of pharmaceutical immediate<br>• UNIFAC-IL model and GC methods were used to estimate properties of ILs<br>• Employed EDS approach to determine suitable IL<br>• Appropriate when there are only few groups for study |

## 2.4 Property Predictive Models for Ionic Liquids

Successes of computer-aided molecular design (CAMD) methodologies depend to a large extent, on the ability of predict and obtain the necessary properties, which are related to the targeted performance

characteristics (Gani et al., 2003). This shows that the availability and reliability of property prediction models are very important as it determines the applicability of the CAMD approach. Therefore, to design task specific ionic liquids (ILs) using CAMD, property prediction models for ILs are necessary. In the last decade, much work has been dedicated to develop property prediction methods for ILs, but this field is still considered to be new because there are not many prediction models for most of the properties of ILs.

### 2.4.1 Density

The density, $\rho$ is one of the most studied properties of ILs; there are approximately 20,000 data points available for more than 1,000 ILs (Coutinho et al., 2012). Density is an important property, particularly for energetic compounds (e.g. ILs), because density is related to energy packed per unit volume (Ye and Shreeve, 2007). Since density is one of the most fundamental and crucial properties, it has the most correlations and models proposed for estimations.

The first correlation for general application was proposed by Ye and Shreeve (2007). This model is based on group contribution (GC) approach and uses the hypothesis of Jenkins et al. (1999), which states that the molar volume of the salt is the linear sum of molar volumes of both ions. A

parameter table consists of about 60 parameters, covering 12 cation families and 20 anions, was proposed (Ye and Shreeve, 2007). The proposed model can predict ILs densities at high accuracy, where only 5 % of the estimated values have an absolute deviation higher than 0.08 g $cm^{-3}$. However, this model is limited to only 298.15 K and 0.10 MPa.

Gardas and Coutinho (2008a) extended the model by Ye and Shreeve (2007) to wider range of pressures and temperatures. In this extension, the mechanical coefficients of ILs, the isothermal compressibility, and the isobaric expansivity are assumed to be constant, in a wide range of pressures and temperatures. This modifies the initial methods for molar volume estimation, which is now depending on pressure and temperature. Apart from that, Gardas and Coutinho (2008a) also extended the parameter table for more cation families. This model is applicable for pressures at 0.10 to 100 MPa, and temperature at 273.15 to 393.15 K, with reported average deviation of 1.5 %.

Another correlation proposed by Jacquemin et al. (2008a) is also using concept by Jenkins et al. (1999), but this correlation is not based on GC approach. A large temperature dependent parameter table was produced by Jacquemin et al. (2008a). This model is reported to have average deviation of less than 0.5 % for more than 2000 data points. However, this model is limited to pressure at 0.1 MPa only. This model was then revised for estimation of ILs

densities at higher pressure (Jacquemin et al., 2008b). However, the revised model is over parameterised, where one ion requires seven parameters. This rigorous model provides detailed analysis on densities of the molecules, but it might lead to combinatorial explosion when it is applied in CAMD.

Qiao et al. (2010) proposed a GC based model to predict densities of ILs, but unlike the previous models, this model does not predict molar volumes of ILs. This model estimates densities directly, using concept of Jenkins et al. (1999) and Gardas and Coutinho (2008a). This model was correlated to almost 7400 data points for more than 120 ILs. The reported average deviation is 0.88 % for pure ILs, and 1.22 % for binary mixtures of ILs.

Lazzús (2010) presented a model using GC approach to estimate molar volumes of ILs at reference condition of 298.15 K and 0.1 MPa, which will then be corrected to different temperatures and pressures. The parameter table was prepared based on data points for 210 ILs and regression was done based on 3500 data points. This model is reported to produce an average deviation of 1.9 % at reference condition; while the temperature and pressure dependent model has a deviation of 0.73 %.

To date, the most extensive model for ILs densities was proposed by Paduszyński and Domańska (2012). This model was developed based on 20,000 data points for over 1,000 ILs, using the hypothesis by Jenkins et al. (1999) and Gardas and Coutinho (2008a). The Tait equation was adopted in this correlation for better pressure dependency. This model is reported to have average deviation of 0.53 % for the correlation data points, and 0.43 % for other testing points. Coutinho et al. (2012) reviewed that this model is the best prediction model for densities of ILs yet reported.

### 2.4.2 Viscosity

Viscosity is another well-studied property of ILs, which has many prediction models proposed. Most of these models are based on quantitative structure property relationships (QSPR) or GC approach. Abbott (2004) proposed a model which employs the hole theory to describe the viscosity of ionic and molecular liquids. This theory states that an ion must find a hole large enough to move. The author showed that this model can predict viscosities of a range of liquids with reasonable accuracy. This approach was adopted by Bandrés et al. (2011) to estimate the viscosities of pyridinium based ILs. However, the predicted values varied by a lot from the experimental values. The group improved the model by defining effective IL radius, and this yielded an average deviation of 4.5 %.

Gardas and Coutinho (2008b) proposed a prediction model based on GC method, where the viscosities of ILs are estimated using Orrick-Erbar-type equation (Poling et al., 2001). This model was developed based on 500 data points for 30 ILs, with an average deviation of 7.7 %. However, this model requires densities of ILs, which is a drawback when this model is applied in CAMD. The authors improved this model by proposing a new model based on Vogel-Tammann-Fulcher equation (Gardas and Coutinho, 2009). The new model does not require densities, and reference temperature is added. A reference temperature was chosen to be 165.06 K by the authors. The average deviation of this model was reported to be 7.5 %.

Dutt and Ravikumar (2008) proposed an approach, with a reduced form of Arrhenius model. This model was developed 29 ILs, which include imidazolium, pyridinium, and ammonium based ILs. Yet, this model was tested and the deviation was reported to be more than 20 % (Dutt et al., 2013).

Yamamoto (2006) was first to report a QSPR study for ILs viscosities and proposed few models to estimate viscosities of ILs. One of the models was developed for CAMD purpose, and a Java program was developed based on this model (Matsuda et al., 2007). This model consists of the terms of temperature, cation, side chain, and anion. Thus, it is possible to estimate viscosities of ILs solely based on the ions structure. This model was tested on

correlation data set and it showed a correlation coefficient $R^2$ of 0.8971. However, when it was tested on prediction data points, the $R^2$ decreases to only 0.6226. This shows that the model is not suitable for ILs out of the correlation data set.

Han et al. (2011) also presented a new set of QSPR models for ILs viscosities. These sets are based on the cations and anions of ILs. These models showed $R^2$ values between 0.92 to 0.97, and the authors claim that the largest deviation is 13.6 %. However, this model is limited to a small range of ILs, and the temperature dependency descriptors are not included. Mirkhani and Gharagheizi (2012) developed another QSPR model based on 435 data points for 293 ILs. This model showed $R^2$ value of 0.8096, when it was tested with 348 correlation data points and 87 data points. This model was reported to have deviation of about 9 %.

Valderrama et al. (2011) proposed the use of artificial neural networks (ANN) to describe viscosities of ILs. This work was done based on the molecular mass of ions, the mass connectivity, and density at temperature of 298 K. This model was tested on 31 data points and it showed average deviation of 1.68 %. Paduszyński and Domańska (2014) also presented a new model based on feed-forward ANN. This model requires input variables of temperature, pressure, and GC of each group. The model was developed based

on 13,000 data points of more than 1000 ILs, which is the most extensive model to date for viscosities of ILs. The $R^2$ value obtained from testing was reported to be about 0.98, and average deviation of about 13 %.

### 2.4.3 Solubility of Carbon Dioxide in Ionic Liquids

Since carbon dioxide ($CO_2$) absorption using ILs has gained the interest of researchers, efforts have been dedicated to develop predictive thermodynamic models for IL-$CO_2$ systems. There are various types of predictive models available currently to predict $CO_2$ solubility in ILs, including regular solution theory (RST), statistical associating fluid theory (SAFT) equation of state (EoS), conductor-like screening model for real solvents (COSMO-RS), and UNIFAC model.

Camper et al. (2004) first reported that RST can be used to model gas solubility in ILs at low pressures. This work has shown that RST is able to explain the solubility trends of $CO_2$ in ILs, depending only on the gas. Scovazzo et al. (2004) also explained that the solubility parameters can be reasonably related to the gas solubility in ILs instead of a curve-fitting exercise due to predominant van der Waals force between $CO_2$ and ILs. Hence, extension of RST model to application of IL-$CO_2$ systems does not violate the assumption used to define solubility parameters. RST model offers simple method to predict the gas solubility in ILs. However, this model is only

limited to low pressures application and the solubility parameters cannot be extrapolated to other conditions (Camper et al., 2004; Lei et al., 2013).

Karakatsani et al. (2007) proposed to use a truncated perturbed chain-polar SAFT EoS to predict $CO_2$ solubility in 1-butyl-3methylimidazolium hexafluorophosphate IL, and showed good agreement. Later, Ji and Adidharma (2010) presented a heterosegmented-SAFT EoS to represent $CO_2$ solubility in ILs. In this model, $CO_2$ is taken as a molecule; while IL is broken down into several alkyl, cation head, and anion groups. This model is reported to produce good estimation of $CO_2$ solubility in ILs at temperatures up to 473 K and pressures up to 200 bar, especially at low pressures. Chen et al. (2012) used perturbed chain SAFT EoS to reproduce solubility of $CO_2$ in imidazolium-based ILs in a wide range of temperatures and pressures. This model generally can estimate $CO_2$ solubility in ILs in good agreement with available experimental data, but higher accuracy was observed by the authors at low pressures. However, SAFT EoS has more complicated formulations; many parameters are to be considered, and hence limit the application of SAFT EoS in CAMD (Lei et al., 2014).

Manan et al. (2009) first evaluated the predictive capability of COSMO-RS model for 15 gases including $CO_2$ in 27 ILs. It was reported that the results are consistent for correlation data points only; the results for

predicting data points varied by a lot. Palomar et al. (2011) continued to explore the molecular interaction between $CO_2$ and ILs at molecular level by means of COSMO-RS model. The results showed that this model does not always produce good results of $CO_2$ solubility, compared to the experimental data. Nevertheless, Gonzalez-Miquel et al. (2012) used COSMO-RS model to estimate thermodynamic properties of ILs, such as $CO_2$ solubility, solvent regeneration enthalpy, and solvent reversal temperature. This work suggested that COSMO-RS model can act as a guide in designing new ILs for carbon capture purpose.

Lei et al. (2013) was first to proposed to extend UNIFAC model to predict $CO_2$ solubility in ILs. This work was done based on the model by Gmehling et al. (1982), and new group binary interaction parameters between $CO_2$ and 22 IL groups were added. UNIFAC model can also be extended to predict $CO_2$ solubility in pure ILs for a wide range of temperatures. Solubility of $CO_2$ in binary mixtures of ILs can also be predicted using UNIFAC model, with an average deviation of about 10 % (Lei et al., 2013). However, similar to all GC models, UNIFAC model cannot distinguish among isomers because the group proximity effect is not considered (Lei et al., 2014).

Lee and Lin (2015) demonstrated the use of predictive COSMO-SAC model for Henry's Law constant, selectivity of $CO_2$ over other gases in IL, and

their temperature dependency solubility. According to Lee and Lin (2015), the predicted results of Henry's Law constants of $CO_2$ in ILs have an average absolute relative deviation of 17 %. This proposed model includes quantum mechanical calculations, which are complicated and time consuming. The prediction model was also used to screen for potential IL candidates for $CO_2$ capture in the mentioned work.

## 2.5 Integrated Process and Product Design

Process design and molecular design have been treated as two separate problems generally, with little to no feedback between the two problems. Approaches developed to solve individual process design and molecular design problems show limitations, due to lack of information required prior to start the design algorithm. For example, in molecular design techniques, input of desired target properties is always required to start the design procedure, which is assumed ahead of the design and usually based on previous experience or knowledge. This situation can lead to a sub-optimal design. Similarly, a list of pre-defined candidate components are given generally when considering conventional process design methodologies, and hence limits the performance of process to the listed components. These limitations can be overcome through considering the interactions between both problems as shown in Figure 2-4 (Eden et al., 2004). The necessary input to this methodology is the molecular building blocks to form the desired product for molecular design problem and the desired process performance for process

design problem. The outputs of this methodology are design variables that fulfil the desired process performance target, and molecules that satisfy the property targets identified from solution of the process design problem. The interconnections between molecular design and process design enable exchange of information; hence avoid pre-deciding of any specific compounds and assumption on target property values.

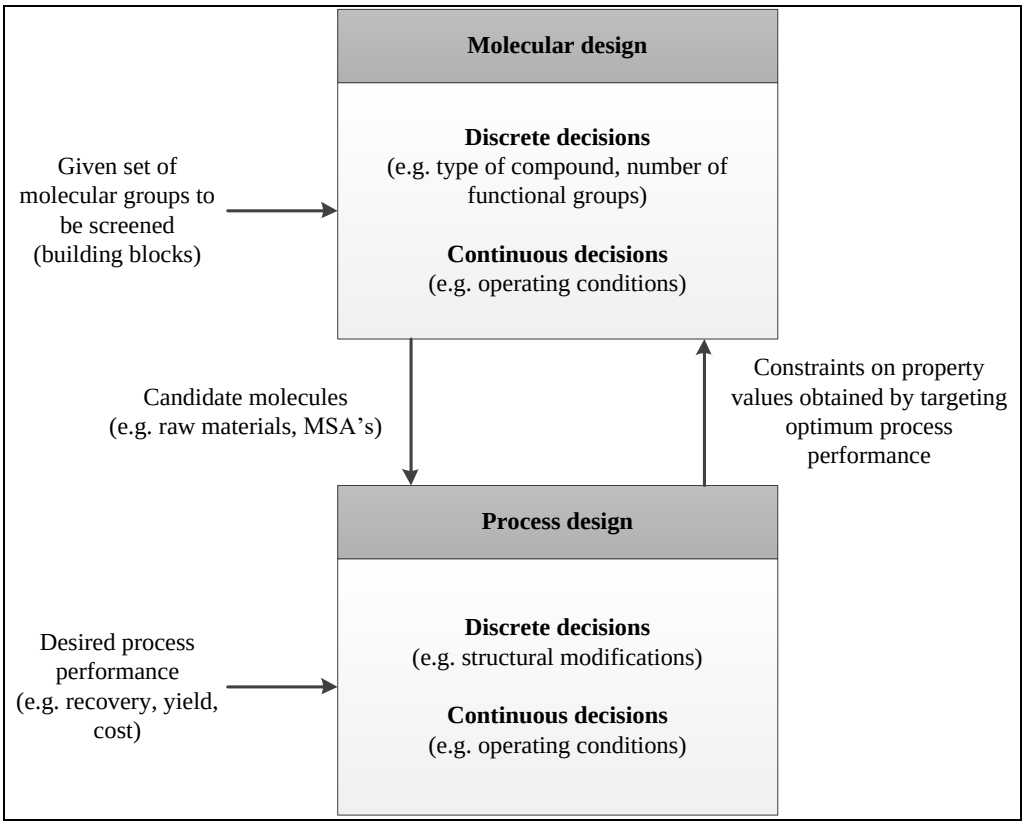


**Figure 2-4**: Integrated process-product design

Various works have been done on integrating process and product design problems to solve both problems sequentially or simultaneously. Lee et

al. (2002) proposed a selection method combining thermodynamics and non-linear programming techniques for optimal refrigerant mixture compositions, and developed a systematic design tool for mixed refrigerant systems. Eden et al. (2004) introduced a systematic framework for simultaneous solution of process and product design problems based on property clustering technique. The proposed methodology reformulates the conventional forward problems into two reverse problem formulations: reverse of simulation problem and reverse of property prediction problem. Papadopoulos and Linke (2005) presented a unified framework for integrated solvent design and process system design, which allows the identification of solvent molecules, based on process performance criteria. Papadopoulos and Linke (2006) later proposed to incorporate the solvent design information into process synthesis stage through molecular clustering approach, within an integrated design of solvent and process system. Optimal solvent candidates are identified using multi-objective optimisation, and subsequently evaluated in a process synthesis stage.

Eljack et al. (2007) proposed a systematic property based framework for simultaneous process and molecular design. Using this approach, process design problem is solved in terms of properties and property targets corresponding to the desired process performance is obtained. Potential molecular will be determined to match the obtained targets. For a process and product design problem that can be described by three properties, it can be

solved visually and simultaneously using this framework. Kazantzi et al. (2007) presented a graphical approach for simultaneous process and molecular design, and derived design rules for this purpose. In this proposed approach, process requirements and objectives, as well as molecular group properties were integrated to simultaneously target process design and material design. Property clustering technique was combined with GC methods to map the system from process level to molecule level using this approach, and vice versa. Therefore, the process design problem can be reversely mapped to define the constraints for molecular design problem. Nonetheless, mathematical optimisation based approaches can easily extend the application range to include more properties (Eljack et al., 2008).

Chemmangattuvalappil et al. (2010b) developed a combined property clustering and $GC^{+}$ algorithm to identify molecules that meet the property targets identified during the process design stage. This approach is useful when property contributions of some molecular groups are not available. To design simple monofunctional molecules, a modified visual approach was proposed; while mathematical optimisation method was developed to design more complicated structures. Besides, higher order groups can be considered to increase the accuracy of prediction when mathematical approach is used. Bardow et al. (2010) presented continuous-molecular targeting method (CoMT-CAMD) to solve integrated process and product design problem. An optimal process and a hypothetical solvent are first obtained using CoMT-

CAMD, and the parameters of hypothetical solvent are mapped onto an existing optimal solvent afterwards.

Bommareddy et al. (2012) proposed a hybrid method combining computer-aided flowsheet design (CAFD) and CAMD, based on GC approaches. Therefore, evaluation of the solution alternatives for both problems is straightforward and rapid. Ng et al. (2015) presented a two-stage optimisation approach to design optimal biochemical products and synthesise optimal conversion pathways in a biorefinery. The optimal biochemical products that meet the customer requirements are first identified using signature based molecular design techniques, followed by determining optimal conversion pathways to convert biomass into the identified products through superstructural mathematical optimisation approach. Ng et al. (2015b) later extended the approach to integrate mixture design and process design for biorefinery.

## 2.6 Research Gap

In short, ionic liquids (ILs) are currently the most promising substitute to conventional carbon capture solvent, as they have negligible vapour pressure and they can be tailored according to the requirements set by consumers. However, the process of designing an optimal IL is time consuming and costly, but there is no work reported on systematic approaches

for IL design specifically for carbon capture yet. Firstly, property clustering technique shows the possibility to solve IL design problem visually on ternary diagram and generate a list of potential ILs. There is a need for an insight-based methodology for IL design because it can provide useful insights to designers, assisting designers to make decision based on observation via a diagram. The insight-based methodology enables visualisation of feasibility and availability for different molecular groups clearly through the diagram. In order to identify an optimal IL solvent to fulfil design objective and relevant target properties, a comprehensive methodology is required. This can be done through computer-aided molecular design (CAMD), where a single IL can be targeted according to design objective.

Sometimes, IL mixture is desired instead of pure ILs due to economic and performance limitations. Yet, there is no reported work on IL mixture design via systematic design tools, and hence it is necessary to explore into this area. Property clustering technique can be employed to develop an insight-based approach to design IL mixture, so that users can understand and observe the feasibility of an IL constituent as part of the mixture. The literature study shows that the property prediction models for ILs are not widely available yet, except for density and viscosity of ILs. Besides, most of the prediction models are for pure IL systems, which are not applicable when IL mixture is desired. This gap should be addressed since the CAMD methodologies and property clustering technique are greatly dependent on prediction models. One option is

to consider and incorporate any newly available experimental data in the developed approach.

Apart from that, there is still a lack of work done to integrate ILs design and process design up to date. The operating conditions are always considered only during process design stage, which is always done separately with IL design stage. However, the choice of solvent will always affect the operating conditions of a process, and vice versa. There is a need to incorporate process conditions into IL design stage to ensure the optimum performance of designed IL solvent. This is the first step to integrate process design with IL design. On top of that, the choice of solvent is also affecting the process that is implementing carbon capture unit (in terms of economic performance, utility consumption, and etc.), but this problem has not been addressed thus far. Therefore, the entire process should be integrated with IL solvent design problem, to guarantee the optimality of results. These research gaps are investigated in details and addressed in the following chapters.

# CHAPTER 3

# RESEARCH SCOPES AND METHODOLOGY

## 3.1 Scopes of Research

Based on the research gaps identified in Chapter 2, this research work is divided into five main scopes, by focusing on different aspects of ionic liquid (IL) or IL mixture design specifically as carbon capture solvent. The five research scopes presented in this thesis are summarised as follows:

i. Systematic insight-based approach to identify potential ILs as carbon capture solvents with multi properties consideration

   With at least a million possible ILs, the process to identify potential IL solvents specifically for carbon capture purpose, through generate-and-test, is time consuming and expensive. In order to determine suitable IL-based carbon capture solvents, a systematic insight-based methodology was developed. The design problem can be visualised on a diagram using this developed approach, and multiple properties of IL can be considered on the diagram. Visualisation of the design problem provides useful insights to users with little mathematical programming background. Designers can choose which properties to be optimised,

and observe the feasibility or availability of different molecular groups visually at the same time using the proposed approach.

ii. Systematic approach to design optimal IL as replacement of current commercial carbon capture solvents

From the previous approach, designers can understand the design problem and which groups are useful for the design problem. Following that, an optimal IL should be chosen based on considerations of target properties and constraints. However, there is no work reported on systematic approach to design an optimal IL specifically for carbon capture purpose. To address this problem, a systematic methodology that is able to choose optimal IL based on considerations of target properties and constraints was developed. Carbon dioxide ($CO_2$) solubility and viscosity are main concerns in designing carbon capture solvent, high solubility of $CO_2$ in IL and low viscosity of IL are desired for the IL to be an efficient and green solvent (Kuhlmann et al., 2007). Structural constraints are important in molecular design because they will restrict the final results to feasible IL structure only. Due to lack of understanding of chemical absorption of $CO_2$ in ILs, only physical absorption was considered during the development of the approach. Selectivity of $CO_2$ over other gases was excluded in this work, which means it was assumed that only $CO_2$ is absorbed by the designed IL solvent. Experimental work can be done

afterwards as supplementary to verify the performance of chosen IL. Using the proposed approach, time and expenses needed for experimental work are reduced significantly.

iii. IL mixture design for carbon capture purpose using existing predictive models and newly available experimental data

There are approximately $10^{12}$ binary IL mixture, and up to $10^{18}$ possible tertiary IL mixture (Holbrey and Seddon, 1999). With this number of possibilities, trial-and-error approach is not practical to determine an optimum IL mixture for specific task. Therefore, a systematic approach is needed to determine or design optimum task-specific IL blend. During the process of designing IL mixture, property prediction models are needed to estimate thermophysical properties of ILs. However, these predictive models do not always cover wide range of ILs, since this field is considered still in its infancy. Thus, a methodology that is able to utilise both prediction models and experimental data to design IL mixtures should be developed. The proposed approach in first scope was further extended to determine potential IL mixtures as carbon capture solvents under this scope. Similarly, this approach is easy to be applied by designers or understood by decision makers with little mathematical programming background. The proposed approach takes multiple properties into consideration during IL mixture design, and also newly experimental

data of ILs can be incorporated directly into the proposed methodology.

iv. Systematic methodology to identify optimal operating conditions for carbon capture using the designed IL

Varying the process conditions will affect the thermophysical properties of IL, for example higher temperature will lower viscosities and $CO_2$ solubility of ILs. This will directly affect the performance of IL in capturing $CO_2$, and the overall cost of the process as well. However, operating conditions are usually considered during process design stage only, even though they are equally important for IL design. IL designed based on a fixed operating condition may not be the optimal results, given that a process is usually feasible within a range of temperatures and pressures. Therefore, there is a need to identify the operating conditions properly during the stage of designing optimal IL to capture $CO_2$. The proposed approach for previous research scope was further extended under this scope, by implementing the idea of identification of the optimal operating conditions for the process simultaneously while designing IL solvent. The developed approach is able to determine optimal IL and its optimal operating conditions, by targeting a single property, subject to relevant constraints. In this work, $CO_2$ solubility in IL is the target property, while viscosity, process model and structural constraints are included.

Similar to previous scope, only physical absorption was considered during the development of this approach due to lack of understanding of chemical absorption of $CO_2$ in ILs. Selectivity of $CO_2$ over other gases was not studied as well, so it was assumed that only $CO_2$ is absorbed by designed IL.

v. Integrated carbon capture process design and IL solvent design

Process design and product design are always related in such a way that they are affecting each other. When solvent design and process design are done separately, there is no guarantee of optimal results for both problems. For example, an optimal IL designed solely based on solubility of $CO_2$ can give high $CO_2$ absorption, but may need high energy or larger tower for regeneration. On the other hand, designing a process using one IL solvent may produce a profitable process, but the solvent may not be the most efficient among all. Hence, the design of carbon capture process should be done in conjunction with the IL design to ensure the optimality of results. To address these problems, a systematic approach was developed to determine the optimal IL solvent and carbon capture process design simultaneously. IL solvent is determined using the information of process that will implement carbon capture system. Installation of carbon capture system with the designed IL can be evaluated and retrofitting can be done accordingly.

## 3.2 Research Methodology

Based on the research gaps discussed in Section 2.7, various computer-aided molecular design (CAMD) techniques and mathematical optimisation approaches were applied to achieve the aim and objectives of this research within the mentioned scopes. First and foremost, detailed literature review on carbon capture technologies and solvent used for carbon capture, as well as properties and prediction models of ionic liquids (ILs) was done. The information obtained from literatures was used to identify the main properties that affect the performance of carbon capture solvents. A graphical approach was developed for identification of potential ILs as carbon capture solvents, when multiple properties are considered in design problem. This approach is aimed to produce a list of possible structures of ILs, fulfilling all property constraints. Mathematical optimisation approach was then applied to solve IL design problem and identify the optimal structure of IL as carbon capture solvent, focusing on single target optimisation. The same graphical approach was further extended to determine potential IL mixtures for carbon capture purpose. The developed approach is targeted to be able to utilise both predicted models and experimental data to determine properties of IL mixtures.

As a first step to integrate IL design and process design, one of the mathematical programming approaches was introduced to simplify the process of identification of optimal operating conditions for a designed IL. This

approach was further utilised and integrated with process design problem, aiming to identify suitable IL for carbon capture process and the whole systematically. The overall methodology to design IL specifically for carbon capture purpose is presented in Figure 3-1.

### 3.2.1 Systematic insight-based approach to identify potential ILs as carbon capture solvents with multi properties consideration

To identify the potential IL solvents for carbon capture purpose, a visual approach was developed by considering multiple properties at the same time. When two or more target properties are to be considered, multi objective optimisation is needed but it is complicated for designers with little mathematical programming background. In order to simplify the problem, a systematic visual approach based on property clustering technique is proposed in Chapter 4. This is an extension of visual approach presented by Eljack and Eden (2008), which was originally for organic compound design. The developed approach can transform the property-based problem onto a diagram and provide useful insights to user visually, and it can then be solved on the very same diagram. The properties of IL solvents were estimated using group contribution (GC) type prediction models. Several rules were developed to assist the users for design of IL solvents using this approach. The proposed approach is able to produce multiple solutions based on the target properties considered. Designers can make the final decision based on other screening criteria.

### 3.2.2 Systematic approach to design optimal IL as replacement of current commercial carbon capture solvents

The approach mentioned in Section 3.2.1 is able to generate a list of potential solutions. In order to identify the optimal IL-based solvent, a systematic mathematical optimisation approach was developed by targeting the performance of IL solvents, as presented in Chapter 5. This is based on CAMD technique that is already established for organic compound design, and now further extended to design IL for carbon capture purpose. The target performance of solvent was first identified as measurable properties. In the case where they are not measurable, they should be correlated or expressed in terms of measurable properties. Since some of the IL structures are novel and do not have available property data, the properties of ILs were estimated by using GC type property prediction models. Besides, relevant constraints must be included to ensure the IL designed is feasible. Finally, mathematical optimisation approach was employed to solve the IL design problem, based on target property chosen at the very beginning.

### 3.2.3 IL mixture design for carbon capture purpose using existing predictive models and newly available experimental data

When using a task-specific IL solvent is impractical for either economic or performance reason, IL mixture may be desired as mixture can provide better mix of properties. To determine possible IL mixtures for carbon capture purpose, the visual approach presented for the first scope was

extended. Multiple target properties can be considered simultaneously during design of IL mixture as carbon capture solvents. Similar to previous scopes, these properties were estimated via GC type property prediction models. However, the data of pure ILs and IL mixtures is still scarce, where some of the prediction models do not cover all ILs considered in the design. Thus, this approach was developed in such a way that experimental data of pure ILs can be utilised, in order to estimate the properties of mixtures. Rules were developed as well to aid the mixture design process for users. The approach is able to generate a list of possible solutions to users, and the final decisions can be made accordingly, through further screening or experimental validations. The proposed approach is presented in Chapter 6.

### 3.2.4 Systematic methodology to identify optimal operating conditions for carbon capture using the designed IL

The importance of identifying the optimal operating conditions for a solvent was discussed in Section 3.1. The proposed methodology for second scope was extended to simultaneously identify optimal IL solvent and optimal operating conditions of carbon capture process using the designed IL solvent. This developed methodology is similar to the previously developed mathematical approach, except that operating conditions (i.e. temperature and pressure) were modelled as variables here, but this will cause the model to be more complex. The proposed approach is presented in Chapter 7. To simplify the optimisation model, disjunctive programming was implemented to

discretise the continuous variables of temperature and pressure. GC prediction models were employed to predict the properties of designed IL. Mathematical optimisation approach was then utilised to solve the design problem and identify both optimal IL solvent and its optimal operating conditions.

### 3.2.5 Integrated carbon capture process design and IL solvent design

Identification of the optimal solvents solely based on properties or performance is insufficient, where the process design considerations (economic and equipment design) are not included. Process design and product design problems should be considered together, to ensure the optimality for both. In the approach presented in Chapter 8, data of the process that will implement carbon capture system was obtained through input-output modelling (Duchin, 1992), and adapted to design IL solvent by targeting the optimum carbon capture performance. The algorithm approaches developed for forth scope was implemented here to identify pure IL solvent and its operating conditions. In this developed approach, GC models were employed to determine the properties of IL solvents. Mathematical optimisation approach was used to solve the design problem and identify both optimal IL solvent and its optimal operating conditions. The results will then be utilised to study the effect of carbon capture system on the overall process using the developed approach, decision about retrofitting of overall process can be done accordingly.

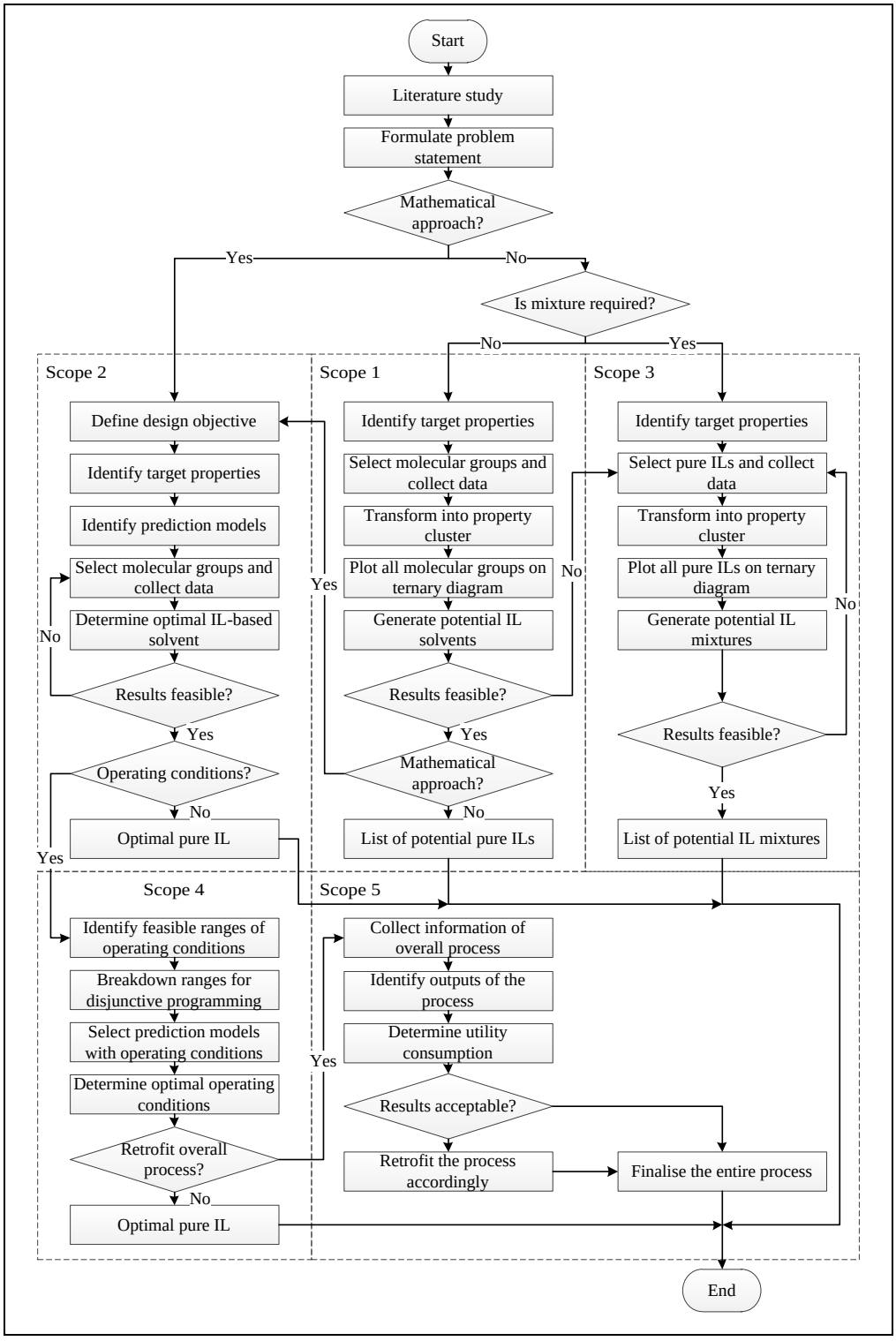


**Figure 3-1**: Approaches to design IL-based solvent for carbon capture purpose

## 3.3 Summary

The research gaps identified in Chapter 2 led to five research scopes defined and presented in this chapter. Methodologies to achieve the objectives within the defined scopes were also discussed in this chapter. The presented research scopes will be addressed in details in the following chapters via proposed research methodologies.

# CHAPTER 4

# DESIGNING IONIC LIQUID SOLVENT FOR CARBON CAPTURE USING SYSTEMATIC VISUAL APPROACH

## 4.1 Introduction

A systematic visual approach to determine potential ILs, using a diagram, specifically for the purpose of carbon capture is presented in this chapter. The presented approach allows multiple target properties consideration through portraying these targets clearly on a diagram, and hence trade-off between these properties is possible. Property clustering technique was employed in this approach, where the design problem can be mapped from property domain into cluster domain. Since some non-existent ILs may occur during the design process, group contribution (GC) method was included in the framework to estimate the properties of ILs. By combining property clustering technique and GC method, the proposed approach is able to provide a property based platform to visualise the performance of designed ILs on a ternary diagram. A case study was investigated to illustrate the validity of proposed approach.

## 4.2 Problem Statement

The overall problem to be addressed can be stated as follows: Given a set of target properties and constraints, also a set of cation cores, anions, and organic functional groups, it is desired to develop a systematic technique to identify the molecular structure of ionic liquid (IL) that is potential substitute to conventional carbon capture solvents. The designed IL must satisfy all the property constraints and design rules. The performance of designed ILs will be evaluated based on the properties (or functionalities such as cost and environmental impact), which are used to represent characteristics or attributes that are not measurable. A superstructure representation of the allowed combinations of all groups is shown in Figure 4-1.

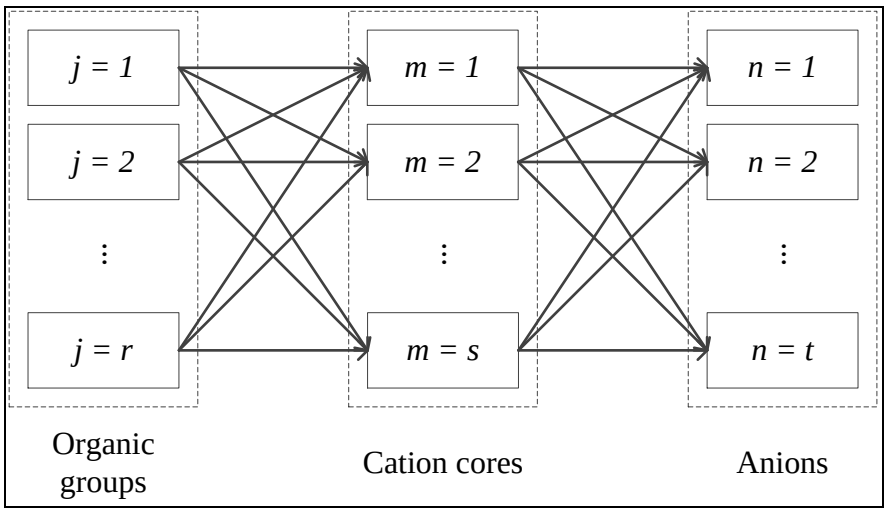


**Figure 4-1**: Schematic representation of combinations of all molecular fragments

## 4.3 Visualisation Design Approach

Property clustering technique was applied in this approach, to represent and track physical properties (Shelley and El-Halwagi, 2000). Property clusters are conserved surrogate quantities that are functions of the original non-conserved properties. The clusters are formed from property operators, which are functions of the original properties and tailored to obey linear mixing rules. The newly developed graphical tool, which takes the form of a ternary diagram, is able to provide insights and assist user in solving the design problem, by showing the directions in searching for solutions. Each vertex of ternary diagram represents one property or functionality, therefore only three dominant properties or functionalities are considered. Other properties that are not included in ternary diagram can serve as screening properties. Screening properties can act as extra criteria in assisting designers to eliminate infeasible ILs. Besides, properties with no available group contribution (GC) prediction models can also be included as screening properties, as long as there are appropriate prediction models for these properties. Figure 4-2 shows the procedure of solving ionic liquid (IL) design as carbon capture solvent, and detailed description of each step is given as below.

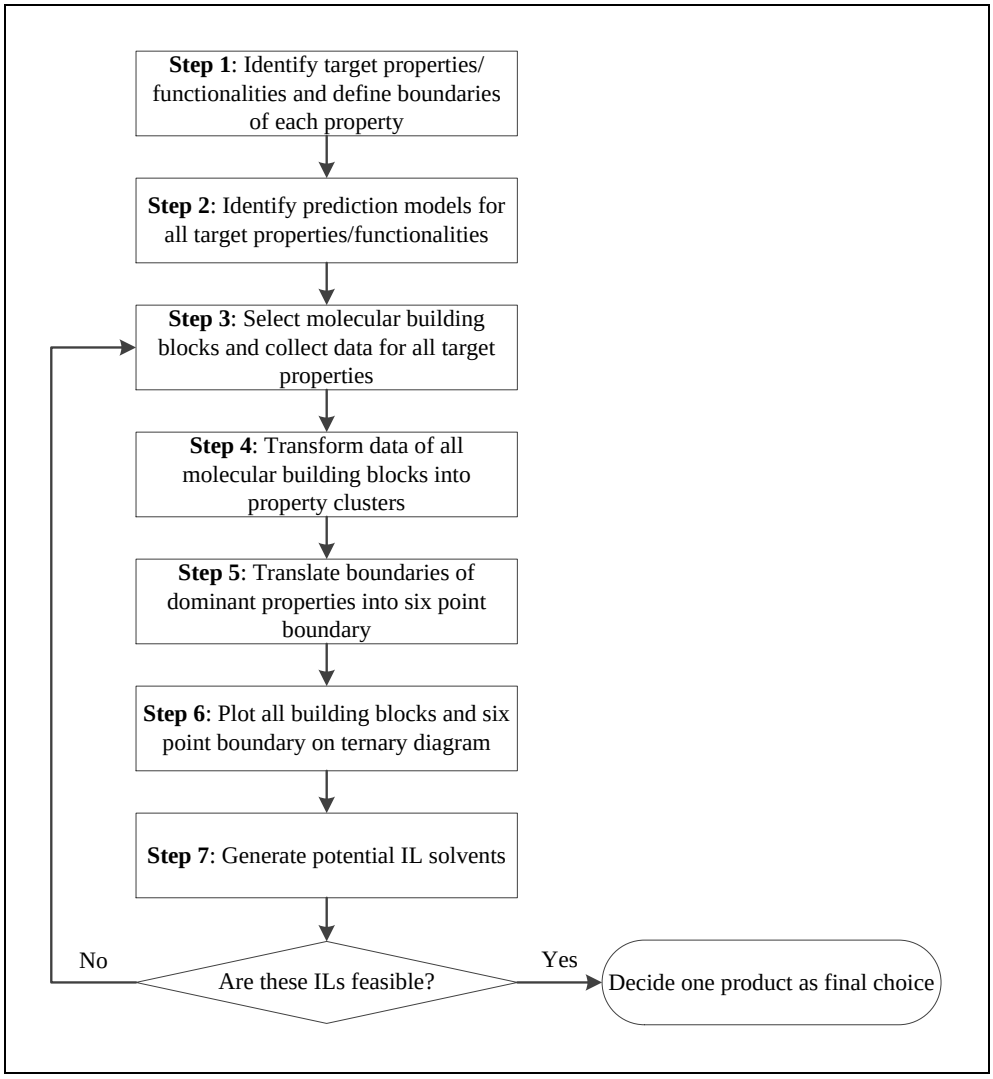


**Figure 4-2**: Property-based visual approach to design IL-based carbon capture solvent

Step 1: All necessary target properties or functionalities (including cost, environmental impact and etc.) should be identified to design IL as carbon capture solvent. The upper and lower limits for these properties will be kept as targets in solving the design problem. These properties can be expressed as Equation (4.1).

$$\tau_d^{\min} \leq \tau_d \leq \tau_d^{\max} \tag{4.1}$$

where $\tau_d$ is the $d^{\text{th}}$ property, $\tau_d^{\min}$ and $\tau_d^{\max}$ are the lower and upper bound of $d^{\text{th}}$ property. As discussed, only three properties can be included in ternary diagram, therefore user should decide the dominant properties in this step if there are more than three target properties.

Step 2: Reliable prediction models should be identified to estimate the target properties of pure ILs, for all target properties. The accuracy of chosen prediction models will affect the overall accuracy of the proposed approach.

Step 3: Suitable molecular building blocks will be selected in this step. These building blocks consist of cation cores, anions, and organic groups, as shown in Figure 4-1, to form a complete IL structure. The molecular building blocks should be selected such that the properties of the designed ILs are similar to the conventional carbon capture solvent. It is assumed that the newly designed ILs will possess properties or functionalities similar to that of conventional products. In this step, the data of all selected molecular groups is collected for all target properties and functionalities.

Step 4: The collected data in Step 3 is converted into molecular property clusters using Equations (4.2) to (4.5).

$$\psi_d(\tau_{di}) = \sum_{k=1}^{q} v_k \psi_d(\tau_{dk}) \tag{4.2}$$

$$\Omega_{dk} = \frac{\psi_d(\tau_{dk})}{\psi_d^{ref}(\tau_d)} \tag{4.3}$$

$$AUP_k = \sum_{d=1}^{N_P} \Omega_{dk} \tag{4.4}$$

$$C_{dk} = \frac{\Omega_{dk}}{AUP_k} \tag{4.5}$$

Property operators are described by Equation (4.2), where $\psi_d(\tau_{di})$ is the property operator of $d^{\text{th}}$ property of component $i$, $v_k$ is the number of group $k$, $q$ is the total number of functional groups, while $\psi_d(\tau_{dk})$ is the molecular property operator of $d^{\text{th}}$ property of functional group $k$. As shown by Equation (4.2), the property operators will follow simple linear mixing rules regardless of the non-linearity of the properties (Shelley and El-Halwagi, 2000). Using molecular property operators, property clusters can be obtained according Equations (4.3) to (4.5). Given the properties are of various functional forms and units, the molecular property operator will first be divided by a properly chosen reference value, $\psi_d^{ref}(\tau_d)$ to make it dimensionless and obtain a normalised molecular property operator for $d^{th}$ property of group $k$, $\Omega_{dk}$. All the normalised molecular property operators for group $k$ are then summed together to obtain an augmented property index (AUP) for group $k$, $AUP_k$. Finally, the property cluster $C_{dk}$ for

property *d* of group *k* is determined using Equation (4.5). The summation of all cluster values for group *k* is equal to unity as shown in Equation (4.6).

$$\sum_{d=1}^{N_P} C_{dk} = 1 \tag{4.6}$$

Step 5: The design problem can now be visualised on a ternary diagram using these obtained cluster values for all functional groups. For the properties included in ternary diagram, the constraints can be represented as a feasibility region defined by six unique points (El-Halwagi et al., 2004). These six points are characterised by the following values of normalised operators, where solutions should fall inside the boundary formed by these points.

$$\left(\Omega_1^{\min}, \Omega_2^{\min}, \Omega_3^{\max}\right)\left(\Omega_1^{\min}, \Omega_2^{\max}, \Omega_3^{\max}\right)\left(\Omega_1^{\min}, \Omega_2^{\max}, \Omega_3^{\min}\right)$$
$$\left(\Omega_1^{\max}, \Omega_2^{\max}, \Omega_3^{\min}\right)\left(\Omega_1^{\max}, \Omega_2^{\min}, \Omega_3^{\min}\right)\left(\Omega_1^{\max}, \Omega_2^{\min}, \Omega_3^{\max}\right)$$

Step 6: IL design problem can now be plotted and visualised on a ternary diagram using calculated molecular property clusters and six point boundary determined in Step 5.

Step 7: A list of possible pure ILs can be determined now using plotted ternary diagram in Step 6. Design and optimisation rules were previously developed by Eden et al. (2004) for process design problems, and extended by Eljack et al. (2006) for organic compound design problems. In this work, a new set of rules have

been developed, based on the previous rules, to ensure the designed ILs are valid solutions. Following these rules, the IL molecular structure can be determined using ternary diagram. Rules 1 to 3 ensure the designed IL is a valid molecular structure. Given a valid IL structure is obtained, Rule 4 must be satisfied for the IL structure to be a valid solution to the IL design problem.

Rule 1: When two functional groups, $K_1$ and $K_2$ are added linearly on the diagram, the AUP values and distance between them provide information of $K_1$-$K_2$ structure.

$$D_1 = \frac{v_1 AUP_1}{v_1 AUP_1 + v_2 AUP_2} \tag{4.7}$$

Rule 2: The molecular structure of final formulation must consist of at least two groups. More groups can be added if the free bond number (FBN) of the structure is not zero. FBN is the number of free molecular bonding of the molecular structure. In Equation (4.9), $n_k$ is the available free bond of functional group *k*. The final IL molecular structure must not have any free bond, to ensure the structure is complete and feasible (i.e. FBN = 0).

$$\sum_k v_k \geq 2 \tag{4.8}$$

$$FBN = \sum_k v_k n_k - 2\left(\sum_k n_k - 1\right) \tag{4.9}$$

Rule 3: In pure IL design, only one cation core and one anion group can be chosen.

Rule 4: The cluster value of the designed IL must be located within the feasibility region on the ternary diagram. The AUP value of the designed IL must be within the range of target AUP. The target AUP range is determined from the six property constraints on ternary diagram. If the AUP value is outside the range of target AUP, the IL is not a feasible solution.

Rule 5: All AUP values of the groups must be positive.

It is common that there is negative GC data, and this will lead to negative property operator and cluster value. In this situation, the group will reside outside the ternary diagram, and using this group will violate Rule 1. Solvason et al. (2009) has discussed about this limitation and another rule is developed to overcome this. Without Rule 5, a negative AUP is mathematically possible, but it gives an infeasible solution. This can be avoided by adjusting reference values of the properties. In the case where

screening properties are included in the design problem, these properties must be calculated for the final IL formulation, using appropriate prediction models. Same as dominant properties included in ternary diagram, these screening properties should be within the range of target properties for the designed IL to be a valid solution.

Once the list of potential ILs is obtained, all properties and functionalities should be checked to ensure they are within the targeted range. Feasibility of these generated IL solvents should be checked, if there is no feasible solution, Step 3 should be done again and the whole process shall be repeated. When there are feasible solutions, decision makers can decide on final one IL as the carbon capture solvent.

## 4.4 Case Study

To demonstrate the proposed approach, an illustrative case study was solved and presented in this section. A post-combustion carbon capture unit is using amine-based solvent currently. It is desired to substitute this solvent with ionic liquid (IL) solvent. The main objective of this case study is to determine possible ILs as carbon capture solvent from a set of organic groups, anions, and cation cores, subjecting to relevant property constraints. The system temperature, $T$ and pressure, $P$ are 323.2 K and 0.7 MPa respectively.

### 4.4.1 Step 1: Identify target properties/functionalities and define boundaries of each property

According to Figure 4-2, target properties and functionalities were identified for this case study. Three properties were taken into consideration in this case study, density ($\rho$), viscosity ($\mu$) and carbon dioxide ($CO_2$) solubility ($S$). These properties were included because density is the basic of transport property, viscosity affects overall operating cost, and $CO_2$ solubility is a measurement of carbon capture performance of solvent. Table 4-1 shows the target property ranges for these properties. The designed IL solvent should possess similar properties as current commercial $CO_2$ solvents (i.e. ethanolamines), and hence the ranges of target properties were set according to the properties of ethanolamines (The Dow Chemical Company, 2003). Low viscosity of IL is desired to minimise pumping power required to circulate IL solvent within the system, and hence viscosity target range was set between 0.01 to 0.10 Pa.s. Final IL formulation should has solubility at least as good as the conventional solvent, and hence the solubility was targeted to be between 0.07 and 0.30 (Zhang et al., 2012).

To illustrate the presented approach clearly, more properties were included in the case study, they are heat of vaporisation ($\Delta H_{vap}$) and specific heat capacity ($c_P$). Their target ranges are shown in Table 4-1 as well. Among these five target properties, density ($\rho$), heat of vaporisation ($\Delta H_{vap}$) and

specific heat capacity ( $c_p$ ) were chosen as dominant properties; while viscosity ($\mu$) and $CO_2$ solubility ($S$) remained as screening properties. The three dominant properties that were chosen for visualisation purpose include density, heat of vaporisation, and specific heat capacity; while the other two properties (viscosity and $CO_2$ solubility) remained as screening properties. Density is chosen as dominant property because it is the basic of transport property and require for viscosity calculation. Heat of vaporisation is chosen because it is related to vapour pressure of ILs and provides the idea of the volatility of the designed ILs, which is also related to the environmental and health aspect of designed ILs. Specific heat capacity of IL is crucial because it will affect the energy required during solvent regeneration. When the designed ILs do not fulfil these three criteria, the screening properties of these ILs will not be calculated.

**Table 4-1**: Target property ranges to design IL for carbon capture purpose

| Property | Lower Bound | Upper Bound |
|---|---|---|
| Density, $\rho$ (g $cm^{-3}$) | 1 | 2 |
| Viscosity, $\mu$ (Pa.s) | 0.01 | 0.10 |
| $CO_2$ solubility, $S$ (mol $CO_2$/mol IL) | 0.07 | 0.35 |
| Heat of vaporisation, $\Delta H_{vap}$ (kJ $mol^{-1}$) | 40 | 200 |
| Specific heat capacity, $c_p$ (J $mol^{-1}$ $K^{-1}$) | 100 | 600 |

### 4.4.2 Step 2: Identify prediction models for all target properties/functionalities

The prediction models for all target properties were selected in this step. Density was estimated using Equation (4.10) (Qiao et al., 2010), Equation (4.11) was employed to predict heat of vaporisation (Verevkin, 2008), and specific heat capacity was estimated using Equation (4.12) (Gardas and Coutinho, 2008c). Viscosity was predicted using Equation (4.13) (Gardas and Coutinho, 2008b). $CO_2$ solubility of IL was estimated through vapour liquid phase equilibrium, as given in Equations (4.14) and (4.15).

$$\rho - \rho_0 = \sum_{k=1}^{q} \nu_k \rho_k \tag{4.10}$$

$$\Delta H_{vap} = \sum_{k=1}^{q} \nu_k \Delta H_{vap,k} \tag{4.11}$$

$$\frac{c_P}{R} = \sum_{k=1}^{q} \nu_k c_{P,k} \tag{4.12}$$

$$\ln \frac{1000\mu}{\rho M} = A_\mu + \frac{B_\mu}{T} \tag{4.13}$$

$$y_i P \varphi_i (T, P, y_i) = x_i \gamma_i P_i^S \tag{4.14}$$

$$S_i = x_{CO_2} / x_{IL} \tag{4.15}$$

In Equation (4.10), $\rho_0$ is an adjustable parameter for density given as 0.538 g $cm^{-3}$, $\rho_k$ is the group contribution (GC) data of group *k* for density, $\Delta H_{vap,k}$ is the GC data of group *k* for heat of vaporisation, $c_{p,k}$ is GC data of group *k* for specific heat capacity, and R is gas constant given as 8.314 J $mol^{-1}$ $K^{-1}$. Density is measured in g $cm^{-3}$, and heat of vaporisation is measured in kJ $mol^{-1}$; while the unit for specific heat capacity is J $mol^{-1}$ $K^{-1}$. The viscosity was determined using Orrick-Erbar-type approach that employs GC method (Gardas and Coutinho, 2008b), where *M* is IL molecular weight in g $mol^{-1}$, *T* is the system temperature in K, $A_\mu$ and $B_\mu$ are calculated parameters based on contributions of group *k* to each of them.

The solubility of $CO_2$ was determined through equilibrium relationships as shown in Equation (4.14) and the nonideality of liquid phase was modelled through activity coefficient $\gamma_i$, which was estimated using UNIFAC model. In Equation (4.14), $x_i$ and $y_i$ are the mole fractions of component *i* in liquid and gas phases respectively, $P_i^S$ is the saturated vapour pressure of component *i*, and $\varphi_i(T,P,y_i)$ is the gas-phase fugacity coefficient. UNIFAC model is given in Equation (4.16) consisting combinatorial contribution, ln $\gamma_i^C$, which is essentially due to the differences in size and shape of the molecules, and residual contribution, ln $\gamma_i^R$, which is due to energetic interactions (Skjold-Jørgensen et al., 1979). This model is expressed as a function of composition and temperature; the detailed explanation is given in Appendix Section A.2.1.

$$\ln \gamma_i = \ln \gamma_i^C + \ln \gamma_i^R \tag{4.16}$$

where $\ln \gamma_i^C$ represents the combinatorial contribution and $\ln \gamma_i^R$ represents the residual contribution. Group parameters and binary interaction parameters of IL for UNIFAC model presented by Lei et al. (2013) have been used to predict activity coefficient. According to Lei et al. (2013), IL should be decomposed into one main skeleton of cation and anion, and the alkyl chain connected to cation broken down into respective organic function group, as presented in Figure 4-3. In order to apply the parameters, the cation core was grouped with the anion; while $R_1$, $R_2$ and $R_3$ alkyl chains are broken down into respective organic groups.

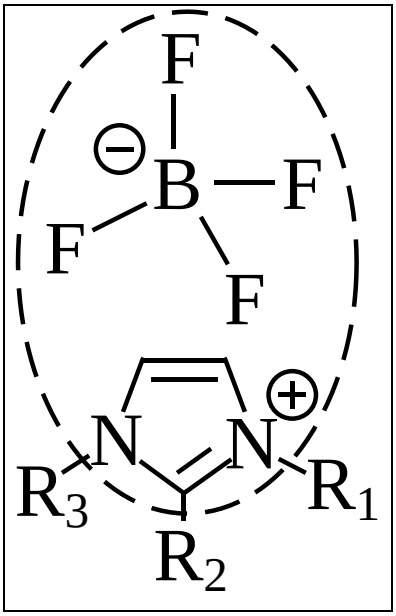


**Figure 4-3**: Decomposition of ionic liquid

Gas-phase fugacity coefficient was determined using equation of state proposed by Span and Wagner (1996) that is given as Equation (4.17), where the details are given in Appendix Section A.2.2. Saturated vapour pressure of $CO_2$ was calculated using the extrapolated Antoine equation proposed by Shiflett and Yokozeki (2006) as described by Equation (4.18); while the saturated vapour pressure of IL was taken as zero due to its extremely low vapour pressure. For the same reason, IL was assumed to be absent in vapour phase (i.e. $y_{IL}$ = 0). Once the mole fraction of $CO_2$ in liquid phase was determined, the $CO_2$ solubility in terms of mole $CO_2$ per mole IL can be calculated using Equation (4.15).

$$\ln \varphi_i = \phi^r + \delta\phi_\delta^r - \ln\left(1 + \delta\phi_\delta^r\right) \tag{4.17}$$

$$\ln P_i^S = A_i - \frac{B_i}{T + C_i} \tag{4.18}$$

where $\delta = \rho/\rho_c$ is the reduced density, $A_i$, $B_i$, and $C_i$ are coefficients of component $i$. The saturated vapour pressure of IL was assumed to be negligible due to its extremely low vapour pressure. For the same reason, IL is assumed to be absent in vapour phase (i.e. $y_{IL}$ = 0). Both Equations (4.17) and (4.18) were employed by Lei et al.(2013) to determine group parameters of ILs for UNIFAC model.

### 4.4.3 Step 3: Select molecular building blocks and collect data for all target properties

The list of pre-selected functional groups is shown in Table 4-2. These are chosen for they are the most widely studied cations and anions (Zhou et al., 2009). The relevant GC data was collected and given in Table 4-3, along with free bond number (FBN) of each functional group.

**Table 4-2**: Organic functional groups, anions, and cation cores considered

| Type | *k* | Groups | Type | *k* | Groups |
|---|---|---|---|---|---|
| Organic groups | 1 | $CH_3$ | Anions | 6 | $[BF_4]^-$ |
| | 2 | $CH_2$ | | 7 | $[Tf_2N]^-$ |
| Cation cores | 3 | $[MIm]^+$ | | 8 | $[OTf]^-$ |
| | 4 | $[Py]^+$ | | | |
| | 5 | $[MPyr]^+$ | | | |

### 4.4.4 Step 4: Transform data of all molecular building blocks into property clusters

With all the properties and constraints defined, the molecular property operators and cluster values of dominant properties was determined in this step. From Equations (4.10) to (4.12), the property operators were determined and included in Table 4-4, along with the suitable reference value for each property. These reference values were chosen such that all augmented property index (AUP) values are positive, and fulfil Rule 5 in Section 4.3.

**Table 4-3**: GC data, free bond number, and molecular weights of all functional groups

| Groups | $k$ | $\rho_k$ | $\Delta H_{vap,k}$ | $c_{P,k}$ | $n_k$ | Molecular weight (g mol$^{-1}$) | $A_{k,\mu}$ | $B_{k,\mu}$ |
|---|---|---|---|---|---|---|---|---|
| $CH_3$ | 1 | -0.0077 | 2.5 | -10.059 | 1 | 15.03 | -0.74 | 250.0 |
| $CH_2$ | 2 | -0.0310 | 2.5 | 4.095 | 2 | 14.03 | -0.63 | 250.4 |
| $[MIm]^+$ | 3 | 0.5273 | 62.6 | 33.789 | 1 | 82.10 | 7.30 | 1507.1 |
| $[Py]^+$ | 4 | 0.5477 | 38.8 | 33.966 | 1 | 79.10 | 7.61 | 1453.6 |
| $[MPyr]^+$ | 5 | 0.4865 | 38.8 | 32.365 | 1 | 85.15 | 6.17 | 1983.3 |
| $[BF_4]^-$ | 6 | 0.2302 | 77.8 | 9.959 | 0 | 86.80 | -18.08 | 1192.4 |
| $[NTf_2]^-$ | 7 | 0.4505 | 65.3 | 35.450 | 0 | 280.15 | -17.39 | 510.0 |
| $[OTf]^-$ | 8 | 0.3141 | -0.5 | 18.950 | 0 | 149.07 | -17.72 | 905.6 |

Note that the molecular property operator for density is different from the usual property operator which is the reciprocal value of density as shown in Equation (4.19). This is because the property operator in Equation (4.19) is used to determine density of mixture using density of pure components; while the density property operator in Table 4-4 is employed to determine density of pure IL from functional groups.

**Table 4-4**: Molecular property operators and reference values for this case study

| Property | Molecular property operator, $\psi_d(\tau_{di})$ | Reference value |
|---|---|---|
| Density | $\rho$ - $\rho_0$ | 1 |
| Heat of vaporisation | $\Delta H_{vap}$ | 20 |
| Specific heat capacity | $c_P/R$ | 300 |

$$\psi_{density}\left(\tau_{density}\right)=\frac{1}{\rho} \tag{4.19}$$

GC data in Table 4-3 was transformed intro molecular property operators and clusters, as given in Table 4-5 and Table 4-6. As shown in Table 4-5, AUP values are positive even though there are negative property operator values. Table 4-7 shows the normalised molecular property operators of lower bound and upper bound for dominant properties.

**Table 4-5**: Molecular property operator and AUP values of functional groups considered in case study

| Groups | $k$ | $\psi_{density}(\tau_{density,\,k})$ | $\psi_{Hvap}(\tau_{Hvap,\,k})$ | $\psi_{cp}(\tau_{cp,\,k})$ | $AUP_k$ |
|---|---|---|---|---|---|
| $CH_3$ | 1 | -0.0074 | 0.125 | -0.0335 | 0.0837 |
| $CH_2$ | 2 | -0.0310 | 0.125 | 0.0136 | 0.1077 |
| $[Mim]^+$ | 3 | 0.5273 | 3.130 | 0.1126 | 3.7699 |
| $[Py]^+$ | 4 | 0.5477 | 1.940 | 0.1132 | 2.6009 |
| $[MPyr]^+$ | 5 | 0.4865 | 1.940 | 0.1079 | 2.5344 |
| $[BF_4]^-$ | 6 | 0.2302 | 3.890 | 0.0332 | 4.1534 |
| $[NTf_2]^-$ | 7 | 0.4505 | 3.265 | 0.1182 | 3.8337 |
| $[OTf]^-$ | 8 | 0.3141 | -0.025 | 0.0632 | 0.3523 |

**Table 4-6**: Property cluster values for all functional groups considered in case study

| Groups | $k$ | $C_{density,\,k}$ | $C_{Hvap,\,k}$ | $C_{cp,\,k}$ | *Sum* |
|---|---|---|---|---|---|
| $CH_3$ | 1 | -0.0925 | 1.4929 | -0.4005 | 1 |
| $CH_2$ | 2 | -0.2877 | 1.1609 | 0.1268 | 1 |
| $[Mim]^+$ | 3 | 0.1399 | 0.8303 | 0.0299 | 1 |
| $[Py]^+$ | 4 | 0.2106 | 0.7459 | 0.0435 | 1 |
| $[MPyr]^+$ | 5 | 0.1920 | 0.7655 | 0.0426 | 1 |
| $[BF_4]^-$ | 6 | 0.0554 | 0.9366 | 0.0080 | 1 |
| $[NTf_2]^-$ | 7 | 0.1175 | 0.8517 | 0.0308 | 1 |
| $[OTf]^-$ | 8 | 0.8917 | -0.0710 | 0.1793 | 1 |

**Table 4-7**: Normalised molecular property operator values of lower and upper bounds for three dominant properties

| Property | Normalised molecular property operator, $\Omega_d$ | $\Omega^{min}$ | $\Omega^{max}$ |
|---|---|---|---|
| Density | $\Omega_{density}$ | 0.4624 | 1.4624 |
| Heat of vaporisation | $\Omega_{Hvap}$ | 2 | 10 |
| Specific heat capacity | $\Omega_{cp}$ | 0.0401 | 0.2405 |

### 4.4.5 Step 5: Translate boundaries of dominant properties into six point boundary

The feasibility region of this IL design problem was determined using the molecular property operators and six point bounding presented by El-Halwagi et al. (2004). This feasibility region on ternary diagram is shown in Figure 4-4. From these six points, the AUP values of each were determined; while the minimum and maximum AUP values were identified as 2.703 and 11.502. According to Rule 4, the designed IL solvent must have AUP value within this range to be a valid solution.

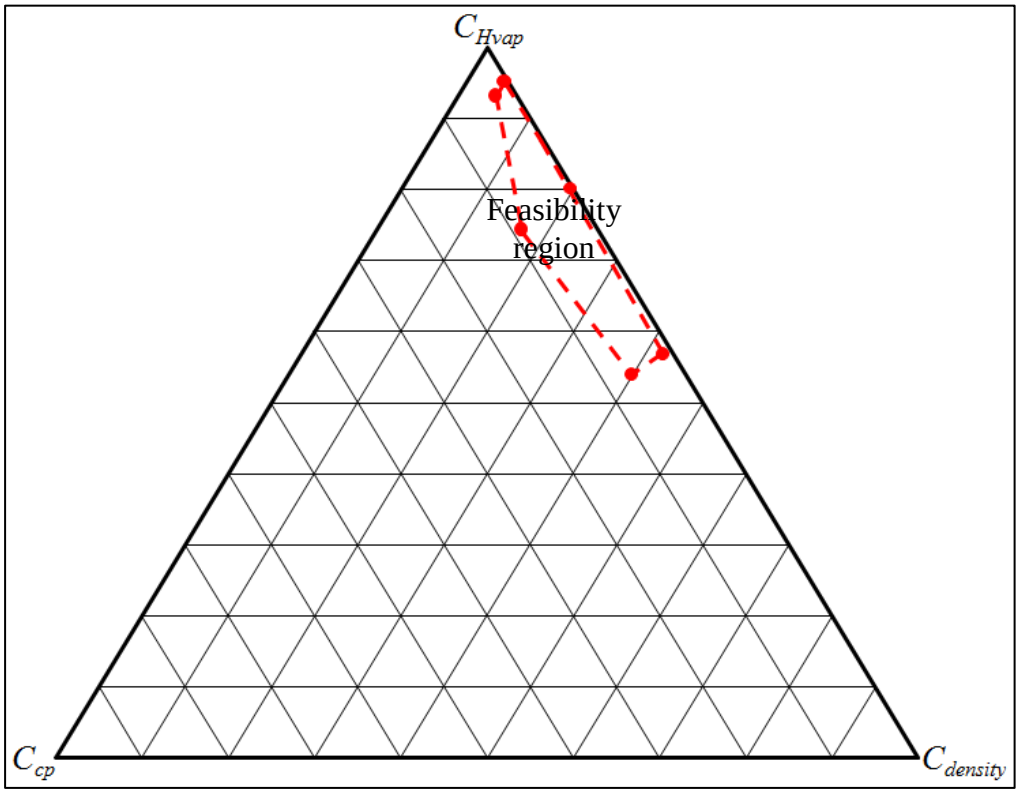


**Figure 4-4**: Feasibility region of this case study

### 4.4.6 Step 6: Plot all building blocks and six point boundary on ternary diagram

Using these cluster values, the functional groups can be plotted on ternary diagram, as shown in Figure 4-5. The IL design problem was visualised on a ternary diagram, where the dominant properties of all functional groups is represented by cluster values. Groups 1 and 2 reside out of the ternary diagram, due to their negative property cluster values. In Figure 4-5, different types of functional groups are labelled using different shapes and colours, to ease the design process. According to Rule 3, only one cation core and one anion group can be chosen, thus only one red triangle and one green diamond on the ternary diagram can be matched together at once. The advantage of using visual approach is that user can know which groups will be helpful for the design problem even before solving the problem. For example, in Figure 4-5, Group 8 is far away from the feasibility region, it is obvious that this group is not helpful at all in building an IL within feasibility region. Thus, this group can be omitted during the design process.

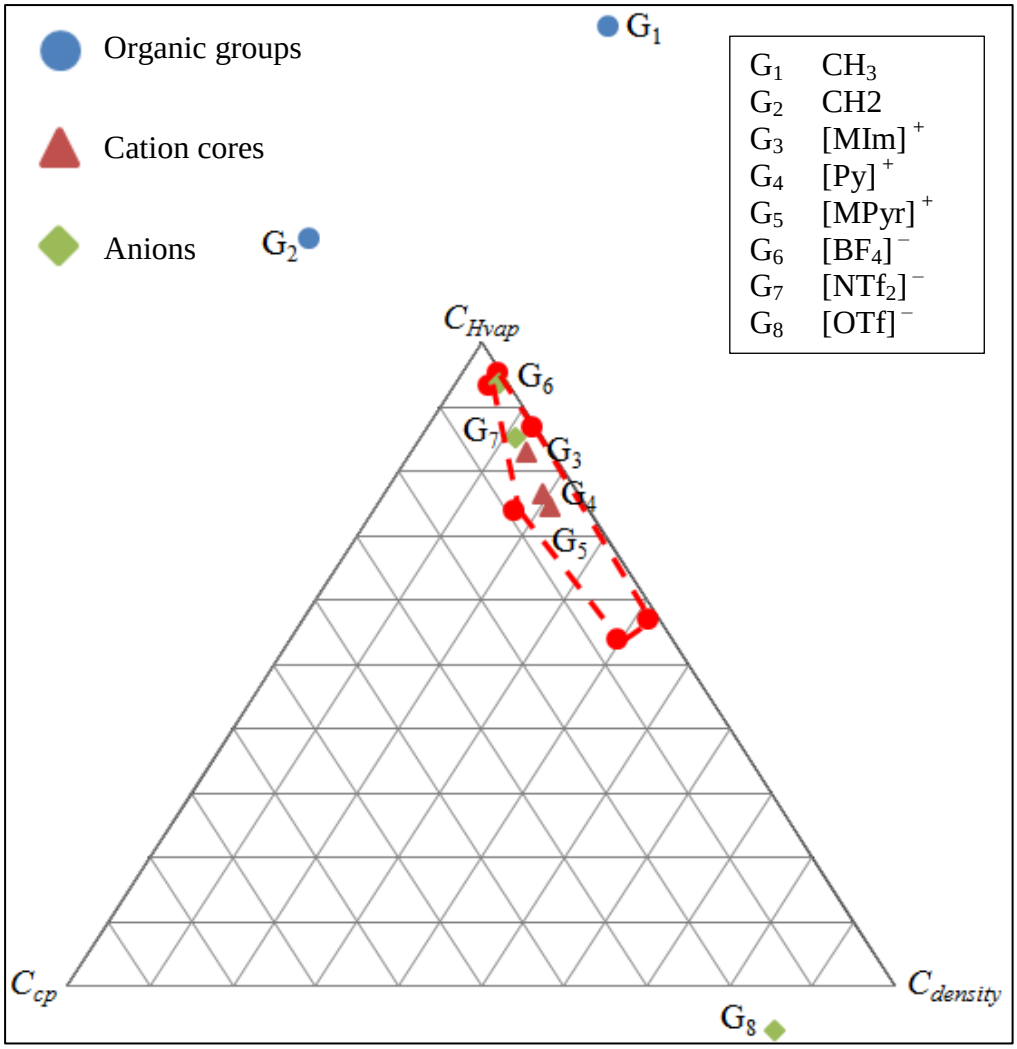


**Figure 4-5**: Ternary diagram representing IL design problem

### 4.4.7 Step 7: Generate potential IL solvents

In this step, potential IL solvents were generated using Figure 4-5. An example of synthesising an IL using proposed approach is shown in Figure 4-6. First of all, a cation core and an anion are to be chosen, $[MPyr]^+$ (red triangle) and $[NTf_2]^-$ (green diamond) were chosen in this example. Since this combination has one free bond (-$[MPyr]^+$- $[NTf_2]^-$), more organic functional groups (blue circle) can be added to it; a $CH_3$ group was added in this case, to fill up the free bond. The formulation designed here is $[C_1MPyr][NTf_2]$ ($CH_3$-$[MPyr]^+$- $[NTf_2]^-$), which obeys Rules 1 to 3. Rules 4 and 5 will be used to examine to validity of this solution.

Using the location of this final formulation on ternary diagram and Equation (4.7), the dominant properties of this IL were determined to be 1.467 g $cm^{-3}$, 106.6 kJ $mol^{-1}$, and 480.2 J $mol^{-1}$ $K^{-1}$, and its viscosity is 0.015 Pa.s while $CO_2$ solubility is 0.0841 mol $CO_2$/mol IL. All these are within the target property ranges. The AUP value of this IL formulation was calculated to be 6.452, which is also between the lower and upper bound values. Therefore, this formulation is a valid solution for this case study. Seven other candidate ILs were formulated on ternary diagram, as shown in Figure 4-7, and the properties were determined and presented in Table 4-8.

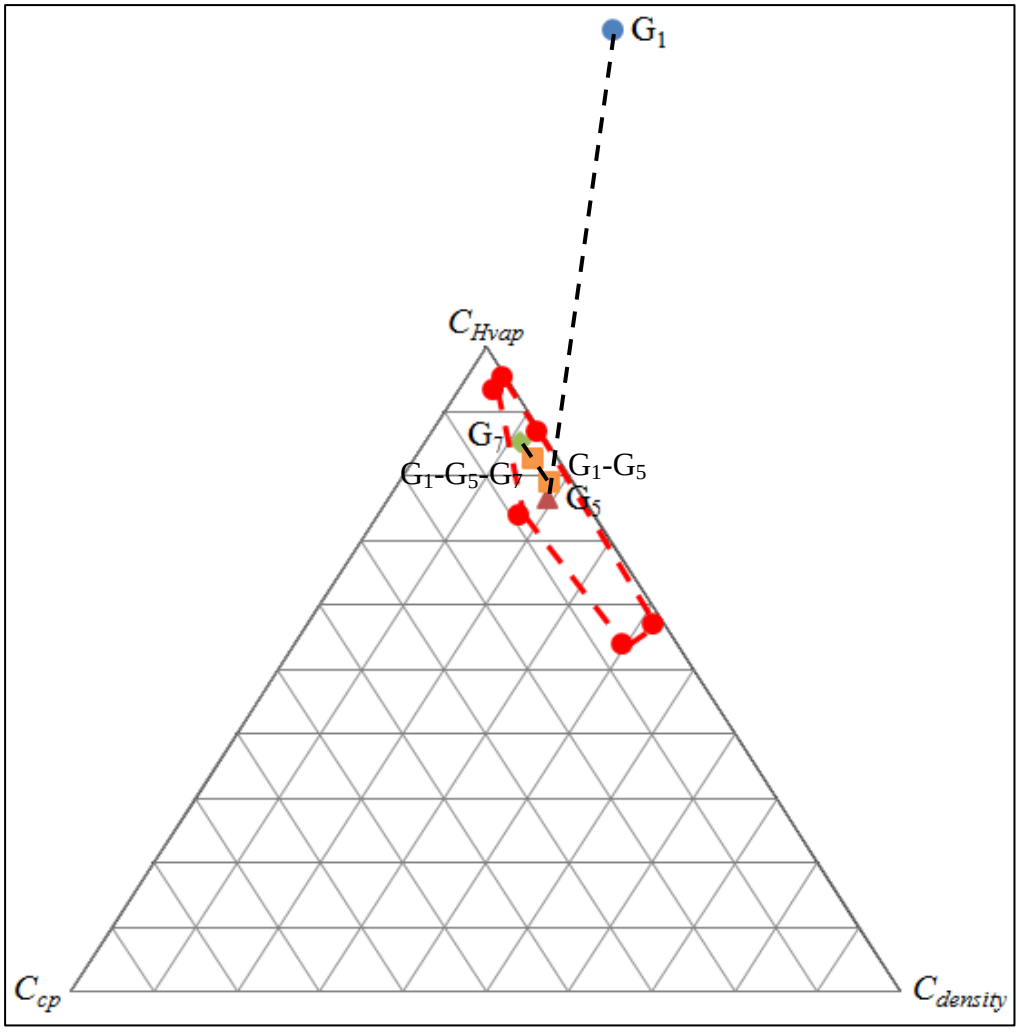


**Figure 4-6**: Synthesis path of [$C_1$MPyr][$NTf_2$]

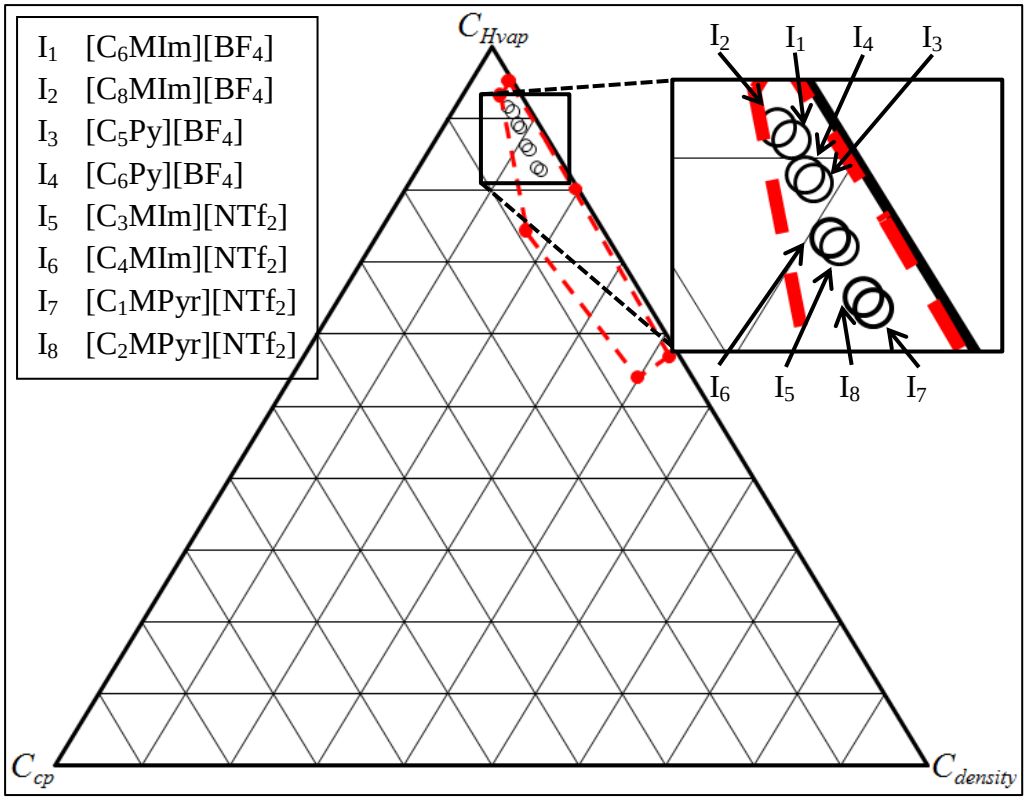


**Figure 4-7**: Ternary diagram representing IL design results

As shown in Table 4-8, the dominant and screening properties of these designed ILs are within the target property ranges. AUP values for all ILs are also in between the minimum and maximum AUP values (2.703 and 11.502) determined previously from six point bounding. Therefore, these ILs are valid solutions for this case study. According to results in Table 4-8, the combination of $[MIm]^+$ and $[NTf_2]^-$ has the highest $CO_2$ solubility, and the viscosity is relative low. This combination of properties is generally desired as $CO_2$ capturing solvent. The combination of $[MIm]^+$ and $[BF_4]^-$ has lower $CO_2$ solubility as compared to the former combination. This agrees with the work

by Ramdin et al. (2012), which showed that the $CO_2$ solubility in IL with $[NTf_2]^-$ anion is greater than that in IL with same cation but $[BF_4]^-$ anion. The results also show that $CO_2$ solubility of IL, with same cation and anion combination, increases when the alkyl chain attached to cation is longer, the same trend is observed for IL viscosity.

**Table 4-8**: IL design results

| Ionic Liquids | $\rho$ (g $cm^{-3}$) | $\Delta H_{vap}$ (kJ $mol^{-1}$) | $c_p$ (J $mol^{-1}$ $K^{-1}$) | $\mu$ (Pa.s) | $S$ (mol $CO_2$/mol IL) | AUP |
|---|---|---|---|---|---|---|
| $[C_6MIm][BF_4]$ | 1.132 | 155.4 | 450.3 | 0.045 | 0.095 | 8.545 |
| $[C_8MIm][BF_4]$ | 1.070 | 160.4 | 518.4 | 0.061 | 0.114 | 8.761 |
| $[C_5Py][BF_4]$ | 1.184 | 129.1 | 417.8 | 0.044 | 0.071 | 7.269 |
| $[C_6Py][BF_4]$ | 1.153 | 131.6 | 451.8 | 0.052 | 0.078 | 7.376 |
| $[C_3MIm][NTf_2]$ | 1.446 | 135.4 | 560.1 | 0.015 | 0.300 | 7.903 |
| $[C_4MIm][NTf_2]$ | 1.415 | 137.9 | 594.2 | 0.018 | 0.311 | 8.010 |
| $[C_1MPyr][NTf_2]$ | 1.467 | 106.6 | 480.2 | 0.015 | 0.084 | 6.452 |
| $[C_2MPyr][NTf_2]$ | 1.436 | 109.1 | 514.3 | 0.018 | 0.095 | 6.559 |

As demonstrated by this case study, this proposed approach can generate multiple solutions within the given set of property constraints. Of course, changing the lower and upper bound of constraints will produce different solutions as well. The choice of final solution will depend on the decision maker after the solutions are generated, to decide which IL suits the process best. If more considerations (i.e. economic and environmental aspects) or properties are to be included in IL design problem, a mathematical optimisation approach can be used to provide an optimal solution instead.

## 4.5 Summary

A systematic property based visual approach to design ionic liquid (IL) as carbon capture solvent has been presented in this chapter. The significance of this approach is that IL design problem can be solved visually on a ternary diagram. This can provide insights to the user when designing ILs as carbon capture solvents, and can be helpful to user without mathematical programming background. Besides, this approach is suitable when multiple target properties are considered in the design problem. The proposed approach is based on property clustering technique; group contribution (GC) method was included in the framework to solve molecular design problem. The IL design problem is translated into property perspective through property clustering technique and presented on a ternary diagram. On ternary diagram, each vertex represents one pure property cluster, and hence three dominant properties can be included in the diagram. Other properties can be considered as screening properties. For all properties considered during IL design, constraints should be included and final IL formulation must fulfil these constraints. A set of design and optimisation rules were developed to aid the design using this approach. An illustrative case study to design potential IL-based carbon capture solvent was solved to demonstrate this proposed approach. This approach was developed for pure IL design only. Designers can understand the design problem through visualisation using the developed approach, and identify potential IL-based carbon capture solvents. In order to determine the optimal IL solvent, a systematic mathematical approach is needed, and this is presented in Chapter 5.

# CHAPTER 5

# IONIC LIQUID DESIGN FOR ENHANCED CARBON DIOXIDE CAPTURE USING COMPUTER-AIDED MOLECULAR DESIGN APPROACH

## 5.1 Introduction

Previous chapter presents a visual approach to identify potential ionic liquids (ILs) as carbon capture solvent, which allows multiple properties consideration. In this chapter, a mathematical approach based on computer-aided molecular design (CAMD) technique is presented to design IL specifically for the purpose of carbon capture. The developed approach can be applied to design optimal IL as a substitution to conventional carbon capture solvent, based on target properties and constraints. In order to predict the properties of ILs, group contribution (GC) approach was employed in the presented approach. The structural constraints commonly used for organic solvent designs were included, as well as combination constraints of cations and anions. The approach developed in this chapter focused on design of IL based on a physical absorption mechanism, and hence no chemical reaction was involved. The presented approach was illustrated using a case study. Carbon dioxide ($CO_2$) solubility was included as a measure of performance of IL solvent, while density and viscosity of IL were taken into consideration as

constraints for the case study. Predicted properties of the potential candidates were compared to the literature data and both are in good agreement of experimentally measured properties.

## 5.2 Problem Statement

The main objective of the problem is to design an optimal molecular structure of an ionic liquid (IL) from a given set of pre-selected cation cores, anions, and organic functional groups, to replace conventional carbon capture solvent. The designed IL must satisfy target property and related constraints. The performance of designed IL will be evaluated based on the properties. A superstructure representation of the allowed combinations of all groups is shown in Figure 5-1, including organic groups, cation cores, and anions.

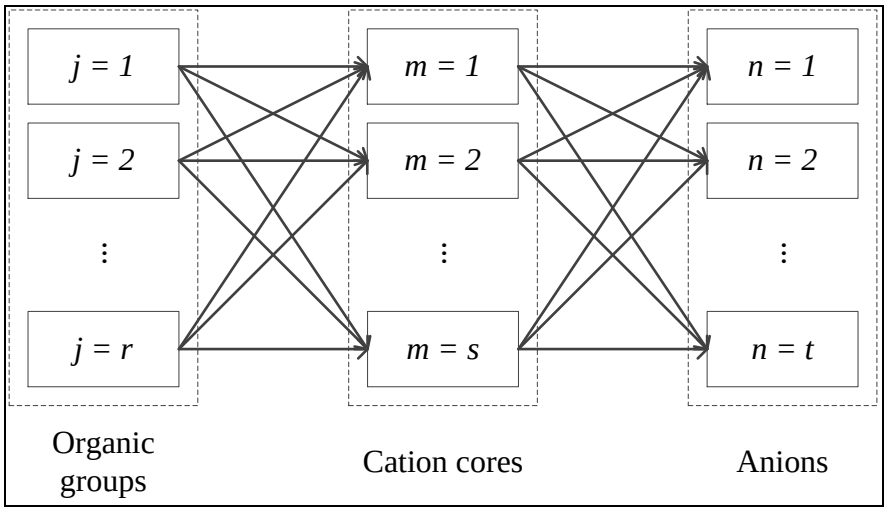


**Figure 5-1**: Schematic representation of combinations of all molecular fragments (replicated from Figure 4-1)

The specific problem to be addressed is stated as follows:

1) Design an IL that fulfils target properties and all constraints, based on the carbon capture performance, from the groups available in the superstructure. The carbon capture performance can be measured using carbon dioxide ($CO_2$) solubility of IL generally.
2) The superstructure comprises of *r* organic functional groups, *s* cation cores, and *t* anions, these groups are selected based on gas absorption and separation performance of IL beforehand (Baltus et al., 2004; Cadena et al., 2004). The choice of cation core and anion is limited to a maximum of one, i.e. only pure IL will be synthesised.
3) The selectivity of other gases over $CO_2$ is assumed to be negligible, only $CO_2$ will be absorbed by selected IL. Also, the IL is chosen based on physical absorption mechanism using the approach, no reaction is involved between $CO_2$ and IL.

## 5.3 Optimisation Model

A generic formulation to design ionic liquid (IL) solvent for carbon capture purpose is presented in this section. Firstly, the design objective and target performance of IL solvent should be identified and expressed in terms of measurable properties. These properties are estimated using reliable group contribution (GC) prediction models, which are based on molecular structure information. Structural constraints must be satisfied as well to make sure that only structurally feasible ILs will be formed from a collection of descriptors,

groups or building blocks. The formulation can be solved to determine the optimal IL solvent which can fulfils all target properties and constraints. Figure 5-2 shows the procedure of solving IL design and followed by detailed explanation of each step.

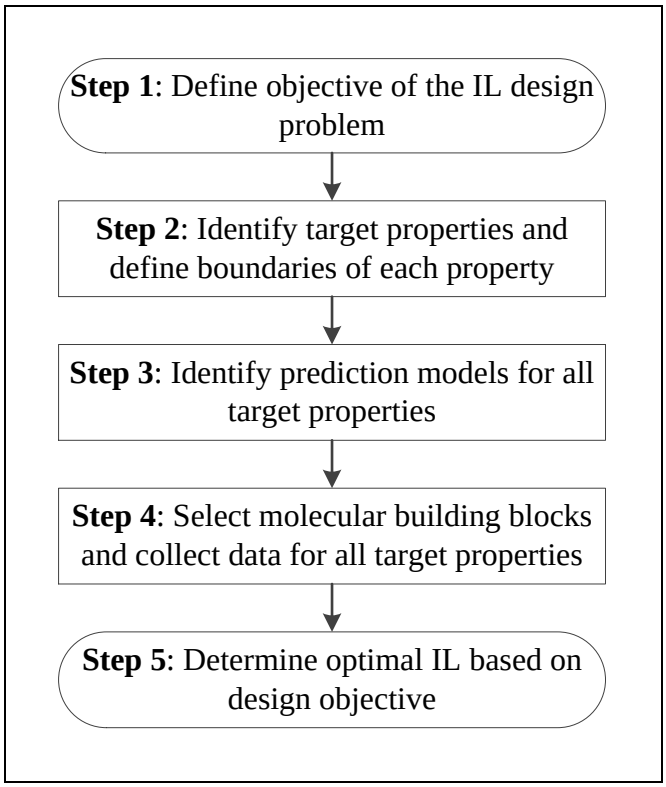


**Figure 5-2**: Systematic approach to design IL for carbon capture system

Step 1: The objective of the design problem must be determined first, by identifying the target property that is most concerned in the design problem. The design objective covers the thermophysical properties that can affect functionality of designed IL, or environmental and

economical performance of IL in carbon capture process. The optimisation objective can be written in general as Equation (4.1).

$$\text{maximise } f \tag{5.1}$$

where $f$ is the objective of design problem. The objective shown in Equation (5.1) is targeted to be max, however maximising or minimising the objective is dependent on the main concern in the process.

Step 2: All target properties for this IL design problem should be determined, and their upper and lower limits will be kept as constraints in solving the design problem. These properties can be expressed as Equation (5.2), where $\tau_d$ is the $d^{\text{th}}$ property, $\tau_d^{\min}$ and $\tau_d^{\max}$ are the lower and upper bound of the target properties.

$$\tau_d^{\min} \leq \tau_d \leq \tau_d^{\max} \tag{5.2}$$

Step 3: Appropriate prediction models are chosen to estimate the target properties of pure IL, for all target properties listed in Step 2. Properties of pure IL are estimated using GC models, which are based on molecular structure information.

Step 4: Suitable molecular building blocks for IL design problem should be identified in this step. The molecular building blocks include organic groups, cations, and anions, to form a complete IL, which are slightly different from design problem for organic compounds. These

building blocks are selected such that designed IL possesses similar properties as the conventional products for the designated application, since the IL is designed to replace conventional carbon capture solvent. Data of all target properties for all chosen molecular building blocks should be collected, which is used to estimate properties of the IL combined using these building blocks.

Step 5: In this step, an optimum IL that can fulfil all target properties is designed based on the design objective. As stated in the problem statement, the selectivity of other gases over $CO_2$ was not considered in this work, i.e. only $CO_2$ will be absorbed by the selected IL. Also, the operating conditions were fixed in this design problem, and hence the effect of operating conditions was not studied. Liquid and gas phases are both involved in carbon capture process, hence equilibrium relationships were considered and it can be described using Equation (5.3).

$$y_i P \varphi_i \left(T, P, y_i\right) = x_i \gamma_i P_i^{\mathrm{S}} \tag{5.3}$$

where $x_i$ and $y_i$ are the mole fractions of component $i$ in liquid and gas phases respectively, $P_i^S$ is the saturated vapour pressure of component $i$, and $\varphi_i(T,P,y_i)$ is the gas-phase fugacity coefficient. Activity coefficient was estimated using UNIFAC model as shown in Equation (5.4), and its details are given in Appendix Section A.2.1.

$$\ln \gamma_i = \ln \gamma_i^{C} + \ln \gamma_i^{R} \qquad \forall i \tag{5.4}$$

As discussed in Section 4.4.2, group parameters and binary interaction parameters of IL for UNIFAC model presented by Lei et al. (2013) have been used to predict activity coefficient. The gas-phase fugacity coefficient was determined using equation of state proposed by Span and Wagner (1996), which is further explained in Appendix Section A.2.2. The saturated vapour pressure of $CO_2$ was calculated using extrapolated Antoine equation proposed by Shiflett and Yokozeki (2006) as presented in Section 4.4.2. The saturated vapour pressure of IL was assumed to be negligible due to its extremely low vapour pressure. For the same reason, IL is assumed to be absent in vapour phase (i.e. $y_{IL} = 0$). To ensure the designed IL is valid solution, some constraints are included. Summation of mole fractions for both phases is included as constraints, as shown in Equations (5.5) and (5.6).

$$\sum_i y_i = 1 \tag{5.5}$$

$$\sum_i x_i = 1 \tag{5.6}$$

Structural constraints for IL design are also included, as given in Equations (5.7) to (5.8). As defined in Equation (5.7), the molecular structure of designed IL must consist of at least two building blocks. The final structure must not have any free bond, as described in

Equation (5.8). In these equations, $v_k$ is the number of group $k$ and $n_k$ is the available free bond of group $k$.

$$\sum_k v_k \geq 2 \tag{5.7}$$

$$\sum_k n_k v_k - 2\left(\sum_k n_k - 1\right) = 0 \tag{5.8}$$

As presented in Section 5.2, only pure IL can be formed, which means one cation and one anion can be chosen. Therefore, Equations (5.9) and (5.10) are added to enforce only a pair of cation and anion will occur, where $\alpha_m$ and $\beta_n$ are the binary variables representing each cation $m$ and each anion $n$, respectively.

$$\sum_m \alpha_m = 1 \tag{5.9}$$

$$\sum_n \beta_n = 1 \tag{5.10}$$

## 5.4 Case Study

To illustrate the proposed approach, a case study is presented in this section. A post-combustion carbon capture system is currently using monoethanolamine (MEA) solvent, and it is desired to replace the carbon capture solvent with ionic liquid (IL) solvent. An IL solvent is to be designed using the presented approach. The system temperature, $T$ and pressure, $P$ are

set at 323.2 K and 0.7 Mpa, which are the operating conditions for current amine scrubbing process (Yu et al. 2012).

$$T = 323.2 \tag{5.11}$$

$$P = 0.7 \tag{5.12}$$

### 5.4.1 Step 1: Define objective of the IL design problem

First and foremost, the design objective for this design problem was identified. Since IL is designed carbon capture purpose, carbon dioxide ($CO_2$) solubility of IL, $S$ is the main concern and hence it is set as the design objective. The $CO_2$ solubility of IL should be maximised for best carbon capture performance. This can be translated into Equation (5.13).

$$\max \quad S \tag{5.13}$$

### 5.4.2 Step 2: Identify target properties and define boundaries of each property

Two target properties were considered in this case study, density ($\rho$) and viscosity ($\mu$) of IL. Density is a basic transport property, and it is required to determine viscosity too. Viscosity of solvent affects the pumping power required to circulate the solvent within the system, and ultimately the operating cost (Kuhlmann et al., 2007). The target range of each property is given in Table 5-1. These target ranges were set according to properties of

conventional carbon capture solvent (The Dow Chemical Company, 2003). Viscosity of IL solvent should be as low as possible to ensure pumping power required is at minimum, and therefore set to be lower than 0.1 Pa.s. Generally, viscosities of ILs range between 0.01 to 100 Pa.s; while organic solvents have viscosities of about 0.0002 to 0.01 Pa.s only (Bonhôte et al. 1996).

**Table 5-1**: Target property ranges to design IL solvent

| Property | Lower bound | Upper bound |
|---|---|---|
| Density, $\rho$ (g cm$^{-3}$) | 1.0 | 2.0 |
| Viscosity, $\mu$ (Pa.s) | 0 | 0.1 |

### 5.4.3 Step 3: Identify prediction models for all target properties

Reliable prediction models were selected in this step, to predict the properties of IL. Equations (5.14) to (5.18) are models to predict density (Gardas and Coutinho, 2008a) and viscosity of IL (Gardas and Coutinho, 2008b). $CO_2$ solubility of IL in terms of mole $CO_2$ per mole IL was determined using Equation (5.19) after the mole fraction of $CO_2$ in liquid phase at equilibrium was obtained.

$$\rho = \frac{M}{NV\left(a + bT + cP\right)} \tag{5.14}$$

$$V = \sum_k v_k V_k \tag{5.15}$$

$$\ln\frac{1000\mu}{\rho M} = A_{\mu} + \frac{B_{\mu}}{T} \tag{5.16}$$

$$A_{\mu} = \sum_{k} \nu_k A_{\mu,k} \tag{5.17}$$

$$B_{\mu} = \sum_{k} \nu_k B_{\mu,k} \tag{5.18}$$

$$S = x_{CO_2} / x_{IL} \tag{5.19}$$

where $\rho$ is IL density in g cm$^{-3}$, $M$ is IL molecular weight in g mol$^{-1}$, $N$ is the Avogadro constant (given as 0.6022), $V$ is the molecular volume of IL in Å$^3$, $T$ is the system temperature K, $P$ is the system pressure in MPa, the coefficients $a$, $b$ and $c$ were estimated as 0.8005, 6.652 × 10$^{-4}$ K$^{-1}$ and -5.919 × 10$^{-4}$ MPa$^{-1}$ respectively. Equation (5.15) shows that molecular volume of IL is equivalent to the sum of molecular volume of each group $k$ ($V_k$) that occurs in the structure. In Equation (5.16), $\mu$ is IL viscosity in Pa.s, $A_{\mu,k}$ and $B_{\mu,k}$ in Equations (5.17) and (5.18) are contributions of group $k$ to parameters $A_{\mu}$ and $B_{\mu}$.

### 5.4.4 Step 4: Select molecular building blocks and collect data for all target properties

Molecular building blocks for this case study were selected in this step and shown in Table 5-2. These building blocks were chosen because they are among the most widely studied cations and anions (Zhou et al., 2009). Data of all the selected molecular building blocks for chosen property prediction

models were also collected and presented in Table 5-3, together with the free bond number of each building blocks. Table 5-4 and Table 5-5 show necessary data for UNIFAC model calculation taken from da Silva and Barbosa (2004) and Lei et al. (2009).

**Table 5-2**: Organic function groups, cation cores, and anions considered in this case study

| Type | $k$ | Groups | Type | $k$ | Groups |
|---|---|---|---|---|---|
| Organic groups | 1 | $CH_3$ | Anions | 5 | $[BF_4]$- |
| | 2 | $CH_2$ | | 6 | $[PF_6]$- |
| Cation cores | 3 | [Mim]+ | | 7 | [Cl]- |
| | 4 | [Im]+ | | | |

**Table 5-3**: Free bond number, molecular weights, and data for target properties of all molecular building blocks

| Building blocks | $k$ | $n_k$ | Molecular weight (g $mol^{-1}$) | $V_k$ | $A_{k,\mu}$ | $B_{k,\mu}$ |
|---|---|---|---|---|---|---|
| $CH_3$ | 1 | 1 | 15.03 | 35 | -0.74 | 250.0 |
| $CH_2$ | 2 | 2 | 14.03 | 28 | -0.63 | 250.4 |
| $[Mim]^+$ | 3 | 1 | 82.10 | 119 | 7.30 | 1507.1 |
| $[Im]^+$ | 4 | 2 | 67.07 | 79 | 8.04 | 1257.1 |
| $[BF_4]^-$ | 5 | 0 | 86.80 | 73 | -18.08 | 1192.4 |
| $[PF_6]^-$ | 6 | 0 | 144.96 | 107 | -20.49 | 2099.8 |
| $[Cl]^-$ | 7 | 0 | 35.45 | 47 | -27.63 | 5457.7 |

**Table 5-4**: Group parameters of volume $R_k$ and surface area $Q_k$ in UNIFAC model

| *m* | Main group | Subgroup | $R_k$ | $Q_k$ |
|---|---|---|---|---|
| 1 | $CH_2$ | $CH_3$ | 0.9011 | 0.8480 |
| | | $CH_2$ | 0.6744 | 0.5400 |
| 2 | $CO_2$ | $CO_2$ | 1.2960 | 1.2610 |
| 3 | [Mim][$BF_4$] | [Mim][$BF_4$] | 6.5669 | 4.0050 |
| 4 | [Mim][$PF_6$] | [Mim][$PF_6$] | 7.6909 | 4.6930 |
| 5 | [Mim][Cl] | [Mim][Cl] | 5.7073 | 4.9741 |

**Table 5-5**: Group binary interaction parameters between group *m* and *n* for the UNIFAC model

| *m* | *n* | $a_{mn}$ | $a_{nm}$ |
|---|---|---|---|
| 1 | 2 | 28.05 | 672.80 |
| | 3 | 1180.51 | 588.74 |
| | 4 | 692.26 | 401.54 |
| | 5 | 2093.97 | 1129.01 |
| 2 | 3 | -14.44 | 430.80 |
| | 4 | -66.74 | 460.25 |
| | 5 | 2693.80 | -67.35 |

### 5.4.5 Step 5: Determine optimal IL based on design objective

With the collected data and property prediction models, the design problem can be solved using presented approach. The formulation entails this design problem as a mixed integer non-linear programming (MINLP) model, as shown below.

$$\max S_g = x_{CO_2} / x_{IL} \tag{5.20}$$

$$\rho = \frac{M}{0.6022(1.0151)\sum_{k=1}^{7} v_k V_k} \tag{5.21}$$

$$\mu = \frac{\rho M}{1000} \exp\left( \sum_{k=1}^{7} v_k A_{k,\mu} + \frac{\sum_{k=1}^{7} v_k B_{k,\mu}}{323.2} \right) \leq 0.1 \tag{5.22}$$

$$x_{CO_2} = \frac{0.7 y_1 \varphi_1(T, P, y_1)}{\gamma_1 P_1^S} \tag{5.23}$$

$$\ln \gamma_i = \ln \gamma_i^{\,C} + \ln \gamma_i^{\,R} \qquad \forall i \tag{5.24}$$

$$\sum_i y_i = 1 \tag{5.25}$$

$$\sum_i x_i = 1 \tag{5.26}$$

$$\sum_{k=1}^{7} v_k \geq 2 \tag{5.27}$$

$$\sum_{k=1}^{7} n_k v_k - 2\left( \sum_{k=1}^{7} n_k - 1 \right) = 0 \tag{5.28}$$

$$\sum_{m=3}^{4} \alpha_m = 1; \quad \sum_{n=5}^{7} \beta_n = 1 \tag{5.29}$$

Equation (5.20) is the objective function for this formulation, Equations (5.21) to (5.24) are the property prediction models for targeted properties, and the rest are structural constraints. The optimal IL obtained for

this case study is $[C_{10}Mim][BF_4]$, namely 1-decyl-3-methylimidazolium tetrafluoroborate. It has a predicted solubility of 0.1320 mol $CO_2$/mol IL at 328.2 K and 0.7 MPa; while its viscosity is predicted to be 0.08627 Pa.s, which is less than the 0.1 Pa.s as defined in Equation (5.22). This IL is able to remove the highest amount of $CO_2$ among all the possible combinations of cations and anions, and still fulfils all the given specifications. However, there is no solubility data for this IL in literature, and hence no comparison can be conducted at this time.

After the first optimal structure of IL was obtained, integer cut are applied to obtain other potential solutions. Nine alternative ILs were determined by doing integer cuts, and the results are shown in Table 5-6. According to the results, ILs with $[BF_4]^-$ anion are more preferable as carbon capture solvents following the constraints set previously. Comparing ILs with $[BF_4]^-$ and $[PF_6]^-$ anions, the $CO_2$ solubility is generally higher in ILs with $[PF_6]^-$ anion, but the viscosity is higher as well. ILs with $[PF_6]^-$ anion can be used as $CO_2$ capturing solvent, only if there is no viscosity constraint. There is no ILs with $[Cl]^-$ anion chosen as potential solvent, this is probably because the $CO_2$ solubility is too low. This is supported by work done by Palomar et al. (2011), which concluded that fluorinated entities in the anion improves $CO_2$ solubility of ILs. IL solvents do not contribute to emissions of harmful compounds due to their extremely low vapour pressure, and hence they are environmental friendly and safe for human health. These ILs are designed for

physical absorption of $CO_2$, the regeneration energy will be low as there is no chemical reaction involved between $CO_2$ and ILs (Ramdin et al. 2012).

The results also show that $CO_2$ absorbed by IL increases with increasing number of carbon in alkyl chain attached to cation, the same trend was observed for IL viscosity. This agrees with a literature study done on solubility of $CO_2$ in a series of imidazolium-based ILs (Baltus et al., 2004). Comparison between predicted values and experimental data were done according to Equation (5.30) and shown in Figure 5-3. The relative deviations of $CO_2$ solubility between both values are shown in Table 5-6.

$$\text{Relative Deviation} = \frac{\left|\text{Experimental data} - \text{Predictedvalue}\right|}{\text{Experimental data}} \times 100 \qquad (5.30)$$

From these comparisons, it can be seen that the relative deviations of results are generally less than 10 %. This difference is mainly due to minor errors present in the chosen property prediction models. From the results, it can be said that the results obtained by solving this model corresponds to the best ILs that one could find from these combinations of anions and cations. This also shows that the proposed approach is able to design optimal IL for $CO_2$ absorption, according to the required specifications or performance targets.

**Table 5-6**: Optimal IL molecular design results

| IL chosen | Predicted solubility, $S$ | Predicted viscosity, $\mu$ (Pa.s) | Experimental solubility | Relative deviation, RD (%) | Reference |
|---|---|---|---|---|---|
| $[C_{10}Mim][BF_4]$ | 0.1320 | 0.08627 | - | - | - |
| $[C_9Mim][BF_4]$ | 0.1231 | 0.07312 | - | - | - |
| $[C_8Mim][BF_4]$ | 0.1141 | 0.06193 | 0.1117 | 2.15 | (Gutkowski et al., 2006) |
| $[C_7Mim][BF_4]$ | 0.1049 | 0.05243 | - | - | - |
| $[C_6Mim][PF_6]$ | 0.0978 | 0.08747 | 0.1086 | 9.97 | (Shariati and Peters, 2004) |
| $[C_6Mim][BF_4]$ | 0.0954 | 0.04436 | - | - | - |
| $[C_5Mim][PF_6]$ | 0.0882 | 0.07509 | - | - | - |
| $[C_5Mim][BF_4]$ | 0.0868 | 0.03753 | - | - | - |
| $[C_4Mim][PF_6]$ | 0.0784 | 0.06454 | 0.0858 | 8.62 | (Shiflett and Yokozeki, 2005) |
| $[C_4Mim][BF_4]$ | 0.0758 | 0.03175 | 0.0778 | 2.57 | (Anthony et al., 2005) |

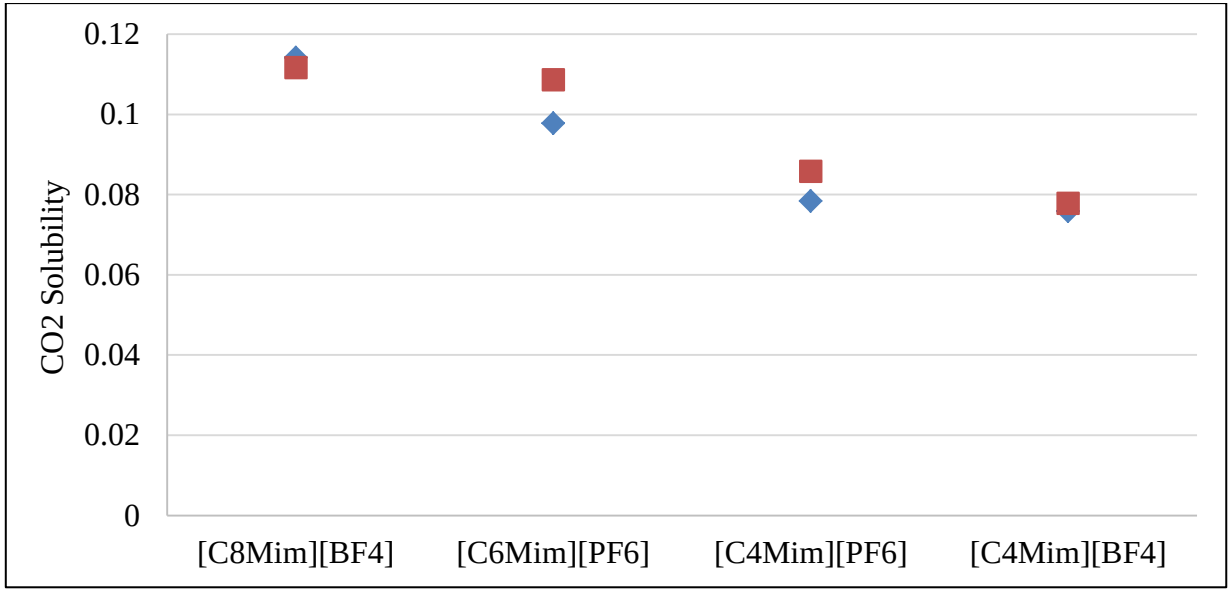


**Figure 5-3**: $CO_2$ solubility of ILs in terms of mole fraction. (♦) Predicted results; (■) Experimental results from literature, $[C_8MIm][BF_4]$ (Gutkowski et al. 2006), $[C_6MIm][PF_6]$ (Shariati and Peters, 2004), $[C_4MIm][PF_6]$ (Shiflett and Yokozeki, 2005), $[C_4MIm][BF_4]$ (Anthony et al. 2005)

However, the proposed approach is highly dependent on the property predictive models that are used to estimate the properties of ILs. According to Coutinho et al.(2012), most properties of ILs have very little data and models even with their importance in common chemical product and process application. Also, the reliability of property predictive models is limited by the number of available ILs. Currently, only $10^3$ out of $10^6$ pure ILs have been synthesised and half of these are commercially available (Coutinho et al. 2012). Another limitation that should be noted is, this formulation utilises GC property predictive models, and thus the design of ILs is confirmed to the list of available group contribution data for cation and anion groups. The current process conditions are fixed and hence the impact on varying it is not taken into consideration in the proposed approach. Process conditions will affect the thermophysical properties of IL, this in turn affect the performance of IL in capturing $CO_2$. The inclusion of the process parameters in an optimisation formulation will be investigated in the future. This will call for simultaneous process and IL molecular design.

## 5.5 Summary

A systematic approach is presented to design optimal pure ionic liquid (IL) solvent specifically for carbon dioxide ($CO_2$) absorption in this chapter. Computer-aided molecular design (CAMD) approach was adapted in this presented approach. The developed approach designs IL-based carbon capture solvent based on a specific design objective, and fulfil all relevant properties.

The valence and octet rules were introduced as constraints to make sure the designed ILs are realistic and feasible for industrial applications. Besides, cation-anion pairing constraint was added in this work to ensure that only one cation and one anion can be chosen in the final molecular structure. An illustrative case study was presented to demonstrate the developed approach. The solubility of $CO_2$ in ILs was set as the design objective in this case study, which should be maximised; while density and viscosity of IL were included as target properties in the case study. As shown by the case study, a mixed integer non-linear programming (MINLP) model was formulated to determine the optimal IL, which is able to absorb the highest amount of $CO_2$. The selectivity of $CO_2$ over other gases was not taken into consideration in this approach. The developed approaches in Chapters 4 and 5 are specifically for pure IL design only, but IL mixtures are required sometimes for economical and performance reason. Therefore, an approach should be developed for pure IL and IL mixture design, which is presented in Chapter 6.

# CHAPTER 6

# A PROPERTY-BASED VISUAL APPROACH TO DESIGN IONIC LIQUID AND IONIC LIQUID MIXTURE AS CARBON CAPTURE SOLVENT

## 6.1 Introduction

In the previous chapters, mathematical approach and visual approach have been developed to design pure ionic liquid (IL) to capture carbon dioxide ($CO_2$). Pure ILs that are specifically designed to capture $CO_2$ can have high $CO_2$ absorption rate and capacity, but studies showed that these ILs are generally more viscous and expensive. Therefore, pure IL solvents may be impractical when economic consideration is a major concern. Instead, a mixture of task specific IL and conventional IL can be combined to improve the overall performance of $CO_2$ solvent and carbon capture process. Given there are many possible IL mixtures, a systematic approach will be helpful to determine the potential mixtures prior to experimental testing. Extended from approach presented in Chapter 4, a property based visual approach to design IL and IL mixture as carbon capture solvent is presented in this chapter. Similar to approach in Chapter 4, the visualisation of problem and solutions is achieved by applying property clustering technique in this proposed methodology, to map the design problem from property domain into cluster

domain. This approach can consider multiple target properties to design potential ILs and IL mixtures. To date, the study of properties of pure ILs and IL mixtures is still in the infant phase, and these data is still scarce. Hence, some of the prediction models do not cover all available ILs. To overcome this problem, the proposed approach is developed to adapt property data of pure ILs directly, together with existing property prediction models to predict the properties of the designed IL mixtures. This methodology provides a property based platform to visualise the overall performance of designed IL mixtures using ternary diagram. An illustrative case study, was solved to demonstrate the proposed approach.

## 6.2 Problem Statement

The problem to be addressed in this chapter is stated as follows: Design potential ionic liquids (ILs) or IL mixtures that are able to replace conventional carbon capture solvents, using the molecular building blocks and available ILs in the superstructure. The designed ILs or IL mixtures must fulfil target property constraints and design rules. The performance of designed IL-based solvents will be evaluated based on the properties (or functionalities like cost and environmental impact), which are used to represent or describe the characteristics or attributes that are not measurable. Figure 6-1 shows the superstructure representation of allowed combinations of all molecular groups (including organic groups, cation cores, and anions) and IL constituents.

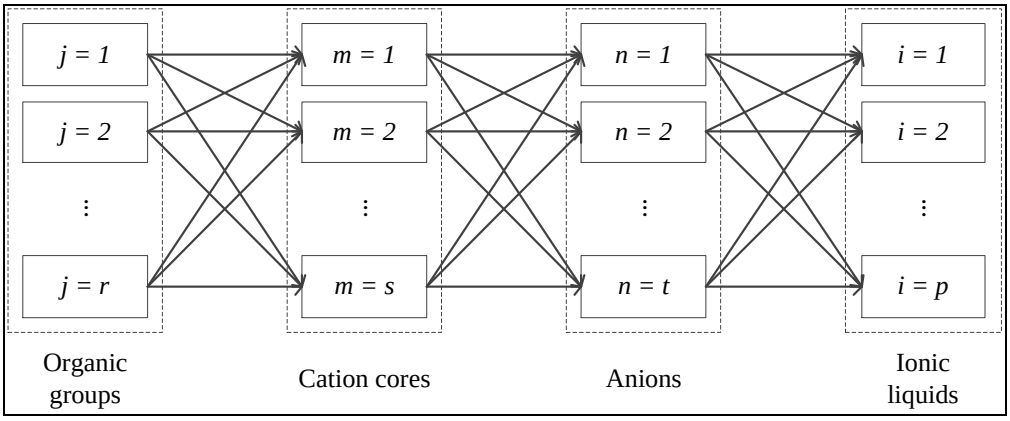


**Figure 6-1**: Schematic representation of combinations of all molecular building blocks and IL constituents

## 6.3 Graphical Tool for Pure Ionic Liquid and Ionic Liquid Mixture Design

Since this approach is an extension of the approach proposed in Chapter 4, property clustering technique was applied in here to represent and track physical properties (Shelley and El-Halwagi, 2000). Similarly, the visualisation tool also takes the form of a ternary diagram, to provide useful insights to user and assist in solving the design problem. As mentioned in Section 4.3, only three dominant properties or functionalities can be considered in ternary diagram, properties that are not presented in ternary diagram remain as screening properties. Note that the ternary diagrams for pure ionic liquid (IL) and IL mixture design are different; they will be solved on different diagrams. Figure 6-2 shows the procedure of solving pure IL and IL mixture design, and it is followed by detailed description of each step.

Step 1: All necessary target properties or functionalities (including cost, environmental impact and etc.) for an IL and mixture design problem should be identified. The upper and lower limits for these properties will be kept as targets in solving the design problem. These properties can be expressed as Equation (6.1), where $\tau_d$ is the $d^{th}$ property, $\tau_d^{min}$ and $\tau_d^{max}$ are the lower and upper bound of these properties.

$$\tau_d^{min} \leq \tau_d \leq \tau_d^{max} \tag{6.1}$$

If there are more than three target properties, three dominant properties should be chosen, and keep the rest as screening properties.

Step 2: For all properties (dominant and screening) considered, appropriate prediction models that estimate the target properties of pure ILs and IL mixtures should be identified. Prediction models for pure ILs and IL mixtures are generally different. Properties of pure ILs are estimated using molecular building blocks while properties of IL mixtures are estimated from pure IL constituents. Hence, two sets of property prediction models should be chosen, one to estimate properties of pure ILs and another for IL mixtures. When this step is done, user can proceed to pure IL design, and followed by IL mixture design afterwards.

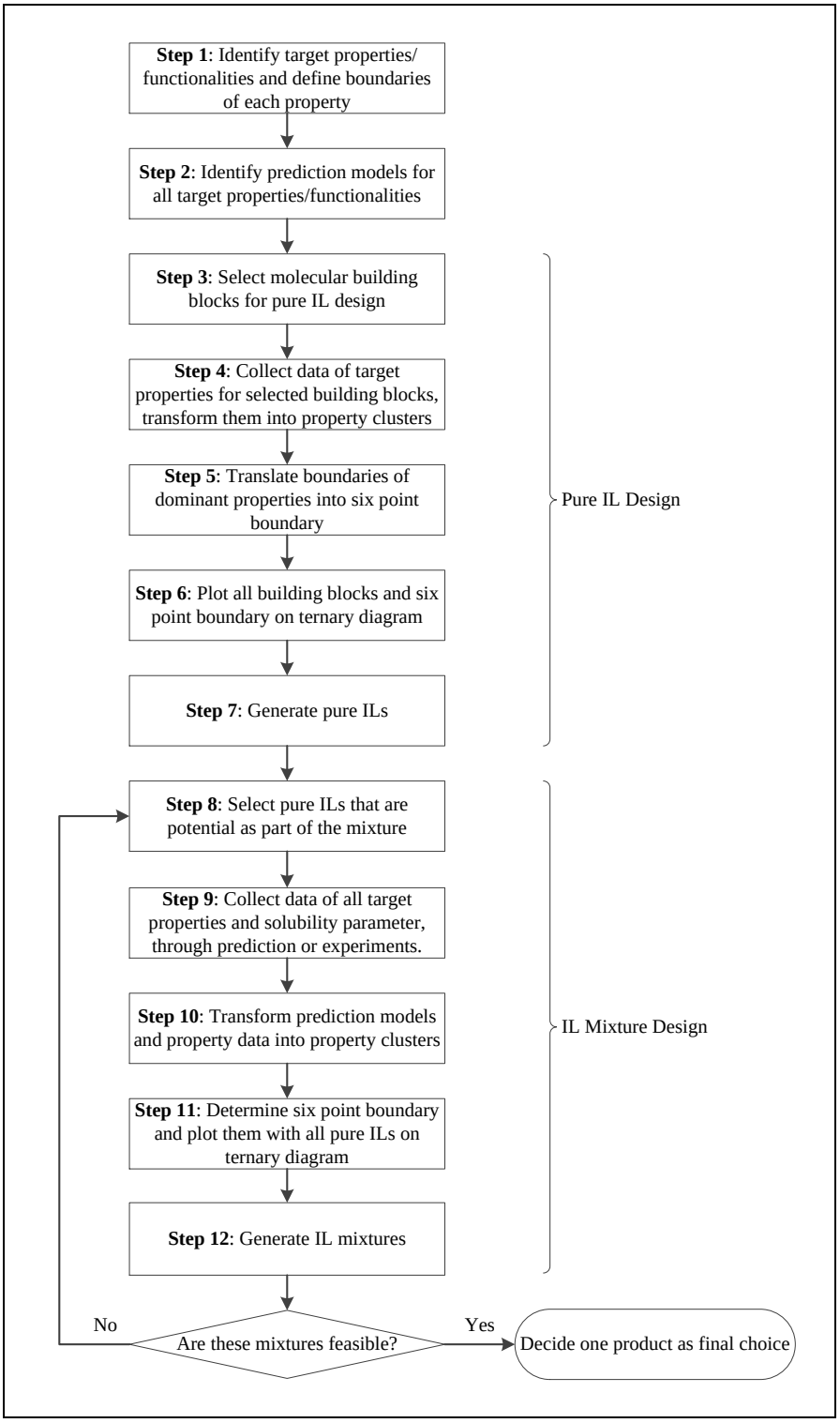


**Figure 6-2**: Procedure to solve IL and IL mixture design problem using property-based visual approach

Step 3: Suitable molecular building blocks for pure IL design should be identified in this step. Different from common product design problem, these molecular building blocks include organic groups, cations, and anions to form a complete IL. The molecular building blocks should be selected such that the properties of the designed ILs are similar to the conventional carbon capture solvent. It is assumed that the newly designed ILs will possess properties or functionalities similar to that of conventional solvent.

Step 4: Data of all target properties and functionalities for all chosen molecular building blocks should be collected. Once these data for all target properties are gathered, data can be translated into molecular property clusters following Equations (6.2) to (6.5).

$$\psi_d\left(\tau_{di}\right)=\sum_{k=1}^{q} v_k \psi_d\left(\tau_{dk}\right) \tag{6.2}$$

$$\Omega_{dk}=\frac{\psi_d\left(\tau_{dk}\right)}{\psi_d^{ref}\left(\tau_d\right)} \tag{6.3}$$

$$AUP_k=\sum_{d=1}^{N_P}\Omega_{dk} \tag{6.4}$$

$$C_{dk}=\frac{\Omega_{dk}}{AUP_k} \tag{6.5}$$

$\psi_d(\tau_{di})$ is the property operator of $d^{\text{th}}$ property of component $i$, $v_k$ is the number of group $k$, $q$ is the total number of building blocks, while

$\psi_d(\tau_{dk})$ is the molecular property operator of $d^{\text{th}}$ property of functional group $k$, $\psi_d^{ref}(\tau_d)$ is a reference value for $d^{\text{th}}$ property, $\Omega_{dk}$ is normalised molecular property operator for $d^{th}$ property of group $k$, $AUP_k$ is augmented property index (AUP) for group $k$, $C_{dk}$ is molecular property cluster for property $d$ of group $k$. Property cluster is defined as the ratio of normalised property operator to AUP. Summation of all cluster values for group $k$ must equal to one.

Step 5: For the properties and functionalities included in ternary diagram, the constraints can be represented as a feasibility region defined by six unique points (El-Halwagi et al., 2004). These six points are characterised by the following values of normalised operators.

$$\left(\Omega_1^{\min},\Omega_2^{\min},\Omega_3^{\max}\right)\left(\Omega_1^{\min},\Omega_2^{\max},\Omega_3^{\max}\right)\left(\Omega_1^{\min},\Omega_2^{\max},\Omega_3^{\min}\right)$$
$$\left(\Omega_1^{\max},\Omega_2^{\max},\Omega_3^{\min}\right)\left(\Omega_1^{\max},\Omega_2^{\min},\Omega_3^{\min}\right)\left(\Omega_1^{\max},\Omega_2^{\min},\Omega_3^{\max}\right)$$

This boundary tells the area where the solutions should fall within. Any solution fall out of the boundary will be infeasible.

Step 6: Pure IL design problem can now be visualised on a ternary diagram using obtained molecular property cluster values and six point boundary determined in Step 5.

Step 7: A list of possible pure ILs can be determined now using plotted ternary diagram in Step 6. Rules I1 to I4 (I stands for pure IL) for pure IL design must be followed to ensure designed ILs are feasible structure and valid solutions. Properties and functionalities of

designed ILs must be calculated and checked whether they fall within the target ranges.

Rule I1: When two molecular building blocks, $K_1$ and $K_2$ (any organic groups, cation or anions) are added linearly on the diagram, the AUP values and distance between them provide information of $K_1$- $K_2$ combination using lever arm rule.

Rule I2: The molecular structure of final formulation must consist of at least two building blocks; this is given by the constraint in Equation (6.6). Besides, Equation (6.7) indicates that final IL molecular structure must not have any free bond. In Equation (6.7), $n_k$ is the available free bond of functional group *k*. Both equations are common structural constraints for organic components design problem, they are now applied in pure IL design here.

$$\sum_k v_k \geq 2 \tag{6.6}$$

$$\sum_k v_k n_k - 2\left(\sum_k n_k - 1\right) = 0 \tag{6.7}$$

Rule I3: In pure IL design, only one cation core and one anion group can be chosen.

Rule I4: The cluster value of the designed IL must be within the feasibility region, and the AUP value of the designed IL must be within the range of target AUP. This target AUP range is determined from the six property constraints on ternary diagram. AUP values of all molecular building blocks must be positive.

Step 8: After pure ILs are designed, user can proceed to IL mixture design stage. Previously identified ILs will be used as part of the design, other potential ILs can also be included. For example, if there are few newly tested ILs that show great potential as part of the IL mixture design, it can be included in this step. These pure ILs can be selected based on their properties or functionalities, by comparing with existing products.

Step 9: Once all potential pure ILs are selected, data of all target properties and functionalities for these ILs should be collected. This can be done through prediction models or experiments. The experimental data comes into application in this step, where they can be included directly into consideration to predict the properties of designed IL mixtures. This is useful when the available data for prediction models does not cover wide range of ILs. By adapting experimental data into this approach, it is more flexible as more ILs can be considered in mixture design problem using the approach. Apart

from target properties and functionalities, solubility parameter of all selected ILs should be identified at this stage, to predict whether ILs will form miscible solution. In order for a mixture to be miscible, the constituents of the mixture must have similar solubility parameters. The solubility parameter can be determined through prediction models or experiments. In this work, a group contribution model (Kulajanpeng et al., 2014) have been used to estimate the solubility parameter of short listed pure IL candidates.

Step 10: Data collected in Step 9 is translated into property clusters using Equations (6.8) to (6.11), this includes data collected through experiments.

$$\psi_d(\tau_d)_M = \sum_{i=1}^{p} x_i \psi_d(\tau_{di}) \tag{6.8}$$

$$\Omega_{di} = \frac{\psi_d(\tau_{di})}{\psi_d^{ref}(\tau_d)} \tag{6.9}$$

$$AUP_i = \sum_{i=1}^{p} \Omega_{di} \tag{6.10}$$

$$C_{di} = \frac{\Omega_{di}}{AUP_i} \tag{6.11}$$

$\psi_d(\tau_d)_M$ is the property operator of $d^{\text{th}}$ property of mixture $M$, $x_i$ is the mole fraction of IL component $i$, $p$ is the total number of components, while $\psi_d(\tau_{di})$ is the property operator of $d^{\text{th}}$ property of

IL component *i*, $\psi_d^{ref}(\tau_d)$ is a chosen reference value, $\Omega_{di}$ is normalised property operator for $d^{th}$ property of IL component *i*, $AUP_i$ is AUP for component *i*, $C_{di}$ is property cluster for property *d* of component *i*. The summation of all cluster values for IL component *i* is equal to unity. Note that these equations are different from Equations (6.2) to (6.5) are meant for molecular building blocks; while Equations (6.8) to (6.11) are meant for IL constituents.

Step 11: Similar to pure IL design, constraints of properties or functionalities included in ternary diagram can be represented as a feasibility region defined by six unique points. A ternary diagram should be prepared for mixture design purpose here, using obtained cluster values for all pure ILs and six point boundary.

Step 12: IL mixtures can be generated at this step, according to Rules M1 to M5 (M stands for IL mixture). These rules are not the same as rules shown in Step 7, where these will ensure the designed IL mixtures are valid and feasible mixtures.

Rule M1: When two IL constituents, $I_1$ and $I_2$ are added linearly on the diagram, the AUP values and distance between them provide information of $I_1$-$I_2$ combination using simple lever arm rule.

Rule M2: The fraction of each IL constituent chosen as part of the mixture must be between zero and one, and final summation of all fractions must be one.

Rule M3: The cluster value of the designed IL mixture must be located within the feasibility region on the ternary diagram.

Rule M4: The AUP value of the designed IL mixture must be within the range of target AUP. The target AUP range is determined from the six property constraints on ternary diagram. If the AUP value is outside the range of target AUP, the IL mixture is not a feasible solution.

Rule M5: ILs that are chosen as part of the mixture should have similar solubility parameter values, to ensure they form a miscible solution.

When IL mixtures are obtained, all properties and functionalities should be checked to ensure they are within the targeted range. Feasibility of these generated mixtures should be checked, if there is no feasible solution, Step 8 should be done again and the whole process shall follow. When there are feasible solutions, decision makers can decide on final one IL or mixture according to the application of this product.

## 6.4 Case Study

A carbon capture solvent design problem will be solved using the proposed approach in this section, where ionic liquids (ILs) and IL mixtures will be designed to replace ethanolamines, one of the conventional carbon capture solvents that are essentially volatile organic compounds (VOCs). The main objective of this case study is to determine possible IL or IL binary mixture as carbon capture solvent, subjecting to relevant property constraints. In this case study, the system temperature and pressure are set as 303.15 K and 0.7 MPa respectively.

### 6.4.1 Step 1: Identify target properties/functionalities and define boundaries of each property

Following steps described in Figure 6-2, target properties and functionalities should be identified. Three target properties included in this case study are density ($\rho$), viscosity ($\mu$) and $CO_2$ solubility ($S$). Density is the basic of transport property, viscosity will affect overall operating cost, and carbon dioxide ($CO_2$) solubility is the performance measurement of a carbon capture solvent. The target property ranges for all properties are included in Table 6-1, this is applicable to both pure IL and IL mixture design. The designed solvent should possess similar properties as ethanolamines, since the IL product is designed to be carbon capture solvent. Therefore, the ranges of target properties are set according to the properties of ethanolamines (The Dow Chemical Company, 2003). Viscosity of designed IL mixtures should be

as low as possible to minimise pumping power required to circulate the solvent within the process. Hence, the target range of viscosity is set to be between 0.01 to 0.10 Pa.s (Bonhôte et al., 1996). $CO_2$ solubility of designed solvent should be at least as good as the conventional solvent, the boundary is therefore set between 0.09 and 0.60 mol $CO_2$/mol solvent (Zhang et al., 2012).

**Table 6-1**: Target property ranges to design pure IL and IL mixture

| Property/functionality | Lower Bound | Upper Bound |
|---|---|---|
| Density, $\rho$ (g cm$^{-3}$) | 1.00 | 2.00 |
| Viscosity, $\mu$ (Pa.s) | 0.01 | 0.10 |
| $CO_2$ solubility, $S$ (mol $CO_2$/mol solvent) | 0.09 | 0.60 |

To further illustrate this proposed approach, more properties and functionalities are added separately to the design problem. Heat of vaporisation ($\Delta H_{vap}$) and specific heat capacity ($c_P$) are included to pure IL design problem, with their target ranges given in Table 6-2; while cost of solvent ($C$) is considered in mixture design problem and the target range is given in Table 6-3. There are five properties to consider during design of pure ILs as carbon capture solvent, and four for IL mixture design. These additional properties or functionalities illustrate the steps of the proposed approach to solve a design problem with more than three target properties. For pure IL design, density, heat of vaporisation, and specific heat capacity are chosen as dominant properties; while the other two properties (viscosity and $CO_2$ solubility) remained as screening properties. Density is chosen because it is

required for viscosity calculation. Heat of vaporisation is selected for its relationship with vapour pressure and volatility of designed ILs; while specific heat capacity of IL provides idea on energy requirement during solvent regeneration. On the other hand, density, viscosity, and cost of solvent are selected as dominant properties/functionalities during IL mixture design stage; $CO_2$ solubility in the mixture is kept as a screening property.

**Table 6-2**: Target property ranges of additional properties to design pure IL

| Property/functionality | Lower Bound | Upper Bound |
|---|---|---|
| Heat of vaporisation, $\Delta H_{vap}$ (kJ mol$^{-1}$) | 40 | 200 |
| Specific heat capacity, $c_P$ (J mol$^{-1}$ K$^{-1}$) | 100 | 600 |

**Table 6-3**: Target property range of additional property to design IL mixture

| Property/functionality | Lower Bound | Upper Bound |
|---|---|---|
| Cost of solvent, $C$ (USD mol$^{-1}$) | 200 | 800 |

### 6.4.2 Step 2: Identify prediction models for all target properties/functionalities

In this step, suitable prediction models are identified to predict the properties and functionalities of designed ILs and IL mixtures. Equations (6.12) to (6.15) are prediction models to estimate density (Qiao et al., 2010), heat of vaporisation (Verevkin, 2008), specific heat capacity (Gardas and Coutinho, 2008c), and viscosity (Gardas and Coutinho, 2008b). These

prediction models are group contribution (GC) models. $CO_2$ solubility of pure ILs was estimated through vapour liquid phase equilibrium.

$$\rho_i - \rho_0 = \sum_{k=1}^{q} \nu_k \rho_k \tag{6.12}$$

$$\Delta H_{vap,i} = \sum_{k=1}^{q} \nu_k \Delta H_{vap,k} \tag{6.13}$$

$$\frac{c_{P,i}}{R} = \sum_{k=1}^{q} \nu_k c_{P,k} \tag{6.14}$$

$$\ln \frac{1000\mu_i}{\rho M} = A_\mu + \frac{B_\mu}{T} \tag{6.15}$$

$$y_i P \varphi_i (T, P, y_i) = x_i \gamma_i P_i^S \tag{6.16}$$

$$S_i = x_{CO_2} / x_{IL} \tag{6.17}$$

In Equation (6.12), $\rho_i$ is density of IL *i*, $\rho_0$ is an adjustable parameter for density given as 0.556 g $cm^{-3}$ as given by Qiao et al. (2010), and $\rho_k$ is the GC data of group *k* for density. $\Delta H_{vap,k}$ in Equation (6.13) is the GC data of group *k* for heat of vaporisation, $c_P$ in Equation (6.14) is GC data of group *k* for specific heat capacity, and R is gas constant given as 8.314 J $mol^{-1}$ $K^{-1}$. Viscosity is determined using Orrick-Erbar-type approach that employs GC method as shown in Equation (6.15), where *M* is IL molecular weight in g

$mol^{-1}$, $T$ is the system temperature in K, $A_\mu$ and $B_\mu$ are calculated parameters based on contributions of group $k$ to each of them.

The mole fraction of $CO_2$ in liquid phase at equilibrium was obtained using Equation (6.16). In this equation, $x_i$ and $y_i$ are the mole fractions of component $i$ in liquid and gas phases respectively, $\gamma_i$ is activity coefficient which is determined using UNIFAC model, $P_i^S$ is the saturated vapour pressure of component $i$, and $\varphi_i(T,P,y_i)$ is the gas-phase fugacity coefficient. Similar to approach presented in Chapter 4, original UNIFAC model was employed to predict activity coefficient in this work, which is discussed further in Appendix Section A.2.1. Group parameters and binary interaction parameters of ILs for UNIFAC model presented by Lei et al. (2013) have been used to predict activity coefficient in this work. Gas-phase fugacity coefficient was determined using equation of state proposed by Span and Wagner (1996), which details are provided in Appendix Section A.2.2. Saturated vapour pressure of $CO_2$ can be calculated using the extrapolated Antoine equation proposed by Shiflett and Yokozeki (2006). The saturated vapour pressure of IL was assumed to be negligible due to its extremely low vapour pressure. For the same reason, IL was assumed to be absent in vapour phase (i.e., $y_{IL} = 0$). When mole fraction of $CO_2$ in liquid phase at equilibrium was determined, Equation (6.17) was then used to determine $CO_2$ solubility of ILs, $S_i$ in terms of mole $CO_2$ per mole IL.

Another set of prediction models was included to estimate all target properties and functionalities of IL mixtures. Equation (6.18) was used to predict density of IL mixture, Equations (6.19) to (6.21) are prediction models to estimate viscosity of mixture (Maples, 2000). Equation (6.22) predicts cost of the designed solvent, where $C_i$ is cost of individual IL *i*. $CO_2$ solubility of IL mixtures was determined using Equations (6.16) and (6.17). The interaction between IL groups are assumed to be zero as they are electrically neutral groups and have similar polarity (Lei et al., 2009).

$$\frac{1}{\rho} = \sum_i x_i \left( \frac{1}{\rho_i} \right) \tag{6.18}$$

$$VBI_i = 10.975 + 14.535 \ln\left[\ln\left(\nu_i + 0.8\right)\right] \tag{6.19}$$

$$\mu_i = \nu_i \rho_i \tag{6.20}$$

$$VBI = \sum_i x_i VBI_i \tag{6.21}$$

$$C = \sum_i x_i C_i \tag{6.22}$$

To estimate viscosity of IL mixture, Refutas method was applied in this work, where viscosity-blending index (VBI) is used. First, the VBI for each IL constituent was determined. The VBI of mixture is equal to summation of all the products of mole fraction and VBI of each component. In Equations (6.19) to (6.21), $VBI_i$ is the viscosity-blending index of IL

constituent *i*, $\nu_i$ is the kinematic viscosity of IL constituent *i* in $m^2\ s^{-1}$, and $\mu_i$ is the dynamic viscosity of constituent *i* in Pa.s.

### 6.4.3 Step 3: Select molecular building blocks for pure IL design

Suitable molecular building blocks for pure IL design were identified in this step. The structures of basic molecular building blocks are dependent on the pre-defined structures used in chosen property prediction models. For this case study, two organic groups, three cation cores and three anions were chosen, as shown in Table 6-4. These were chosen for they are the most widely studied cations and anions (Zhou et al., 2009).

**Table 6-4**: Molecular building blocks selected for pure IL design

| Type | *k* | Groups | Type | *k* | Groups |
|---|---|---|---|---|---|
| Organic groups | 1 | $CH_3$ | Anions | 6 | $[BF_4]^-$ |
| | 2 | $CH_2$ | | 7 | $[Tf_2N]^-$ |
| Cation cores | 3 | $[MIm]^+$ | | 8 | $[OTf]^-$ |
| | 4 | $[Py]^+$ | | | |
| | 5 | $[MPyr]^+$ | | | |

### 6.4.4 Step 4: Collect data of target properties for selected building blocks, transform them into property clusters

For all selected molecular building blocks, the relevant GC data of each target property is given in Table 6-5, along with number of free bond for each functional group. The data was collected according to the prediction

models selected in Step 2. All properties and constraints were defined up to this step, molecular property clusters of dominant properties can be determined using Equations (6.2) to (6.5). First of all, molecular property operators were identified as shown in Table 6-6, and suitable reference values were given. These reference values were chosen such that all AUP values are positive, thus obeying Rule I5. Molecular property operator for density is different from common property operator, which is reciprocal value of density as given in Equation (6.23). This is because the property operator in Equation (6.23) is used to determine density of mixture using density of pure components; while the density property operator in Table 6-6 was employed to determine density of pure IL from functional groups.

$$\psi_{density}\left(\tau_{density}\right)=\frac{1}{\rho} \tag{6.23}$$

GC data was transformed into molecular property operators and clusters. The property operators and AUP values are shown in Table 6-7; while Table 6-8 shows the cluster values for all functional groups. As presented in Table 6-7, all the AUP values are positive even though there are some negative property operator values.

**Table 6-5**: GC data, free bond number, and molecular weights for all molecular building blocks

| Building blocks | $k$ | $\rho_k$ | $\Delta H_{vap,k}$ | $c_P$ | $n_k$ | Molecular weight (g mol$^{-1}$) | $A_{k,\mu}$ | $B_{k,\mu}$ |
|---|---|---|---|---|---|---|---|---|
| $CH_3$ | 1 | -0.0244 | 2.5 | -9.825 | 1 | 15.03 | -0.74 | 250.0 |
| $CH_2$ | 2 | -0.0310 | 2.5 | 3.893 | 2 | 14.03 | -0.63 | 250.4 |
| $[Mim]^+$ | 3 | 0.5542 | 62.6 | 33.857 | 1 | 82.10 | 7.30 | 1507.1 |
| $[Py]^+$ | 4 | 0.5715 | 38.8 | 35.060 | 1 | 79.10 | 7.61 | 1453.6 |
| $[MPyr]^+$ | 5 | 0.5148 | 38.8 | 32.908 | 1 | 85.15 | 6.17 | 1983.3 |
| $[BF_4]^-$ | 6 | 0.2184 | 77.8 | 8.696 | 0 | 86.80 | -18.08 | 1192.4 |
| $[NTf_2]^-$ | 7 | 0.4431 | 65.3 | 33.557 | 0 | 280.15 | -17.39 | 510.0 |
| $[OTf]^-$ | 8 | 0.3067 | -0.5 | 17.899 | 0 | 149.07 | -17.72 | 905.6 |

**Table 6-6**: Molecular property operators and reference values for pure IL design

| Property | Molecular property operator, $\psi_d(\tau_{di})$ | Reference value |
|---|---|---|
| Density | $\rho - \rho_0$ | 1.8 |
| Heat of vaporisation | $\Delta H_{vap}$ | 16 |
| Specific heat capacity | $c_P/R$ | 300 |

**Table 6-7**: Molecular property operator and AUP values of molecular building blocks for dominant properties in pure IL design

| Groups | $k$ | $\psi_{density}(\tau_{density,\,k})$ | $\psi_{Hvap}(\tau_{Hvap,\,k})$ | $\psi_{cp}(\tau_{cp,\,k})$ | $AUP_k$ |
|---|---|---|---|---|---|
| $CH_3$ | 1 | -0.0135 | 0.1563 | -0.0328 | 0.1100 |
| $CH_2$ | 2 | -0.0173 | 0.1563 | 0.0130 | 0.1519 |
| $[Mim]^+$ | 3 | 0.3079 | 3.9125 | 0.1129 | 4.3332 |
| $[Py]^+$ | 4 | 0.3175 | 2.4250 | 0.1169 | 2.8594 |
| $[MPyr]^+$ | 5 | 0.2860 | 2.4250 | 0.1097 | 2.8207 |
| $[BF_4]^-$ | 6 | 0.1214 | 4.8625 | 0.0290 | 5.0128 |
| $[NTf_2]^-$ | 7 | 0.2462 | 4.0813 | 0.1119 | 4.4393 |
| $[OTf]^-$ | 8 | 0.1704 | -0.0312 | 0.0597 | 0.1988 |

**Table 6-8**: Molecular property cluster values of molecular building blocks for dominant properties pure IL design

| Groups | $k$ | $C_{density,\,k}$ | $C_{Hvap,\,k}$ | $C_{cp,\,k}$ | Sum |
|---|---|---|---|---|---|
| $CH_3$ | 1 | -0.1231 | 1.4210 | -0.2978 | 1 |
| $CH_2$ | 2 | -0.1142 | 1.0287 | 0.0854 | 1 |
| $[Mim]^+$ | 3 | 0.0710 | 0.9029 | 0.0260 | 1 |
| $[Py]^+$ | 4 | 0.1110 | 0.8481 | 0.0409 | 1 |
| $[MPyr]^+$ | 5 | 0.1014 | 0.8597 | 0.0389 | 1 |
| $[BF_4]^-$ | 6 | 0.0242 | 0.9700 | 0.0058 | 1 |
| $[NTf_2]^-$ | 7 | 0.0555 | 0.9193 | 0.0252 | 1 |
| $[OTf]^-$ | 8 | 0.8571 | -0.1572 | 0.3001 | 1 |

### 6.4.5 Step 5: Translate boundaries of dominant properties into six point boundary

The property constraints of dominant properties were transformed into normalised molecular property operators and the results are shown in Table 6-9. The feasibility region of this IL design problem was also determined using these molecular property operators and six point bounding presented by El-Halwagi et al. (2004). From these six points, the AUP values of each were determined; while the minimum and maximum AUP values were identified as 2.987 and 13.064.

**Table 6-9**: Normalised molecular property operator values of lower and upper bounds for three dominant properties

| Property | Normalised molecular property operator, $\Omega_d$ | $\Omega^{min}$ | $\Omega^{max}$ |
|---|---|---|---|
| Density | $\Omega_{density}$ | 0.2466 | 0.5243 |
| Heat of vaporisation | $\Omega_{Hvap}$ | 2.5 | 12.5 |
| Specific heat capacity | $\Omega_{cp}$ | 0.0401 | 0.2405 |

### 6.4.6 Step 6: Plot all building blocks and six point boundary on ternary diagram

With all cluster values and six point boundary obtained, this pure IL design problem was visualised on a ternary diagram, as shown in Figure 6-3. Red dotted lines represent the feasibility region bound by six points determined in Step 5. In Figure 6-3, different types of functional groups were

labelled using different shapes and colours, to ease the design process. According to Rule I3, only one cation core and one anion group can be chosen, thus only one red triangle and one green diamond on the ternary diagram can be matched together at once. The advantage of using visual approach is that user can know which groups will be helpful for the design problem even before solving the problem. For example, in Figure 6-3, Group 8 is far away from the feasibility region, it is obvious that this group is not helpful at all in building an IL within feasibility region. Thus, this group can be omitted during the design process.

### 6.4.7 Step 7: Generate pure ILs

Potential pure ILs was generated using Figure 6-3. An example of synthesising $[C_2MPyr][NTf_2]$ using the presented approach is shown in Figure 6-4. A $CH_3$ group was connected to a $CH_2$ group to form the carbon chain ($CH_3 – CH_2$), and this carbon chain was added to the desired cation core (e.g. $[MPyr]^+$ in this case). Following this, $[C_2MPyr]^+$ cation was combined with $[NTf_2]^-$ anion to form a complete IL structure ($CH_3 – CH_2 – [MPyr]^+ – [NTf_2]^-$ ). A total of four IL candidates were formulated using proposed approach, as shown in Figure 6-5, and their properties were back calculated and presented in Table 6-10. The dominant and screening properties of these ILs are within targeted ranges, their AUP values are in between the minimum and maximum AUP values as well (2.987 and 13.064). Thus, these ILs are valid solutions for this design problem.

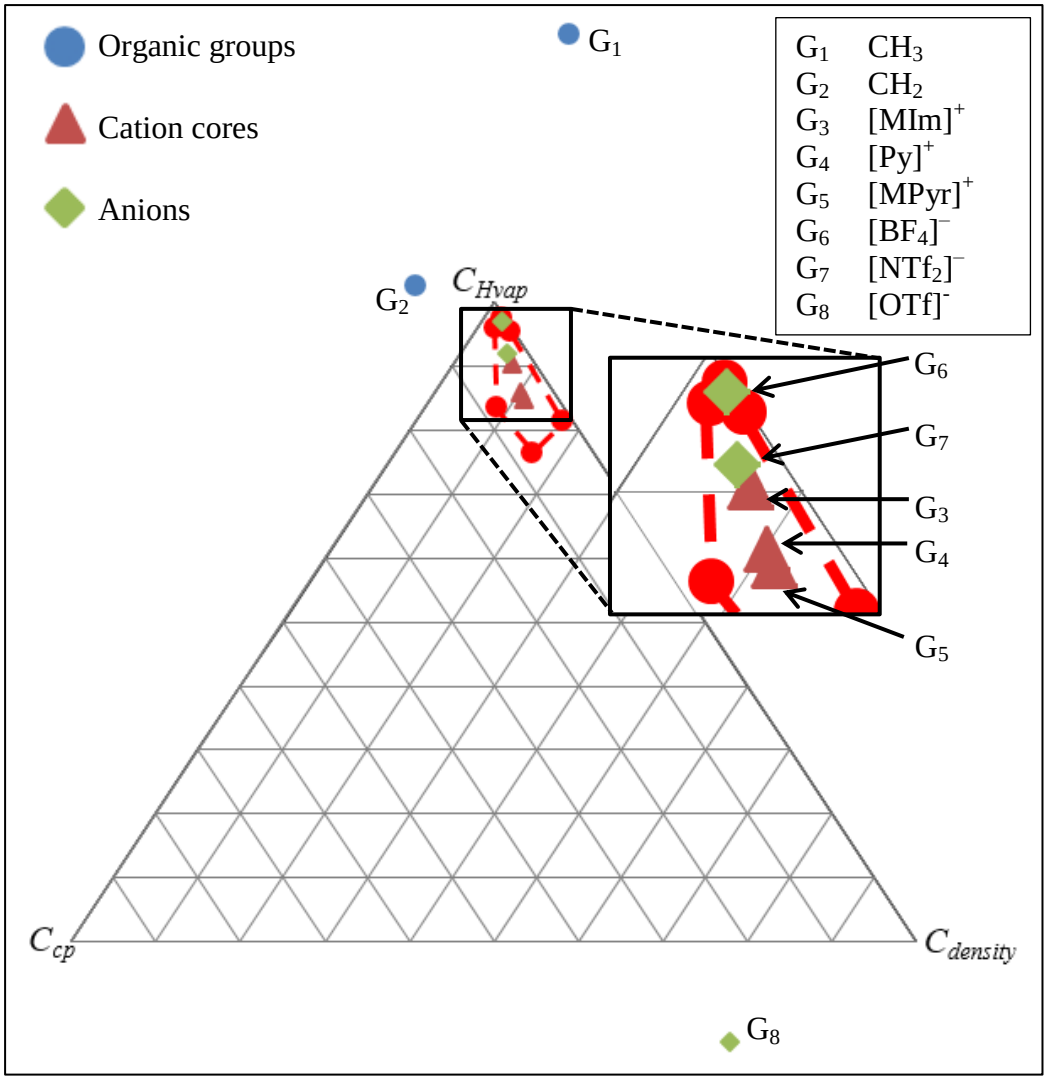


**Figure 6-3**: Ternary diagram representing pure IL design problem

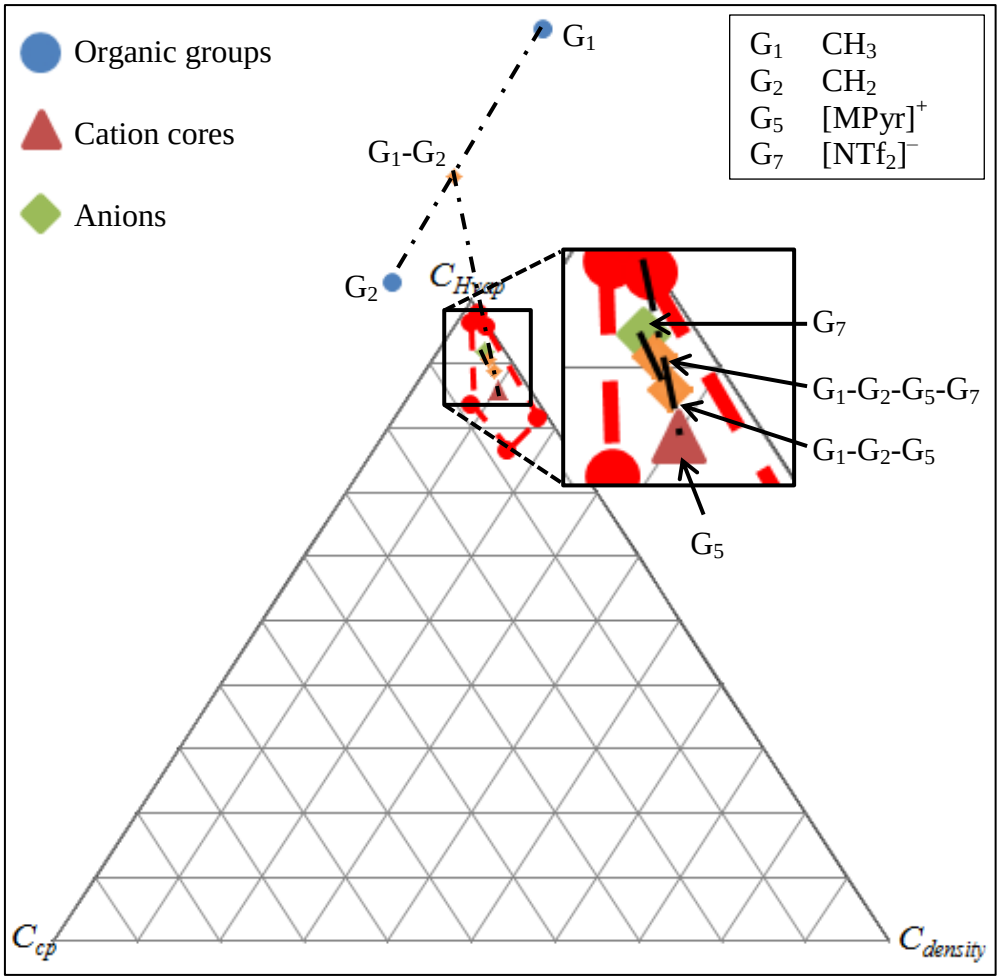


**Figure 6-4**: Synthesis path of $[C_2MPyr][NTf_2]$

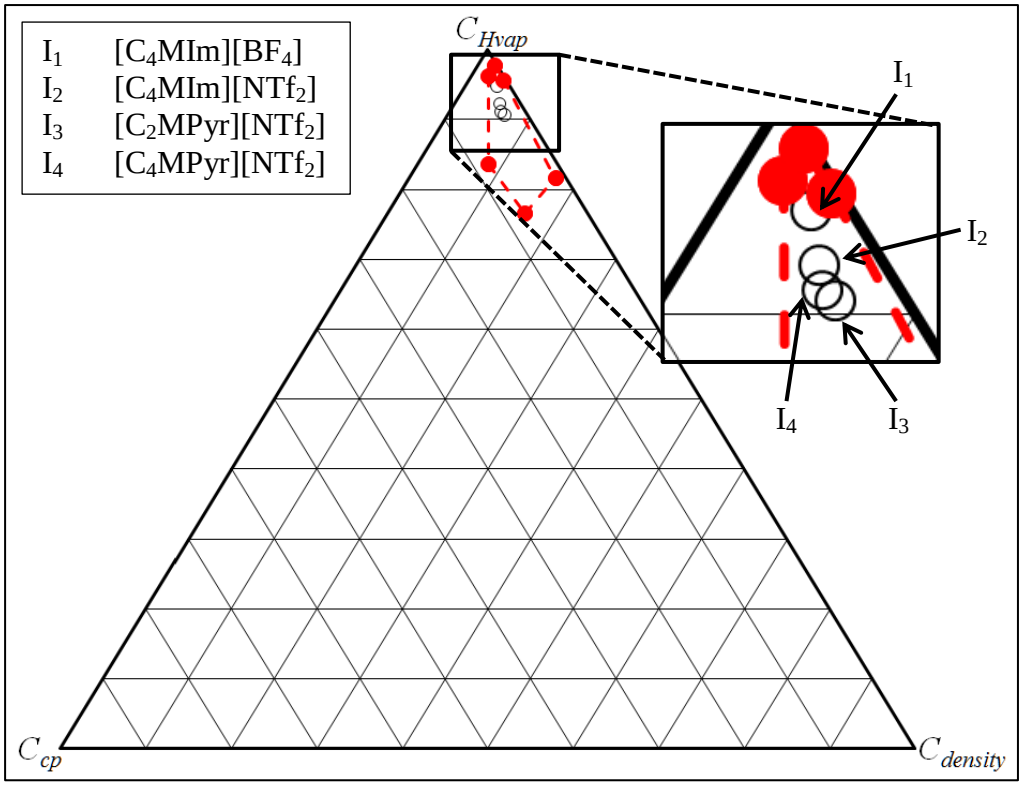


**Figure 6-5**: Ternary diagram representing pure IL design results

**Table 6-10**: Pure IL design results

| ILs | $i$ | $\rho$ (g cm$^{-3}$) | $\Delta H_{vap}$ (kJ mol$^{-1}$) | $c_P$ (J mol$^{-1}$ K$^{-1}$) | $\mu$ (Pa.s) | $S$ (mol $CO_2$/mol IL) | AUP |
|---|---|---|---|---|---|---|---|
| [$C_4$MIm][$BF_4$] | 1 | 1.211 | 150.4 | 369.2 | 0.082 | 0.097 | 9.912 |
| [$C_4$MIm][$NTf_2$] | 2 | 1.435 | 137.9 | 575.9 | 0.038 | 0.218 | 9.338 |
| [$C_2$MPyr][$NTf_2$] | 3 | 1.459 | 109.1 | 503.3 | 0.038 | 0.132 | 7.522 |
| [$C_4$MPyr][$NTf_2$] | 4 | 1.396 | 114.1 | 568.0 | 0.058 | 0.174 | 7.826 |

### 6.4.8 Step 8: Select pure ILs that are potential as part of the mixture

Designed ILs was used to design IL mixtures, additional ILs can also be added into the selection. These additional ILs can be some newly tested ILs that show great potential to replace conventional VOC (carbon capture solvent in this case study). For example, ammonium-based ILs are recently tested and show high $CO_2$ solubility (Nonthanasin et al., 2014), but some of them have high viscosity. In this case study, they were added into the list of possible IL constituents that can make up IL mixtures. By mixing them with other ILs that have low viscosity, the viscosity of mixture can be lowered and yet maintain reasonable $CO_2$ solubility. The list of potential IL constituents is given in Table 6-11, including ILs designed in Step 9.

**Table 6-11**: Potential IL constituents for IL mixture design

| ILs | *i* |
|---|---|
| $[C_4MIm][BF_4]$ | 1 |
| $[C_4MIm][NTf_2]$ | 2 |
| $[C_2MPyr][NTf_2]$ | 3 |
| $[C_4MPyr][NTf_2]$ | 4 |
| $[N_{4111}][NTf_2]$ | 5 |
| $[N_{1888}][NTf_2]$ | 6 |

### 6.4.9 Step 9: Collect data of all target properties and solubility parameter, through prediction or experiments

ILs $I_1$ to $I_4$ in Table 6-11 were designed previously, and their properties were taken from Table 6-10. The two additional ILs ($I_5$ to I6) were tested through experiments to obtain their densities at temperature of 303.15 K and pressure of 700 kPa; while the viscosity was obtained from literature. The cost of pure ILs was provided by vendor. The data was given in Table 6-12, along with properties of the other four designed ILs. The solubility parameter of each IL was determined and presented in Table 6-12 as well. In this case study, the Hildebrand solubility parameter, $\delta_{\mathbf{IL}}$ is used, and it is determined using a GC model as shown in Equation (6.24) (Kulajanpeng et al., 2014). $P_k$ is the contribution of group $k$ to solubility parameter.

$$\delta_{\mathbf{IL}} = \sum n_k P_k \tag{6.24}$$

**Table 6-12**: Property data of potential IL constituents for IL mixture design

| ILs | $i$ | Density, $\rho_i$ (g cm$^{-3}$) | Viscosity, $\mu_i$ (Pa.s) | Cost, $C_i$ (USD mol$^{-1}$) | Solubility parameter (MPa$^{1/2}$) |
|---|---|---|---|---|---|
| $[C_4MIm][BF_4]$ | 1 | 1.211 | 0.082 | 280.00 | 31.59 |
| $[C_4MIm][NTf_2]$ | 2 | 1.435 | 0.038 | 790.00 | 25.70 |
| $[C_2MPyr][NTf_2]$ | 3 | 1.459 | 0.038 | 900.00 | 26.35 |
| $[C_4MPyr][NTf_2]$ | 4 | 1.396 | 0.058 | 990.00 | 25.87 |
| $[N_{4111}][NTf_2]$ | 5 | 1.390 | 0.105 (Bhattacharjee et al., 2014) | 840.00 | 26.44 |
| $[N_{1888}][NTf_2]$ | 6 | 1.095 | 0.403 (Fröba et al., 2008) | 1350.00 | 22.12 |

### 6.4.10 Step 10: Transform prediction models and property data into property clusters

With all the properties and constraints defined, the property operator and cluster values of dominant properties can be determined using the proposed approach. Using Equations (6.18) to (6.22), the property operators were determined and included in Table 6-13, along with the suitable reference value for each property. Following the procedures provided, the properties of all selected ILs were transformed into property operators and clusters. The property operator and AUP values are shown in Table 6-14; while Table 6-15 shows the cluster values for all pure IL constituents.

**Table 6-13**: Property operators and reference value for IL mixture design

| Property/functionality | Property operator, $\psi_d(\tau_d)_M$ | Reference value |
|---|---|---|
| Density | $1/\rho$ | 1 |
| Heat of vaporisation | *VBI* | 40 |
| Cost | *C* | 400 |

**Table 6-14**: Property operator and AUP values of pure ILs considered in IL mixture design

| ILs | $i$ | $\psi_{density}(\tau_{density,\,i})$ | $\psi_{viscosity}(\tau_{viscosity,\,i})$ | $\psi_{cost}(\tau_{cost,\,i})$ | $AUP_i$ |
|---|---|---|---|---|---|
| $[C_4MIm][BF_4]$ | 1 | 0.8258 | 0.7984 | 0.7000 | 2.3241 |
| $[C_4MIm][NTf_2]$ | 2 | 0.6969 | 0.7088 | 1.9750 | 3.3806 |
| $[C_2MPyr][NTf_2]$ | 3 | 0.6854 | 0.7074 | 2.2500 | 3.6428 |
| $[C_4MPyr][NTf_2]$ | 4 | 0.7163 | 0.7539 | 2.4750 | 3.9452 |
| $[N_{4111}][NTf_2]$ | 5 | 0.7195 | 0.8074 | 2.1000 | 3.6269 |
| $[N_{1888}][NTf_2]$ | 6 | 0.9132 | 0.9200 | 3.3750 | 5.2082 |

**Table 6-15**: Property cluster values for all pure ILs considered in IL mixture design

| ILs | $i$ | $C_{\text{density},\,i}$ | $C_{\text{viscosity},\,i}$ | $C_{\text{cost},\,i}$ | Sum |
|---|---|---|---|---|---|
| $[C_4MIm][BF_4]$ | 1 | 0.3553 | 0.3435 | 0.3012 | 1 |
| $[C_4MIm][NTf_2]$ | 2 | 0.2061 | 0.2097 | 0.5842 | 1 |
| $[C_2MPyr][NTf_2]$ | 3 | 0.1882 | 0.1942 | 0.6177 | 1 |
| $[C_4MPyr][NTf_2]$ | 4 | 0.1816 | 0.1911 | 0.6273 | 1 |
| $[N_{4111}][NTf_2]$ | 5 | 0.1984 | 0.2226 | 0.5790 | 1 |
| $[N_{1888}][NTf_2]$ | 6 | 0.1753 | 0.1766 | 0.6480 | 1 |

### 6.4.11 Step 11: Determine six point boundary and plot them with all pure ILs on ternary diagram

The property constraints in Table 6-1 were transformed to normalised property operators, as shown in Table 6-16. Using six point bounding (El-Halwagi et al., 2004), the feasibility region of this design problem was determined and plotted as red dotted line in Figure 6-6. The minimum and maximum AUP values were identified as 1.830 and 3.479. Therefore, this is the target AUP range for this IL mixture design problem. Using cluster values in Table 6-15, the ILs are plotted on ternary diagram, as shown in Figure 6-6.

**Table 6-16**: Normalised property operator values of lower and upper bounds for three dominant properties in IL mixture design

| Property | Normalised property operator, $\Omega_d$ | $\Omega^{\text{min}}$ | $\Omega^{\text{max}}$ |
|---|---|---|---|
| Density | $\Omega_{\text{density}}$ | 0.500 | 1.000 |
| Viscosity | $\Omega_{\text{viscosity}}$ | 0.479 | 0.830 |
| Cost | $\Omega_{\text{cost}}$ | 0.500 | 2.000 |

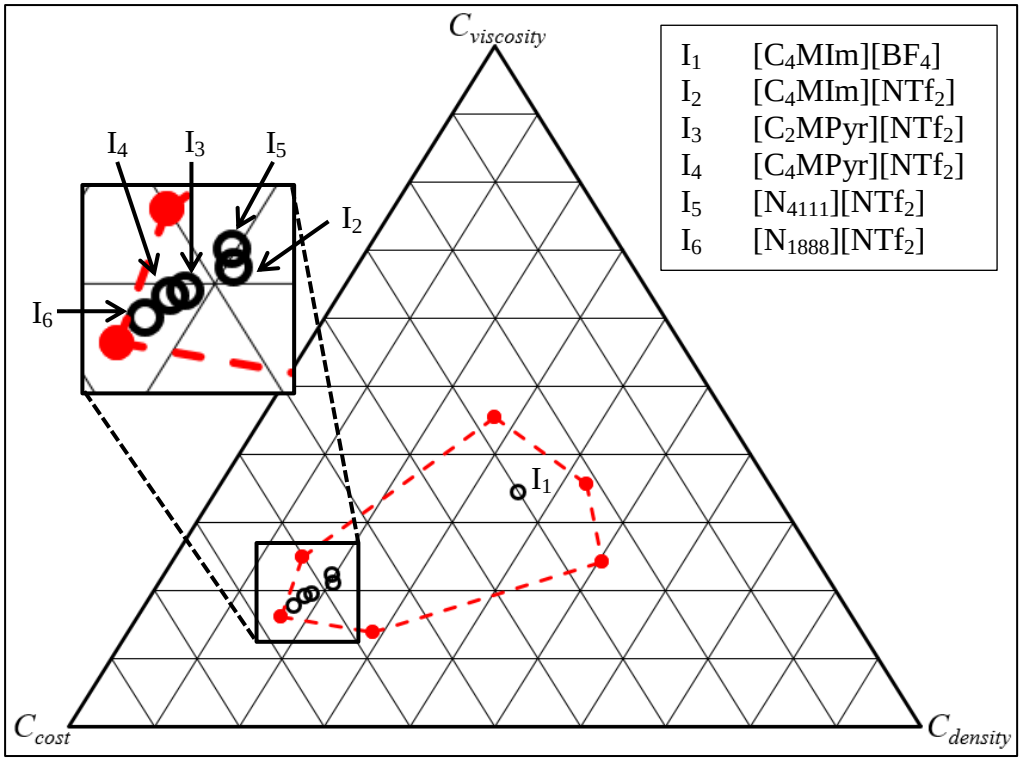


**Figure 6-6**: Ternary diagram representing IL binary mixture design problem

### 6.4.12 Step 12: Generate IL mixtures

Given the objective of this case study is to design IL binary mixtures only, therefore only two pure IL constituents can be chosen as a result. Four IL mixtures were formulated as potential carbon capture solvents using the proposed visual approach and the results are presented in Figure 6-7. The properties were back calculated and included in Table 6-17. As shown, the AUP values of all designed solvents are within the targeted range. All designed IL mixtures fulfil the constraints set in Table 6-1 and Table 6-3. From the results, a mixture of 95 mol % of [$C_4$MIm][$NTf_2$] and 5 mol % of [$C_2$MPyr][$NTf_2$] has the lowest viscosity; while the mixture of 20 mol % of

[$C_4MIm][BF_4$] and 80 mol % of [$N_{4111}$][$NTf_2$] has the highest viscosity yet fulfil all constraints. The first mixture was expected because [$C_4MIm][NTf_2$] and [DEMA][OTF] have the lowest viscosity among all pure ILs. The cost of mixture consisting 95 mol % of [$C_4MIm][BF_4$] and 5 mol % of [$C_4MIm][NTf_2$] is lowest among all combinations, as they are among the most inexpensive ILs. $CO_2$ solubility of all designed mixture was also calculated using Equations (6.16) and (6.17), and the results are given in Table 6-17.

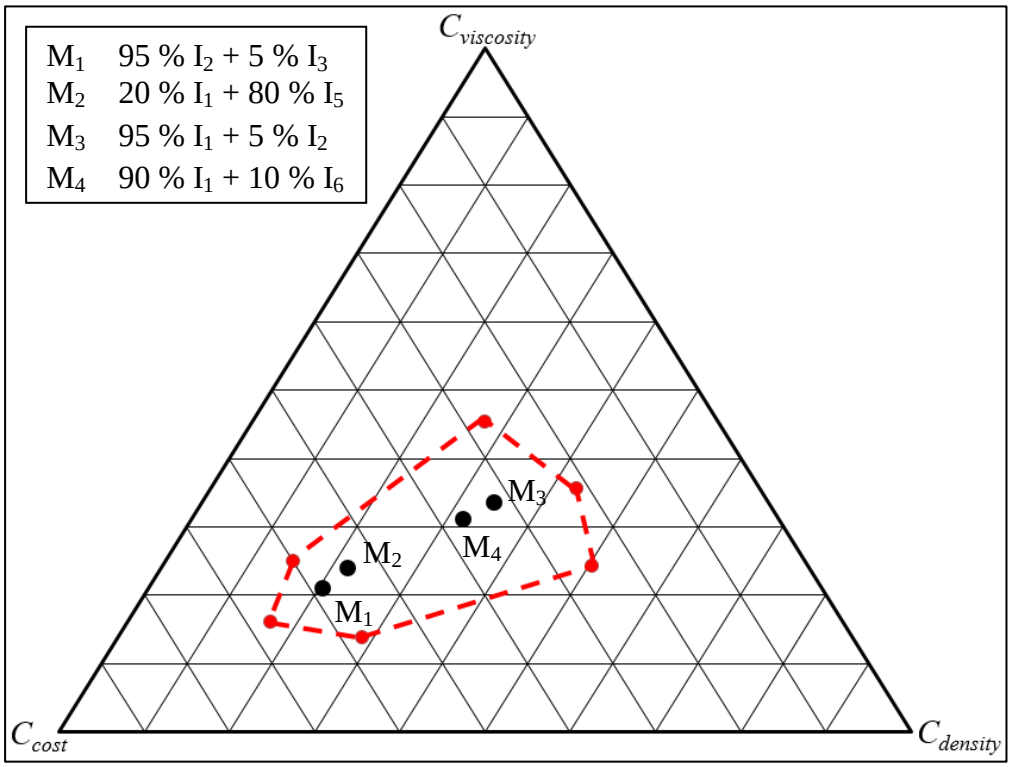


**Figure 6-7**: Ternary diagram representing IL binary mixture design results

**Table 6-17**: IL mixture design results

| IL mixtures | IL constituent 1 | | IL constituent 2 | | $\rho$ (g cm$^{-3}$) | $\mu$ (Pa.s) | $C$ (USD mol$^{-1}$) | $S$ (mol $CO_2$/mol solvent) | AUP |
|---|---|---|---|---|---|---|---|---|---|
| | IL | mol % | IL | mol % | | | | | |
| $M_1$ | $I_2$ | 95 | $I_3$ | 5 | 1.436 | 0.038 | 795.50 | 0.214 | 3.394 |
| $M_2$ | $I_1$ | 20 | $I_5$ | 80 | 1.350 | 0.100 | 728.00 | 0.168 | 3.366 |
| $M_3$ | $I_1$ | 95 | $I_2$ | 5 | 1.221 | 0.079 | 305.50 | 0.116 | 2.377 |
| $M_4$ | $I_1$ | 90 | $I_6$ | 10 | 1.198 | 0.094 | 387.00 | 0.130 | 2.613 |

## 6.5 Summary

A systematic property based visual approach to design ionic liquid (IL) and IL mixture as carbon capture solvent has been presented in this chapter. This approach introduces a property platform to solve IL and IL mixture design problem, through property clustering technique. Using this presented approach, an IL-based solvent problem can now be solved visually using ternary diagrams, which provides user useful insights to both the problem and solutions. On ternary diagram, each vertex is representing one pure property cluster, so only three dominant properties can be displayed on the diagram. Nonetheless, more properties can be considered as screening properties. Mathematical optimisation approach can be utilised if many properties or considerations are included in the mixture design problem. For all properties considered, constraints should be included and final IL formulation must fulfil these constraints. Design and optimisation rules were developed to aid the design of IL and IL mixture using this approach. To overcome the problem of lacking prediction models for IL mixture, this approach can utilise both experimental data and prediction models. An illustrative case study to design potential IL and IL mixture as carbon capture solvent was solved to demonstrate the application of the proposed approach. So far, all the developed approaches only solve IL-based solvent design problem, without considering any aspect from process design. However, the designed IL and process conditions are affecting each other closely, hence they should be considered simultaneously, which will be further discussed in Chapter 7.

# CHAPTER 7

# A SYSTEMATIC APPROACH TO DETERMINE TASK-SPECIFIC IONIC LIQUID AND OPTIMAL OPERATING CONDITIONS USING DISJUNCTIVE PROGRAMMING

## 7.1 Introduction

This chapter presents a systematic approach for the selection of optimal ionic liquid (IL) specifically for the purpose of carbon dioxide ($CO_2$) capture, and identification the optimal system conditions for carbon capture process simultaneously. This is the first step to integrating IL design and process design, by considering the operating conditions during IL design stage. The proposed approach in this chapter is an extension of approach presented in Chapter 5. Since most of the ILs to be designed are novel solvents, their thermophysical properties will be estimated using group contribution (GC) method. Appropriate structural constraints were defined to ensure the structure of the synthesised IL is feasible. Besides, it is necessary to identify the optimal conditions of the carbon capture processes, as the performance of ILs changes according to the operating conditions, which in turn affects the overall performance of the carbon capture process. This was done through disjunctive programming, as it can discretise continuous variables and reduce search space for results. An illustrative case study was solved to demonstrate the

proposed approach. $CO_2$ solubility of IL was set to be design objective, density and viscosity were taken into consideration in the design problem. Ten potential ILs were obtained as results. The regeneration energy required to reproduce designed IL solvents for the case study was estimated through simulation, and compared to the regeneration energy for conventional $CO_2$ capturing solvent to ensure these IL solvents are viable for industry. Besides, the proposed approach was used to study the effect of temperature on $CO_2$ solubility and viscosity of different ILs, and presented in this chapter.

## 7.2 Problem Statement

The main problem is aimed to design an optimal ionic liquid (IL) for carbon capture purpose, from a given set of pre-selected cation cores, anions, and organic functional groups, and to determine the optimal operating conditions for this designed IL, based on a specific design objective, fulfilling target properties and relevant constraints. A superstructure representation of allowed combinations of all molecular fragments is shown in Figure 7-1.

The specific problem to be addressed is stated as below:

1) Design an IL based on carbon capture performance that satisfies all target properties and specified constraints. The carbon capture performance can be defined by carbon dioxide ($CO_2$) solubility of IL.

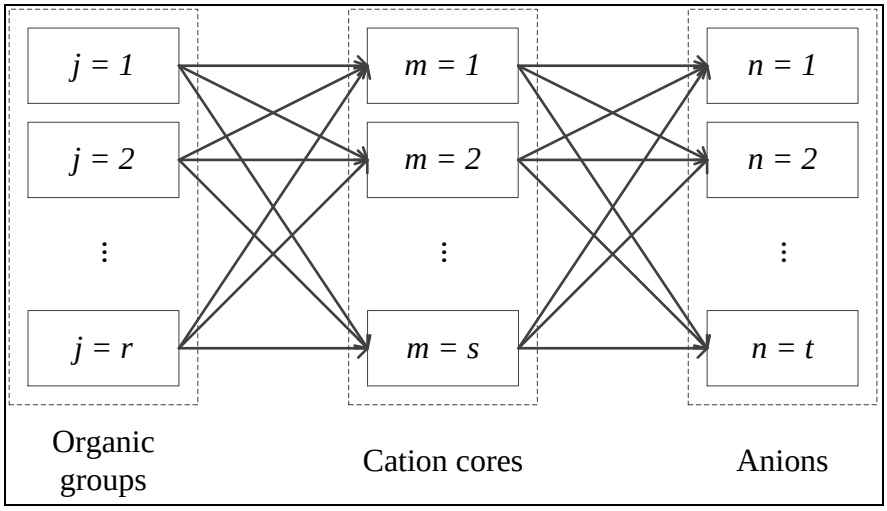


**Figure 7-1**: Schematic representation of combinations of all molecular groups (replicated from Figure 4-1)

2) The superstructure comprises of *r* organic functional groups, *s* cation cores, and *t* anions, which are selected based on gas absorption and separation performance of IL beforehand (Baltus et al., 2004). Since this work aims to design pure IL for carbon capture, the choice of cation core and anion is limited to one each.
3) Operating temperature, *T* and operating pressure, *P* are modelled as variables so that the model will determine the optimal operating conditions for carbon capture process using the designed IL.
4) The selectivity of other gases over $CO_2$ is assumed to be negligible during the development of this approach. Besides, the proposed approach considers only physical absorption mechanism; hence no reaction is involved between $CO_2$ and IL.

## 7.3 Optimisation model

In this section, the formulation to identify optimal ionic liquid (IL) as carbon capture solvent is presented and discussed in detail. Similar to the methodology presented in Chapter 5, the design objective and target performance of IL solvent should be identified and translated into measurable properties. All properties are estimated using suitable group contribution (GC) models. Structural constraints must be fulfilled by the designed IL. As mentioned in Section 7.2, the operating conditions were modelled as variables in this proposed approach. Since the carbon dioxide ($CO_2$) solubility in ILs changes according to temperature and pressure, the operating conditions of the carbon capture process becomes part of the optimisation objective. Temperature and pressure can be modelled as continuous variables to provide good results to the problem. However, the model is more complex to be solved, because the search space for results is much larger, as compared to a model which only considers fixed operating conditions. To avoid solve the model effectively, it can be modelled using disjunctive programming.

### 7.3.1 Optimal Operating Conditions via Disjunctive Programming

Disjunctive programming reformulates continuous non-linear function as piecewise linear functions over discrete domains (El-Halwagi, 2012). As shown in Figure 7-2, the feasible operating temperatures and pressures were broken down into few ranges. According to El-Halwagi (2012), when more ranges are included, the better resemblance of the original function can be

obtained. However, this is unrealistic because the total number of variables in the model will be too high and this will make the model more complicated as well. Hence, a reasonable number of ranges should be selected to provide a proper balance between accuracy in representing the function against the number of ranges. Next, operating temperatures and pressures were discretised with each range represented by its midpoint. The discretisation function with disjunctive programming can be described by the following equations.

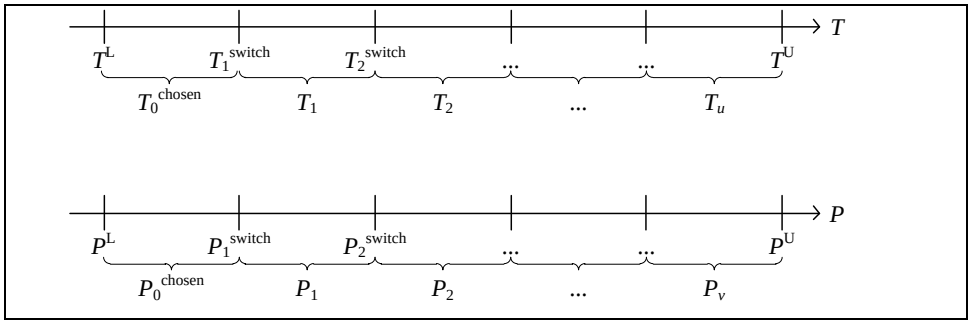


**Figure 7-2**: Operating temperature and pressure ranges

$$T_g^{chosen} = T_{g-1}^{chosen} I_g + T_g (1 - I_g) \tag{7.1}$$

$$(T^L - T_g^{switch}) I_g < T - T_g^{switch} \le (T^U - T_g^{switch})(1 - I_g) \tag{7.2}$$

$$P_h^{chosen} = P_{h-1}^{chosen} I_h + P_h (1 - I_h) \tag{7.3}$$

$$(P^L - P_h^{switch}) I_h < P - P_h^{switch} \le (P^U - P_h^{switch})(1 - I_h) \tag{7.4}$$

where $T^{L}$ and $T^{U}$ are lower and upper bounds to any feasible operating temperature, $P^{L}$ and $P^{U}$ are lower and upper bounds for operating pressure, $T_g^{chosen}$ and $P_h^{chosen}$ are chosen system temperature and chosen system pressure, $T_g$ and $P_h$ are temperature range $g$ and pressure range $h$, $T_g^{switch}$ is boundary temperature between temperature ranges and $P_h^{switch}$ is boundary pressure between pressure ranges.

Binary integers $I_g$ and $I_h$ were introduced in the model for temperature and pressure selection. In Equation (7.2), the first part of the inequality is always negative because $T_g^{switch}$ is always larger than $T^{L}$. In contrast to that, the last part of the inequality is always positive, as $T_g^{switch}$ is always smaller than $T^{U}$. When the temperature value $T$ is higher than $T_g^{switch}$, the middle part of the inequality will be positive, $I_g$ is then forced to be 0 in Equation (7.2) so that the inequality is valid. This also forces $T_g$ to be chosen in Equation (7.1). On the other hand, if the temperature is lower than $T_g^{switch}$, $I_g$ is forced to be 1, while $T_{g\text{-}1}^{chosen}$ will be chosen. Similar trend occurs for pressure selection using Equations (7.3) and (7.4). By including Equations (7.1) to (7.4) in the model, whenever temperature or pressure falls into one of the pre-defined ranges, it will be represented by the midpoint of the range. For example, any temperature value falls between $T^{L}$ and $T_1^{switch}$, it is now represented as $T_0^{chosen}$. In this manner, the continuous variable temperature is now translated to discrete variable. Once the operating conditions are determined, temperature and pressure dependent variables will be computed accordingly.

### 7.3.2 Solution Procedure

The proposed method to design IL as carbon capture solvent, and determine the optimal operating conditions of the designed IL is discussed in details. Figure 7-3 summarises the procedure.

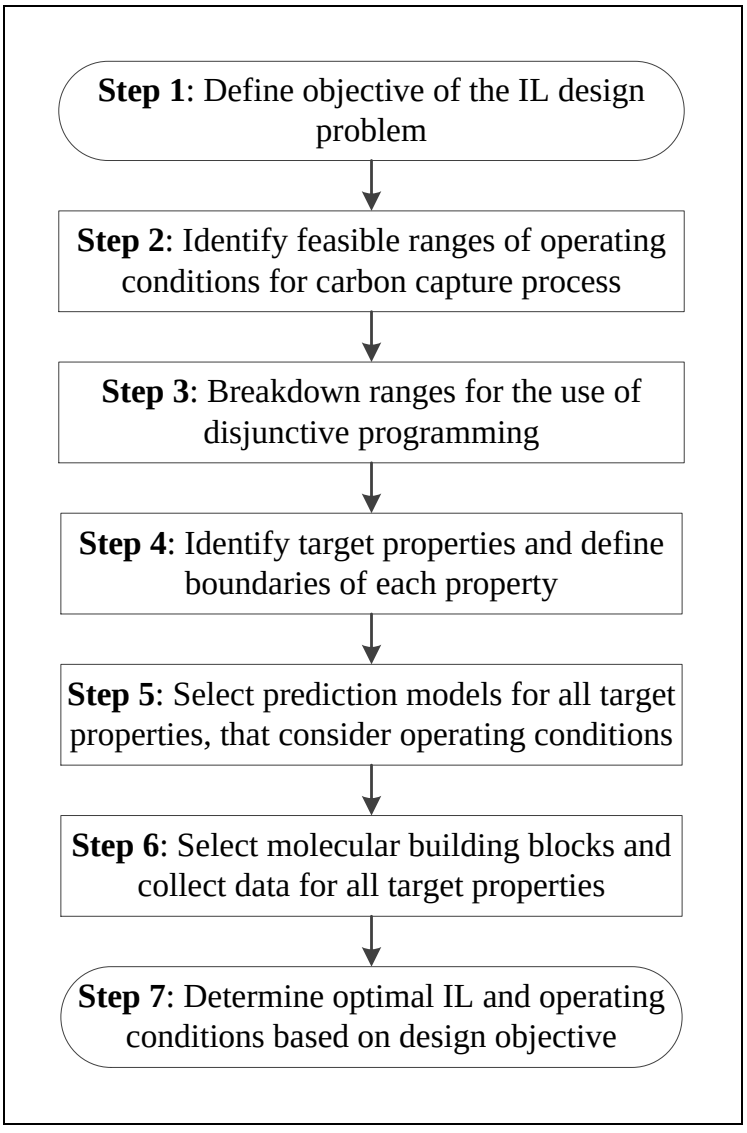


**Figure 7-3**: Proposed approach to design IL-based carbon capture solvent and determine its optimal operating conditions

Step 1: Firstly, the objective of IL design problem is identified by specifying the most concerned target property in this design problem. The design objective can be thermophysical properties that can affect functionality, environmental and economical performance of designed IL in carbon capture process. The operating conditions of carbon capture process are included as part of the optimisation objective, because they affect the performance of IL and the process. This optimisation objective can be written in general as below.

$$\text{maximise} \quad f_{g,h} \qquad \forall g,h \tag{7.5}$$

where $f_{g,h}$ is the design objective in temperature range $g$ and pressure range $h$. The objective shown in Equation (7.5) is targeted to be max, but maximising or minimising the objective is dependent on the main concern in the process.

Step 2: The feasible ranges of operating conditions for carbon capture process should be identified. Since the designed IL solvent is meant to replace conventional solvent, the ranges of operating conditions should follow that of conventional solvent.

Step 3: The operating conditions for the design problem should be broken down into smaller ranges in this step. As discussed in Section 7.3.1, a reasonable number of ranges must be selected to have a proper balance between accuracy in representation of the model against number of ranges. Each range is then represented by its midpoint.

Step 4: Target properties for the IL design problem are determined, along with their respective upper and lower limits. These target properties will be kept as constraints for the IL design problem. They can be expressed as Equation (7.6), $\tau_d$ is the $d^{th}$ property, $\tau_d^{min}$ is lower bound and $\tau_d^{max}$ is upper bound of $d^{th}$ property.

$$\tau_d^{min} \leq \tau_d \leq \tau_d^{max} \tag{7.6}$$

Step 5: Reliable property prediction models are identified for all target properties, to estimate properties of IL. The choice of prediction models is important because it will affect the overall accuracy of the formulation.

Step 6: Molecular groups should be identified for the IL design problem in this step. Similar to the approach proposed in Chapter 5, these groups consist of organic groups, cations, and anions, to form a complete IL. The building blocks are chosen such that designed IL can possess similar properties as conventional products for the designated application, as the designed IL is substituting conventional carbon capture solvent. Data of all chosen molecular building blocks should be collected, which is used to estimate properties of IL structure with these building blocks.

Step 7: The optimal IL that satisfies all target properties is designed based on the design objective, and its operating conditions is determined simultaneously. The selectivity of other gases over $CO_2$ was not part

of this work, i.e. only $CO_2$ will be absorbed by the selected IL. As discussed in Section 5.3, equilibrium relationships must be considered.

$$y_i P_h^{\text{chosen}} \varphi_i(T, P, y_i) = x_i \gamma_i P_i^{\text{S}} \tag{7.7}$$

where $x_i$ and $y_i$ are the mole fractions of component $i$ in liquid and gas phases respectively, $\gamma_i$ is activity coefficient, $P_i^S$ is the saturated vapour pressure of component $i$, and $\varphi_i(T,P,y_i)$ is the gas-phase fugacity coefficient. The activity coefficient was determined using Original UNIFAC model, consisting of combinatorial contribution, $\ln \gamma_i^{\text{C}}$ and residual contribution, $\ln \gamma_i^{\text{R}}$ as given in Equation (7.8). The details of UNIFAC model are given in Appendix Section A.2.1. Group parameters and binary interaction parameters of IL for UNIFAC model presented by Lei et al. (2013) have been used to predict activity coefficient. Cation core should be combined with anion when using these parameters presented by Lei et al. (2013), which is presented in Section 5.3.

$$\ln \gamma_i = \ln \gamma_i^{\text{C}} + \ln \gamma_i^{\text{R}} \qquad \forall i \tag{7.8}$$

Equation of state proposed by Span and Wagner (1996) was employed to calculate the gas-phase fugacity coefficient, with the details explained in Appendix Section A.2.2. Saturated vapour pressure of $CO_2$ was calculated using extrapolated Antoine equation proposed by Shiflett and Yokozeki (2006). To ensure the designed IL

is valid solution, relevant constraints should be included. Summation of mole fractions for both phases is included as constraints because both liquid and gas phases are involved in carbon capture process, as given in Equations (7.9) and (7.10).

$$\sum_i y_i = 1 \tag{7.9}$$

$$\sum_i x_i = 1 \tag{7.10}$$

where $y_i$ and $x_i$ are vapour and liquid fractions respectively. Equations (7.11) and (7.12) are structural constraints for IL design. The final structure of designed IL must consist of at least two building blocks according to Equation (7.11), and it must not have any free bond, as described in Equation (7.12). In these equations, $v_k$ is the number of group $k$ and $n_k$ is the available free bond of group $k$.

$$\sum_k v_k \geq 2 \tag{7.11}$$

$$\sum_k n_k v_k - 2\left(\sum_k n_k - 1\right) = 0 \tag{7.12}$$

Since this proposed methodology focuses on pure IL design, only one cation and one anion can be chosen. Equations (7.13) and (7.14) are included to make sure only a pair of cation and anion will be chosen,

$$\sum_m \alpha_m = 1 \tag{7.13}$$

$$\sum_n \beta_n = 1 \tag{7.14}$$

where $\alpha_m$ and $\beta_n$ are the binary variables representing each cation $m$ and each anion $n$.

## 7.4 Case Study

An illustrative case study was solved to demonstrate the presented approach. A post-combustion carbon capture unit in a coal-fired power plant is treating vent gas stream consisting of nitrogen, carbon dioxide ($CO_2$), water vapour, oxygen, and some other trace gases. The compositions of these gases are given in Table 7-1, data was adapted from Global CCS Institute (2012). The $CO_2$ absorption process is running at 323.15 K and 0.1 MPa (Yu et al., 2012). Amine-based carbon capture solvent is currently being used in the carbon capture process, and it is desired to replace this solvent with ionic liquid (IL) solvent. Since the carbon capture performance of solvent can be affected by operating conditions, hence the optimal operating conditions for IL solvent is yet to be determined. The suitable IL solvent is to be designed using the proposed approach, together with its optimal operating conditions.

### 7.4.1 Step 1: Define objective of the IL design problem

The design objective was identified in this step. The IL is designed for carbon capture purpose, and carbon capture performance is the main concern.

This can be measured by $CO_2$ solubility of IL ($S$) in terms of mole $CO_2$ per mole IL. The $CO_2$ solubility must be maximised for best carbon capture performance, as given in Equation (7.15).

$$\max S_{g,h} \quad \forall g,h \tag{7.15}$$

where $S_{g,h}$ stands for the $CO_2$ solubility of selected IL in temperature range $g$ and pressure range $h$. By introducing this objective function, the model will compare $CO_2$ solubility of all possible ILs between temperature ranges $g$ and $g$+1 in Equations (7.1) and (7.2), and also between pressure ranges $h$ and $h$+1 in Equations (7.3) and (7.4). The IL, with the corresponding temperature and pressure ranges, that has the highest $CO_2$ solubility will be chosen, and then compared with next temperature and pressure range. Taking the first two temperature ranges as example, the first range will be $T_0^{\text{chosen}}$ by default, and this will be compared with $T_1$. If an IL in $T_1$ is determined to be the optimal IL among all combinations in both temperature ranges, $T_1$ will be chosen as $T_1^{\text{chosen}}$ according to Equation (7.1). This result will then be compared with all possible ILs in $T_2$. The comparisons will be carried on for all pre-defined temperature ranges up to $T_u$, similar procedure will be carried out for pressure.

**Table 7-1**: Compositions of flue gases from coal-fired power plant

| Gas constituent | Composition (wt%) |
|---|---|
| Nitrogen | 70 |
| Carbon dioxide | 15 |
| Water vapour | 10 |
| Oxygen | 4 |
| Trace gases ($SO_x$, $NO_x$, others) | 1 |

### 7.4.2 Step 2: Identify feasible ranges of operating conditions for carbon capture process

The designed IL will be replacing an amine-based solvent being used currently, which is operating at 323.15 K and 1.0 bar. The range can be set around the current operating temperature and pressure. For illustration purpose, feasible operating temperature range was set to be 323.15 to 373.15 K in this case study; while feasible pressure range was set between 0.5 and 1.0 MPa.

### 7.4.3 Step 3: Breakdown ranges for the use of disjunctive programming

In this step, the ranges defined in Step 2 were broken down into smaller ranges according to the conditions. As discussed in Section 7.3, reasonable temperature and pressure ranges should be chosen to represent the model for this design problem. Both the operating temperature and pressure were broken down into five ranges as illustrated in Figure 7-4. This information will be used as part of disjunctive programming later.

### 7.4.4 Step 4: Identify target properties and define boundaries of each property

Apart from $CO_2$ solubility of IL was set as design objective, density ($\rho$) and viscosity ($\mu$) of IL were chosen as target properties in this case study.

Density is important as it is a basic transport property and required for viscosity calculation. Viscosity affects the pumping power required to circulate the solvent within the system, and hence the operating cost as well. The target ranges of properties were set according to properties of amine-based solvent. Viscosity of IL solvent should be kept as low as possible to ensure pumping power required is at minimum, and therefore set to be lower than 0.1 Pa.s. The targeted property ranges are shown in Table 7-2.

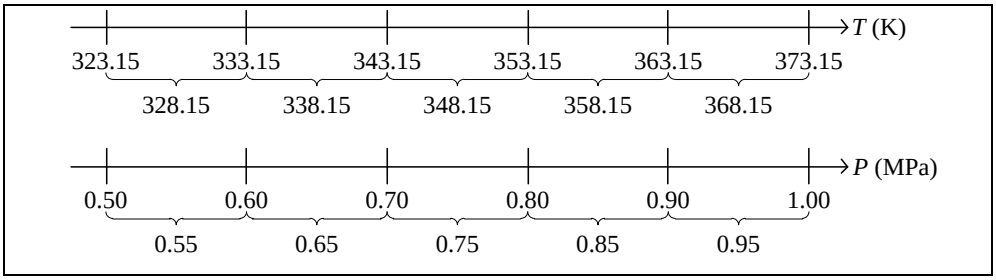


**Figure 7-4**: Midpoints for all temperature and pressure ranges considered in the case study

**Table 7-2**: Target property ranges to design IL solvent

| Property | Lower bound | Upper bound |
|---|---|---|
| Density, $\rho$ (g cm$^{-3}$) | 1.0 | 2.0 |
| Viscosity, $\mu$ (Pa.s) | 0 | 0.1 |

### 7.4.5 Step 5: Identify prediction models for all target properties

Appropriate prediction models were selected for all properties involved in this step. Density can be estimated using Equations (7.16) and (7.17) (Gardas and Coutinho, 2008a), Equations (7.18) to (7.20) are models to predict viscosity of IL (Gardas and Coutinho, 2008b), and Equation (7.21) was used to determine $CO_2$ solubility of ILs, after the mole fraction of $CO_2$ in liquid phase at equilibrium was determined.

$$\rho = \frac{M}{NV\left(a + bT_g^{\text{chosen}} + cP_h^{\text{chosen}}\right)} \tag{7.16}$$

$$V = \sum_k v_k V_k \tag{7.17}$$

$$\ln \frac{1000\mu}{\rho M} = A_\mu + \frac{B_\mu}{T_g^{\text{chosen}}} \tag{7.18}$$

$$A_\mu = \sum_k v_k A_{\mu,k} \tag{7.19}$$

$$B_\mu = \sum_k v_k B_{\mu,k} \tag{7.20}$$

$$S_{g,h} = x_{\text{CO}_2,g,h} \big/ x_{\text{IL},g,h} \tag{7.21}$$

where $N$ is the Avogadro constant (given as 0.6022), $V$ is the molecular volume in $Å^3$, the coefficients $a$, $b$ and $c$ were estimated as 0.8005, $6.652 \times 10^{-4}$ $K^{-1}$ and $-5.919 \times 10^{-4}$ $MPa^{-1}$ respectively. Equation (7.17) shows that molecular volume of IL is equivalent to the sum of molecular volume of each group ($V_k$) that occur in the structure. In Equation (7.18), $\mu$ is IL viscosity in

Pa.s, $\rho$ is IL density in g $cm^{-3}$, $M$ is IL molecular weight in g $mol^{-1}$. For Equations (7.19) and (7.20), $v_k$ is the number of group $k$, $A_{k,\mu}$ and $B_{k,\mu}$ are contributions of group $k$ to parameters $A$ and $B$, respectively.

### 7.4.6 Step 6: Select molecular building blocks and collect data for all target properties

Molecular building blocks were selected for this case study. Table 7-3 shows the molecular fragments that are available for this design problem. These fragments are chosen because they are among the most widely studied cations and anions. Their respective data for all prediction models was collected (Gardas and Coutinho, 2008a, 2008b) as well and presented in Table 7-4. Table 7-5 and Table 7-6 show the necessary parameters for UNIFAC model calculations.

**Table 7-3**: Organic function groups, cation cores, and anions considered

| Type | k | Groups | Type | k | Groups |
|---|---|---|---|---|---|
| Organic groups | 1 | $CH_3$ | Anions | 5 | $[BF_4]^-$ |
| | 2 | $CH_2$ | | 6 | $[PF_6]^-$ |
| Cation cores | 3 | $[Mim]^+$ | | 7 | $[Cl]^-$ |
| | 4 | $[Im]^+$ | | | |

**Table 7-4**: Free bond number, molecular weights, and data for target properties of all molecular building blocks

| Building blocks | $k$ | $n_k$ | Molecular weight (g mol$^{-1}$) | $V_k$ | $A_{k,\mu}$ | $B_{k,\mu}$ |
|---|---|---|---|---|---|---|
| $CH_3$ | 1 | 1 | 15.03 | 35 | -0.74 | 250.0 |
| $CH_2$ | 2 | 2 | 14.03 | 28 | -0.63 | 250.4 |
| $[Mim]^+$ | 3 | 1 | 82.10 | 119 | 7.30 | 1507.1 |
| $[Im]^+$ | 4 | 2 | 67.07 | 79 | 8.04 | 1257.1 |
| $[BF_4]^-$ | 5 | 0 | 86.80 | 73 | -18.08 | 1192.4 |
| $[PF_6]^-$ | 6 | 0 | 144.96 | 107 | -20.49 | 2099.8 |
| $[Cl]^-$ | 7 | 0 | 35.45 | 47 | -27.63 | 5457.7 |

**Table 7-5**: Group parameters of volume $R_k$ and surface area $Q_k$ in UNIFAC model

| $m$ | Main group | Subgroup | $R_k$ | $Q_k$ |
|---|---|---|---|---|
| 1 | $CH_2$ | $CH_3$ | 0.9011 | 0.8480 |
| | | $CH_2$ | 0.6744 | 0.5400 |
| 2 | $CO_2$ | $CO_2$ | 1.2960 | 1.2610 |
| 3 | [Mim][$BF_4$] | [Mim][$BF_4$] | 6.5669 | 4.0050 |
| 4 | [Mim][$PF_6$] | [Mim][$PF_6$] | 7.6909 | 4.6930 |
| 5 | [Mim][Cl] | [Mim][Cl] | 5.7073 | 4.9741 |

**Table 7-6**: Group binary interaction parameters between group $m$ and $n$ for the UNIFAC model

| $m$ | $n$ | $a_{mn}$ | $a_{nm}$ |
|---|---|---|---|
| 1 | 2 | 28.05 | 672.80 |
| | 3 | 1180.51 | 588.74 |
| | 4 | 692.26 | 401.54 |
| | 5 | 2093.97 | 1129.01 |
| 2 | 3 | -14.44 | 430.80 |
| | 4 | -66.74 | 460.25 |
| | 5 | 2693.80 | -67.35 |

### 7.4.7 Step 7: Determine optimal IL and operating conditions based on design objective

In this step, the design problem can be solved using all the collected data and property prediction models. The formulation to solve this problem was modelled as a mixed integer non-linear programming (MINLP) model. The solution of this formulation will predict the molecular structures with the optimal properties. However, it is possible that many of the solutions may be difficult to synthesise or too expensive to use as a solvent. Therefore, integer cuts have been applied to produce multiple solutions in the order of their optimality to provide some flexibility for the decision maker.

The formulation of MINLP model for this case study is given in the following equations.

$$\max S_{g,h} = x_{\mathrm{CO}_2,g,h} / x_{\mathrm{IL},g,h} \tag{7.22}$$

$$T_g^{\text{chosen}} = T_{g-1}^{\text{chosen}} I_g + T_g (1 - I_g) \tag{7.23}$$

$$(T^{\mathrm{L}} - T_g^{\text{switch}}) I_g < T - T_g^{\text{switch}} \le (T^{\mathrm{U}} - T_g^{\text{switch}})(1 - I_g) \tag{7.24}$$

$$P_h^{chosen} = P_{h-1}^{chosen} I_h + P_h (1 - I_h) \tag{7.25}$$

$$(P^L - P_h^{switch}) I_h < P - P_h^{switch} \le (P^U - P_h^{switch})(1 - I_h) \tag{7.26}$$

$$\rho = \frac{M}{0.6022V(1.0151)} \tag{7.27}$$

$$V = \sum_{k=2}^{8} v_k V_k \tag{7.28}$$

$$\mu = \frac{\rho M}{1000} \exp\left( \sum_{k=1}^{7} v_k A_{k,\mu} + \frac{\sum_{k=1}^{7} v_k B_{k,\mu}}{T_g^{\text{chosen}}} \right) \leq 0.1 \tag{7.29}$$

$$x_{\text{CO}_2,g,h} = \frac{y_1 P_h^{\text{chosen}} \varphi_1(T, P, y_1)}{\gamma_1 P_1^S} \tag{7.30}$$

$$\ln \gamma_i = \ln \gamma_i^{\,C} + \ln \gamma_i^{\,R} \tag{7.31}$$

$$\ln \varphi_i = \phi^r + \delta\phi_\delta^r - \ln\left(1 + \delta\phi_\delta^r\right) \tag{7.32}$$

$$\ln P_i^S = A_i - \frac{B_i}{T_g^{\text{chosen}} + C_i} \tag{7.33}$$

$$\sum_i y_i = 1 \tag{7.34}$$

$$\sum_i x_i = 1 \tag{7.35}$$

$$\sum_{k=1}^{7} v_k \geq 2 \tag{7.36}$$

$$\sum_{k=1}^{7} n_k v_k - 2\left( \sum_{k=1}^{7} n_k - 1 \right) = 0 \tag{7.37}$$

$$\sum_{m=3}^{4} \alpha_m = 1; \quad \sum_{n=5}^{7} \beta_n = 1 \tag{7.38}$$

Equation (7.22) is the objective function, and Equations (7.23) to (7.26) are temperature and pressure ranges selection using disjunctive programming. Equations (7.27) to (7.33) are prediction models for target properties and the rest are structural constraints. Solving the MINLP formulation, the optimal results were obtained and $[C_{14}MIm][BF_4]$ was determined as the optimal IL; while the optimal operating temperature range and pressure range were determined as 333.15 to 343.15 K and 0.90 to 1.00 MPa. This results means that $[C_{14}mim][BF_4]$ has the highest $CO_2$ solubility among all possible combinations of cation and anion in the identified temperature and pressure ranges, fulfilling all given constraints at the same time. It has a predicted solubility of 0.1846 mol $CO_2$/mol IL; while its viscosity is predicted to be 0.09431 Pa.s, which is less than the upper limit, i.e. 0.1 Pa.s. However, there is no solubility data for this IL in literature, and hence no comparison can be conducted at this time. Nine alternative ILs are determined by doing integer cuts, along with their respective optimal operating temperature range, and the results are shown in Table 7-7. As shown, the results obtained by solving this model corresponds to the best ILs that one could find from allowed combinations of anions and cations. This means that the proposed approach provide optimal structure of IL for $CO_2$ absorption, according to the given specifications or performance targets.

Given that literature data of ILs is scarce, predicted solubility was only compared to available experimental data, using Equation (7.39). The relative

deviations between literature experimental solubility data and predicted solubility data are shown in Table 7-7. Among all designed ILs, literature data is only available for one, which shows acceptable relative deviations (less than 10 %). The small difference occurs mainly due to the errors present in the chosen prediction models. This can be improved by either using other prediction models, or incorporate newly available experimental data into current models.

$$\text{Relative Deviation} = \frac{\left|\text{Experimental data} - \text{Predictedvalue}\right|}{\text{Experimental data}} \times 100 \tag{7.39}$$

Comparing the results obtained from integer cuts with the optimal result, it can be said that the global optimal is achieved. The proposed approach is shown to be able to design optimal ILs for carbon capture purpose and determine the optimal operating conditions simultaneously. Similar to previous approach in Chapter 5, this approach adapts group contribution (GC) based predictive models, and hence limited by the availability of contribution data.

**Table 7-7**: Optimal IL molecular design results

| IL chosen | Chosen system temperature range, $T_g^{chosen}$ (K) | Chosen system pressure range, $P_h^{chosen}$ (MPa) | Predicted viscosity, $\mu$ (PA.s) | Predicted solubility, $S_{g,h}$ (mol $CO_2$/mol IL) | Experimental solubility | Relative deviation (%) |
|---|---|---|---|---|---|---|
| $[C_{14}MIm][BF_4]$ | 333.15 – 343.15 | 0.90 – 1.00 | 0.09431 | 0.1846 | - | - |
| $[C_{10}MIm][BF_4]$ | 323.15 – 333.15 | 0.90 – 1.00 | 0.08628 | 0.1786 | - | - |
| $[C_{13}MIm][BF_4]$ | 333.15 – 343.15 | 0.90 – 1.00 | 0.08198 | 0.1756 | - | - |
| $[C_9MIm][BF_4]$ | 323.15 – 333.15 | 0.90 – 1.00 | 0.07313 | 0.1667 | - | - |
| $[C_{12}MIm][BF_4]$ | 333.15 – 343.15 | 0.90 – 1.00 | 0.07122 | 0.1665 | - | - |
| $[C_{11}MIm][BF_4]$ | 333.15 – 343.15 | 0.90 – 1.00 | 0.06183 | 0.1571 | - | - |
| $[C_8MIm][BF_4]$ | 323.15 – 333.15 | 0.90 – 1.00 | 0.06194 | 0.1547 | 0.1628(Gutkowski et al., 2006) | 4.98 |
| $[C_{14}MIm][BF_4]$ | 343.15 – 353.15 | 0.90 – 1.00 | 0.05532 | 0.1537 | - | - |
| $[C_{10}MIm][PF_6]$ | 333.15 – 343.15 | 0.90 – 1.00 | 0.09282 | 0.1480 | - | - |
| $[C_{10}MIm][BF_4]$ | 333.15 – 343.15 | 0.90 – 1.00 | 0.05363 | 0.1477 | - | - |

## 7.5 Regeneration Energy for Ionic Liquids and Monoethanolamine

For the designed ionic liquids (ILs) to be viable in industrial process, the energy required to reproduce high purity IL solvent should be lower than or equal to that of monoethanolamine (MEA). Therefore, the desorption process using MEA and all ten ILs shown in Table 7-7 was simulated using Aspen HYSYS version 8.4 (Sittler and Ajikutira, 2013) for comparison. Carbon dioxide ($CO_2$) absorption generally occurs in the range of 40 to 60 $^oC$; while desorption occurs around 110 to 140 $^oC$ (Li et al., 2013). After the absorption process, $CO_2$ rich solvent is preheated prior to the desorption process. $CO_2$ desorption from MEA and IL are simulated based on process described by Li et al. (2013) and Ali et al. (2013). For MEA solvent regeneration, the desorption unit was modelled as desorber with reboiler as shown in Figure 7-5 (Li et al., 2013); while the desorption unit for ILs solvent regeneration was modelled using flash column as presented in Figure 7-6 (Ali et al., 2013a). NRTL fluid package was used to simulate $CO_2$ desorption from MEA solvent (Zhang and Chen, 2013), because the process involves non-ideal system and polar mixtures. On the other hand, Peng-Robinson fluid package was used for simulation of $CO_2$ desorption from ILs, because it was shown that Peng-Robinson is suitable to model this process (Ali et al., 2013a). The total energy required to regenerate different solvents are shown in Table 7-8.

The absorption temperature is the temperature of $CO_2$-rich solvent before entering the heater. As shown, the total energy required to regenerate MEA solvent is highest among all, which indicates that the designed ILs using proposed approach are suitable to replace MEA in $CO_2$ absorption.

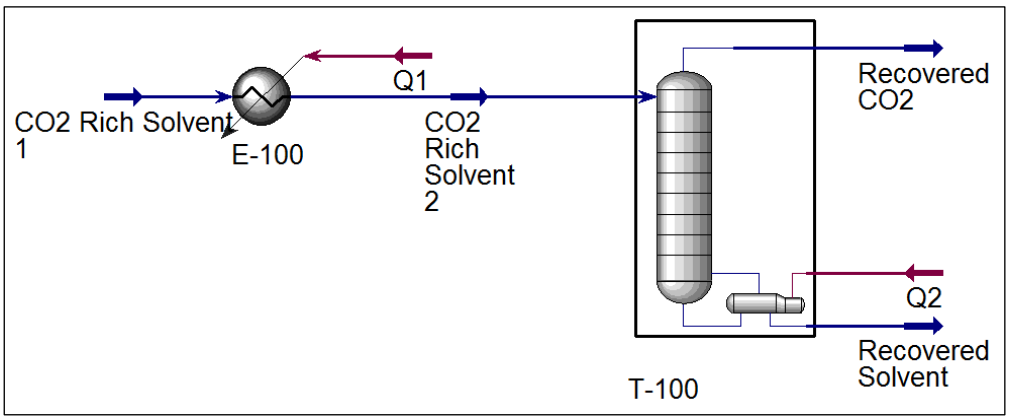


**Figure 7-5**: Desorption of $CO_2$ from MEA solvent

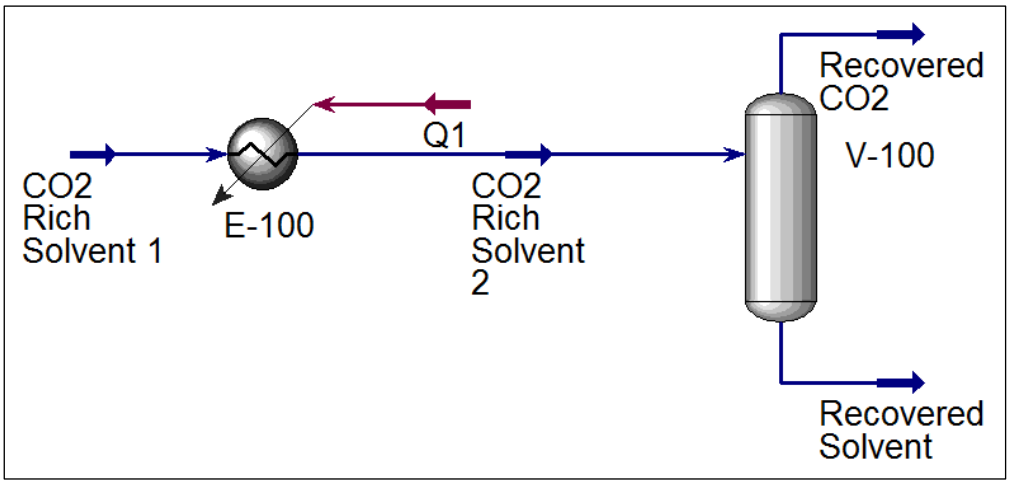


**Figure 7-6**: Desorption of $CO_2$ from IL solvent

**Table 7-8**: Energy required for solvent regeneration

| Solvent | Absorption Temperature (K) | Absorption Pressure (MPa) | Energy required (kJ/mol $CO_2$) |
|---|---|---|---|
| 30 wt% MEA | 328.15 | 0.95 | 136.70 |
| $[C_{14}MIm][BF_4]$ | 338.15 | 0.95 | 64.10 |
| $[C_{10}MIm][BF_4]$ | 328.15 | 0.95 | 75.66 |
| $[C_{13}MIm][BF_4]$ | 338.15 | 0.95 | 62.23 |
| $[C_9MIm][BF_4]$ | 328.15 | 0.95 | 77.97 |
| $[C_{12}MIm][BF_4]$ | 338.15 | 0.95 | 60.50 |
| $[C_{11}MIm][BF_4]$ | 338.15 | 0.95 | 58.23 |
| $[C_8MIm][BF_4]$ | 328.15 | 0.95 | 68.76 |
| $[C_{14}MIm][BF_4]$ | 348.15 | 0.95 | 78.61 |
| $[C_{10}MIm][PF_6]$ | 338.15 | 0.95 | 60.54 |
| $[C_{10}MIm][BF_4]$ | 338.15 | 0.95 | 61.62 |

## 7.6 Effect of Temperature on Carbon Dioxide Solubility and Viscosity of Ionic Liquids

After the potential ionic liquids (ILs) were obtained in the Section 7.4.6, integer cuts were done further to study the effect of temperature on two important properties of ILs, i.e. carbon dioxide ($CO_2$) solubility and viscosity. The ILs that were studied in this work are all imidazolium based with one alkyl chain between C6 to C12 and one methyl group, for three different anions including tetrafluoroborate, hexafluorophosphate, and chloride. The results are shown in Figure 7-7 to Figure 7-12. In general, the figures show that the amount of $CO_2$ solubility increases with the increasing carbon chain length attached to cation core. These results tally with literature study done by Baltus et al. (2004) on $CO_2$ solubility of different imidazolium-based ILs. Apart from that, Figure 7-7, Figure 7-9 and Figure 7-11 also show that, ILs

can absorb more $CO_2$ at lower temperature range. This trend is similar to the experimental results shown by Karadas et al. (2013). In Figure 7-8, Figure 7-10 and Figure 7-12, the ILs viscosity is shown to be decrease with increasing temperature. The study also shows that viscosity of ILs increase when the alkyl chain attached to imidazolium cation core increases. Therefore, the ILs that are chosen for $CO_2$ absorption have longer alkyl chain, and the optimal operating temperature chosen will be as low as possible.

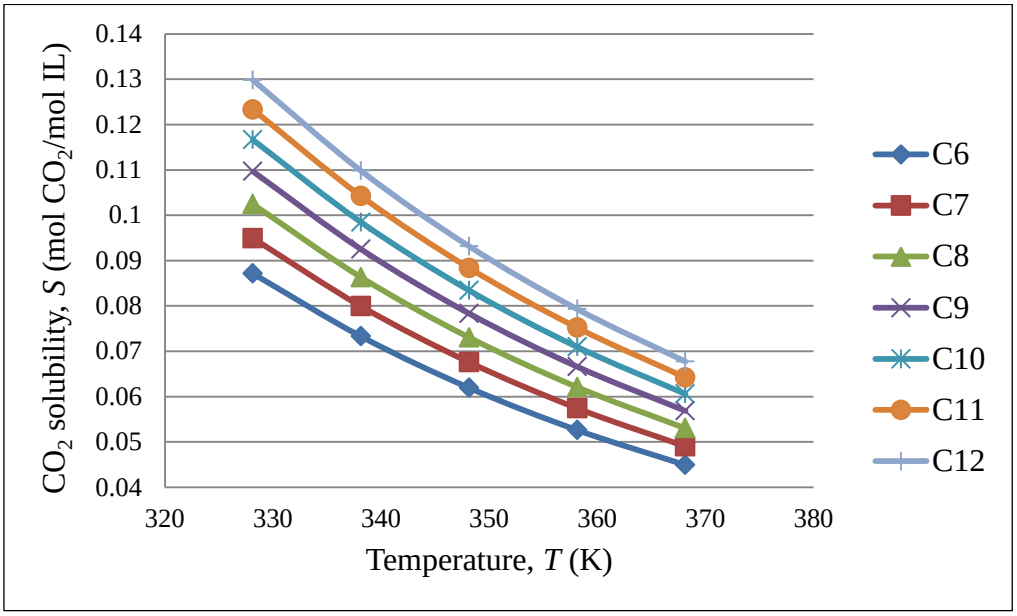


**Figure 7-7**: Effect of temperature on $CO_2$ solubility 1-alkyl-3-methylimidazolium tetrafluoroborate

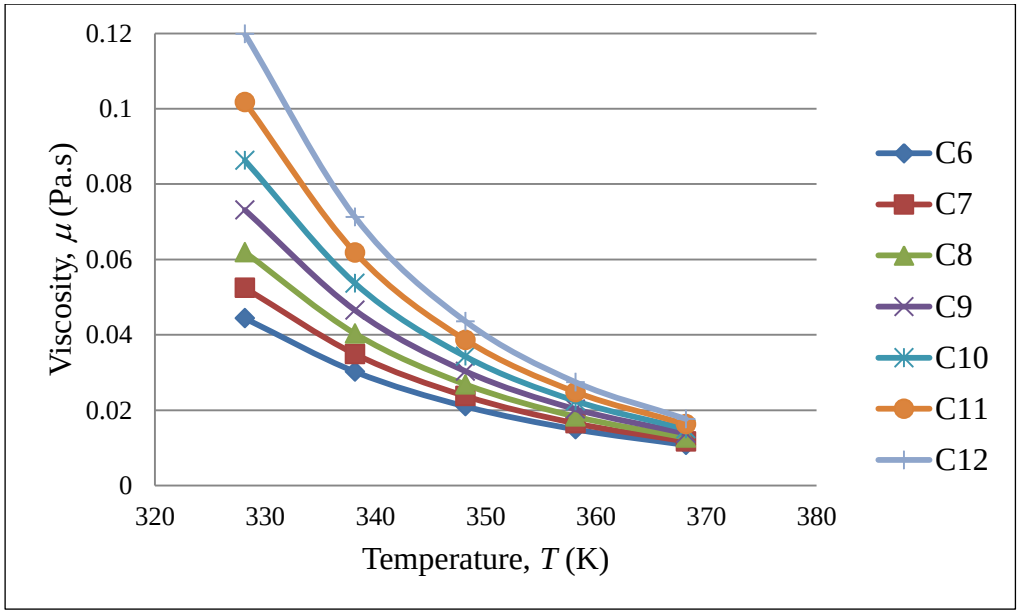


**Figure 7-8**: Effect of temperature on viscosity of 1-alkyl-3-methylimidazolium tetrafluoroborate

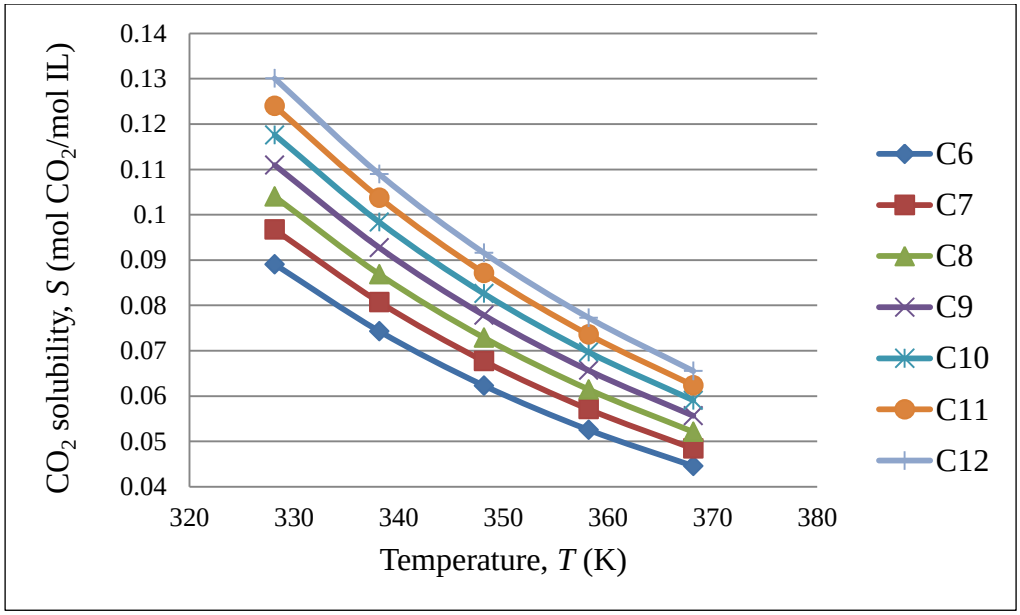


**Figure 7-9**: Effect of temperature on $CO_2$ solubility 1-alkyl-3-methylimidazolium hexafluorophosphate

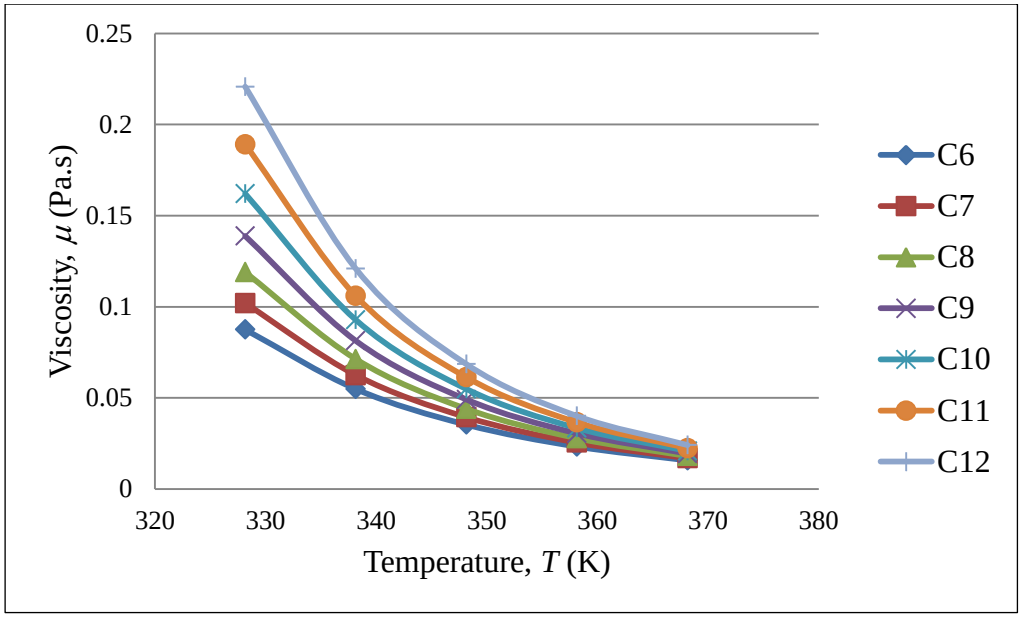


**Figure 7-10**: Effect of temperature on viscosity of 1-alkyl-3-methylimidazolium hexafluorophosphate

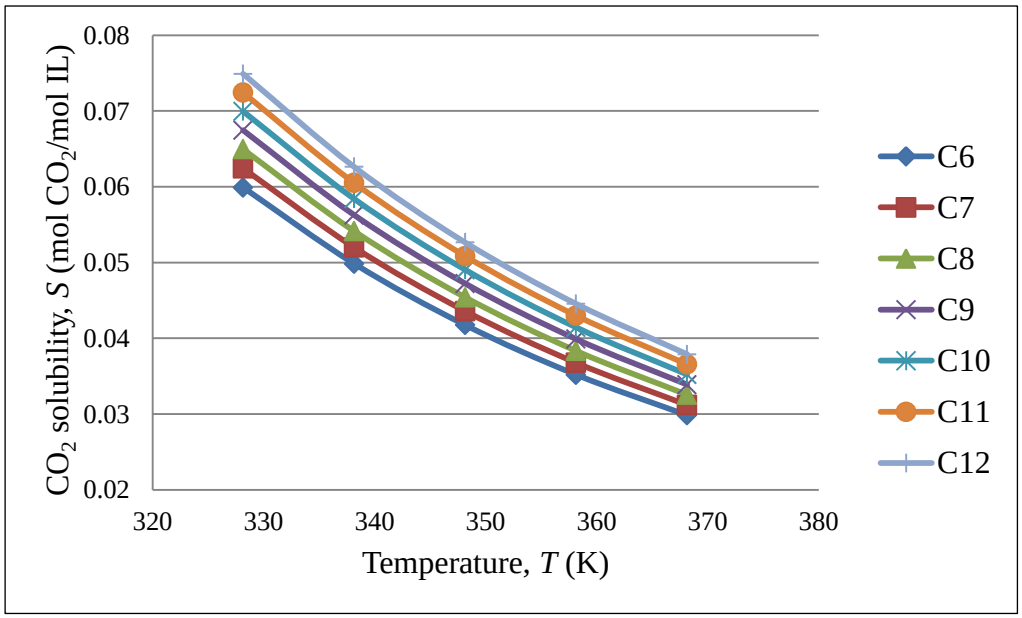


**Figure 7-11**: Effect of temperature on $CO_2$ solubility of 1-alkyl-3-methylimidazolium chloride

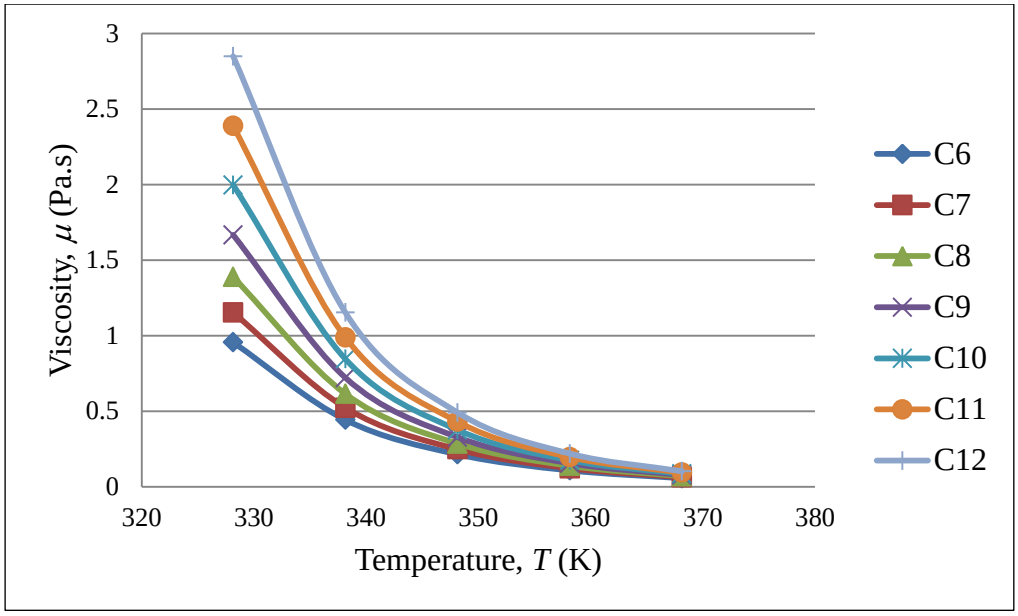


**Figure 7-12**: Effect of temperature on viscosity of 1-alkyl-3-methylimidazolium chloride

## 7.7 Summary

In this chapter, a systematic approach based on computer-aided molecular design (CAMD) technique, was developed for optimal ionic liquid (IL) design and simultaneous target of operating conditions for carbon capture process. The proposed approach was extended from methodology presented in Chapter 5, as a first step to integrate IL design and process design. Optimal IL solvent can be determined for carbon capture purpose using proposed approach, and its optimal operating conditions will be identified through disjunctive programming at the same time. An illustrative case study was presented to show the proposed approach. A mixed integer non-linear programming (MINLP) model was formulated and solved for this case study

to determine the optimal IL with highest carbon dioxide ($CO_2$) solubility, and at the same time determine the optimal operating conditions using designed ILs. The energy demand to regenerate the designed ILs after $CO_2$ absorption ware determined by using Aspen HYSYS simulation, and the results were compared to monoethanolamine (MEA). The results show that ILs need lower amount of energy during solvent regeneration, as compared to MEA. The effect of temperature on $CO_2$ solubility and viscosity of ILs was studied as well. The results suggest that the lower the temperature, the higher the $CO_2$ solubility and viscosity of ILs. Thus, the trade-off between these two properties must be evaluated during ILs design for carbon capture. The formulation utilised group contribution (GC) property predictive models, and thus the accuracy of this approach depends on the accuracy of the accuracy of prediction models used. Similar to approach developed in Chapter 5, the selectivity of $CO_2$ over other gases was not considered. In this approach, only the relationship between operating conditions of carbon capture process and ILs was considered. However, the performance of whole process will be affected by the choice of IL as well. This design consideration will be studied in Chapter 8.

# CHAPTER 8

# INTEGRATION OF IONIC LIQUID DESIGN AND PROCESS DESIGN

## 8.1 Introduction

Different approaches have been developed to solve ionic liquid (IL) and IL mixture design problem for carbon capture purpose. The effects of IL solvent on carbon capture system operating conditions have been demonstrated in previous chapter, but the effect on overall process was not studied. Carbon capture system is implemented commonly to reduce carbon dioxide ($CO_2$) emission from a process and fulfil the emission limit set by authorised organisations. However, performance of the process can be affected when carbon capture system is installed, including the increment in utility consumption and operating cost. Therefore, the integration of IL design and process should be done to study these effects, at the same time to confirm that addition of carbon capture system is favourable from different aspects. Extending the approach proposed in Chapter 7, a systematic approach to design IL as carbon capture solvent with the consideration of effects on overall process is presented in this chapter. The developed approach adapts the data of process involved prior to carbon capture, to design IL solvent by targeting most optimum carbon capture performance within a range of operating conditions. An illustrative example involving bio-energy production system

was solved to demonstrate the proposed approach. Combination of bio-energy system and carbon capture system is one of the potential technologies with negative $CO_2$ emission (i.e. removing $CO_2$ from the atmosphere). The effect of carbon capture system on bio-energy system was studied, specifically on the utilities required by carbon capture system and parasitic loads on bio-energy system. Bio-energy system can supply different energy products to carbon capture system, but it will increase the amount of $CO_2$ produced and also the utilities required by carbon capture system. Therefore, this effect was studied using proposed approach; designers can decide how the bio-energy system should be retrofitted according to the results.

## 8.2 Problem Statement

The overall problem to be addressed is stated as follows: Develop a systematic approach to design an optimal ionic liquid (IL) carbon capture solvent and its optimal operating conditions, from a given set of pre-selected cation cores, anions, and organic functional groups to meet the target properties and constraints. The optimal IL solvent should designed based on design objective, and it must satisfy all target properties and constraints. The approach should also take the effect of carbon capture system on the entire process, and assist in making decision about retrofitting the entire process, to ensure the process is efficient and yet environmental friendly. A superstructure representation of all allowed combinations of molecular building blocks is shown in Figure 8-1. The specific problem to be addressed is stated as follows:

1) Design an IL with the most optimal performance from the groups available in the superstructure, considering the effect of carbon capture system on the entire process. The designed IL must fulfil all target properties and constraints.
2) The superstructure comprises of *r* organic functional groups, *s* cation cores, and *t* anions. These groups are selected based on gas absorption and separation performance of IL beforehand (Baltus et al., 2004). Since this work aims to design pure IL for carbon capture, the choice of cation core and anion is limited to one each.
3) Operating temperature, *T* and operating pressure, *P* are modelled as variables so that the model will determine the optimal operating conditions for the carbon capture system using the chosen IL.
4) The selectivity of other gases over carbon dioxide ($CO_2$) is assumed to be negligible during the development of this approach.

## 8.3 Optimisation Model

A generic formulation to design ionic liquid (IL) solvent and implementing carbon capture system in an existing process is shown in this section. Firstly, all related information of the process should be gathered, and the outputs of the process can be determined by using input-output (IO) models. The collected information is then used to identify the optimal IL solvent that suits the process based on an objective, subject to all relevant constraints, similar to the approach presented in Chapter 7. Once the solvent is

identified, the effect of carbon capture system installation on the entire process will be studied, followed by decision making on modification of the process to accommodate the carbon capture system installation.

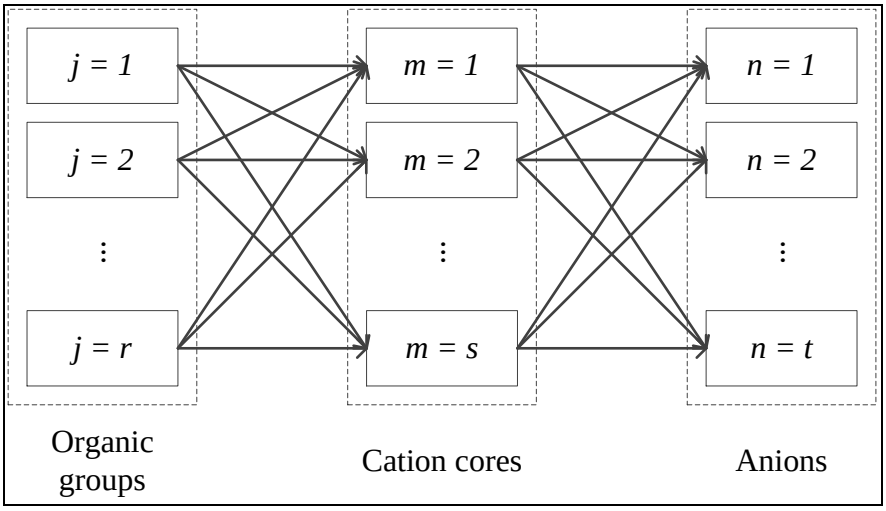


**Figure 8-1**: Schematic representation of combinations of all groups (replicated from Figure 4-1)

### 8.3.1 Input-Output Modelling

IO modelling was used to represent existing process prior to carbon capture system, enabling user to determine the conditions and flowrates of all outputs of the process. The IO models employed are similar to those used in the proposed analytical framework for industrial ecosystems (Duchin, 1992), modelling sudden perturbations to complex industrial networks (Khanna and Bakshi, 2009), and analysing bottlenecks in multi-functional energy systems (Tan et al., 2012). IO modelling is a method to systematically quantify mutual

interrelationships between components of a complex system in one or more time periods (Miller and Blair, 1985). Although this approach was initially developed and used for modelling the quantitative relationships of economic systems (Leontief, 1936), it can be applied to any network or system with various component units such as a bio-energy system. The earliest application of IO models to analyse industrial complexes was demonstrated by Isard and Schooler (1959).

Each component unit is described using only key mass or energy balances and expressed using an IO model in its matrix form, as described by Equation (8.1).

$$\mathbf{Aw} = \mathbf{z} \tag{8.1}$$

where **A** is the process matrix that contains coefficient ratios of mass or energy balances in the system, **w** is the component unit capacity vector, and **z** is the final output vector. Then, a model developed for simultaneous exogenous specifications in the component unit capacity and final output of a given system is used. The approach here is based on the method developed for linear economic systems (Leung et al., 2007) and industrial networks (Khanna and Bakshi, 2009). Equation (8.2) is obtained by rearrangement of Equation (8.1).

$$\begin{bmatrix} 0 & \mathbf{A}' \\ -\mathbf{I} & \mathbf{A}'' \end{bmatrix} \begin{bmatrix} \mathbf{z}'' \\ \mathbf{w}' \end{bmatrix} = \begin{bmatrix} \mathbf{B}' & \mathbf{I} \\ \mathbf{B}'' & 0 \end{bmatrix} \begin{bmatrix} \mathbf{w}'' \\ \mathbf{z}' \end{bmatrix} \tag{8.2}$$

For an $l \times l$ matrix (i.e., a square matrix or a system with $l$ component units with corresponding $l$ main product streams), $p$ is the set of final output (e.g., product streams) with exogenous specifications ($z_1$, $z_2$, …, $z_p$). The remaining ($l$ - $p$) set is the exogenous specification of the capacity vector that contains the component units with reduced capacity ($w_{p+1}$, $w_{p+2}$, …, $w_l$). **A**' is the $p \times p$ matrix containing the elements from the first $p$ rows and first $k$ columns in matrix **A**. **A**'' is the ($l$ - $p$) × $p$ matrix containing the elements from the first ($l$ - $p$) rows and the first $p$ columns in matrix **A**. **B**' is the $p \times (l - p)$ matrix containing the elements from the first $p$ rows and the last ($l$ - $p$) columns in matrix (–**A**). **B**'' is the ($l$ - $p$) × ($l$ - $p$) matrix containing the elements from the first ($l$ - $p$) rows and ($l$ - $p$) columns in matrix (–A). Meanwhile, **w**' is $p$-element column vector containing $w_1$ to $w_p$, which are the endogenous capacity of the component units and **w**'' is the ($l$ - $p$) element column vector containing $w_{p+1}$ to $w_l$, which are the component units with exogenously specified capacity. **z**' is the $k$-element column vector containing elements $z_1$ to $z_p$, which are the exogenously defined final outputs. Lastly, **z**'' is the ($l$ - $p$) element column vector containing elements $z_{p+1}$ to $z_l$, which are the endogenous final output streams.

### 8.3.2 Solution Procedure

The proposed approach to solve an IL design problem for carbon capture, considering its effect on the overall process, is presented in this section and summarised in Figure 8-2.

Step 1: Collect all related information of the process that will install carbon capture system, which will be used to identify the flowrate and conditions output (i.e. input to carbon capture system).

Step 2: Identify the total outputs of the process prior to carbon capture using IO models. The flowrate and conditions of the output with carbon dioxide ($CO_2$) is used to design IL solvent in the following steps. In this step, the total amount of $CO_2$ to be captured is also determined.

Step 3: Identify the design objective and target properties for the IL design problem. Based on IL solvent application and specifications, objective can be defined and the upper or lower limit of target properties is specified as constraints. The operating conditions of the carbon capture process are included as part of the optimisation objective, because they affect the performance of IL and the process. The optimisation objective can be written in general as shown by Equation (8.3).

$$\text{maximise} \quad f_{g,h} \qquad \forall g,h \tag{8.3}$$

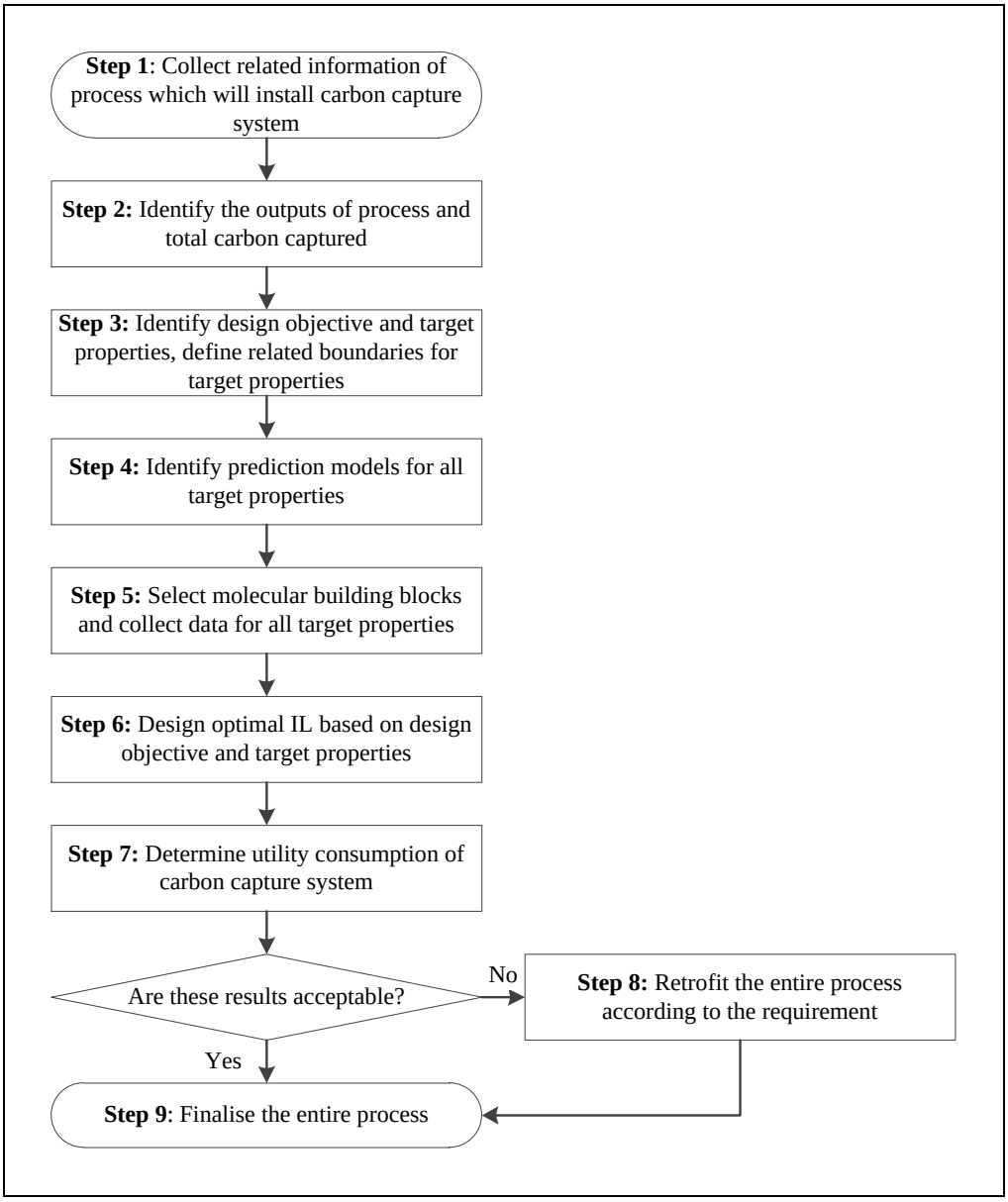


**Figure 8-2**: Systematic approach to design IL for a carbon capture system, considering the effect of carbon capture system installation

where $f_{g,h}$ is the objective of design problem in temperature range *g* and pressure range *h*. Equation (8.3) shows that the objective is maximised, however maximising or minimising the objective is

dependent on the main concern in the process. Disjunctive programming is used in this proposed approach to reformulate continuous variables of temperature and pressure as piecewise functions over discrete domains, as presented in Chapter 5.

Step 4: Choose an appropriate prediction model for each target property that can make accurate estimation. The choice of prediction models is important because they will affect the accuracy of the proposed approach.

Step 5: Select suitable molecular building blocks, including organic groups, cations, and anions, that can form a complete IL. These molecular building blocks are chosen such that IL built using them provides properties similar to the conventional solvent. The data of all target properties for chosen building blocks are collected.

Step 6: Based on the design objective, design an optimal IL that can fulfil all the target properties, with its optimal operating conditions. Similar to mathematical approach presented in Chapters 5 and 7, selectivity of other gases over $CO_2$ is not considered in this approach. The equilibrium relationships are included, as given in Equation (8.4).

$$y_i P_h^{\text{chosen}} \varphi_i\left(T, P, y_i\right) = x_i \gamma_i P_i^{\text{S}} \tag{8.4}$$

$x_i$ and $y_i$ are the mole fractions of component $i$ in liquid and gas phases respectively, $\gamma_i$ is activity coefficient, $P_i^S$ is the saturated vapour pressure of component $i$, and $\varphi_i(T,P,y_i)$ is the gas-phase

fugacity coefficient. The activity coefficient is determined using UNIFAC model, which details are given in Appendix Section A.2.1. Group parameters and binary interaction parameters of IL for UNIFAC model presented by Lei et al. (2013) have been used in this approach. Gas-phase fugacity coefficient are determined using equation of state proposed by Span and Wagner (1996), the details are explained in Appendix Section A.2.2. Extrapolated Antoine equation was applied to determine saturated vapour pressure of $CO_2$ (Shiflett and Yokozeki, 2006). Relevant constraints must be included to ensure the designed IL solvent is a valid solution to the problem. Since carbon capture process involves liquid and gas phases, summation of mole fractions for both phases is included as constraints. This ensures that vapour faction, $y_i$ and liquid fraction, $x_i$ always sum up to unity, as given by Equations (8.5) and (8.6).

$$\sum_i y_i = 1 \tag{8.5}$$

$$\sum_i x_i = 1 \tag{8.6}$$

The molecular structure of designed IL must consist of at least two building blocks, as shown in Equation (87). Equation (8.8) indicates that final IL molecular structure must not have any free bond. In Equations (8.7) and (8.8), $v_k$ is the number of group $k$ and $n_k$ is the available free bond of group $k$.

$$\sum_k v_k \geq 2 \tag{8.7}$$

$$\sum_k n_k v_k - 2\left(\sum_k n_k - 1\right) = 0 \tag{8.8}$$

In a pure IL, only one cation and one anion should occur, and therefore Equations (8.9) and (8.10) are added to enforce only one pair of cation and anion will be selected. In both equations, $\alpha_m$ and $\beta_n$ are the binary variables representing each cation *m* and each anion *n*, respectively.

$$\sum_m \alpha_m = 1 \tag{8.9}$$

$$\sum_n \beta_n = 1 \tag{8.10}$$

Step 7: Determine the total utility consumption of carbon capture system using designed IL solvent. These are important because they affect the final outputs and outcome of the overall process, including economic potential and environmental impact. Figure 8-3 shows a general process flow diagram for carbon capture process using IL solvent, without any integration. As shown in Figure 8-3, power, heating and cooling utilities are required, which can be determined through basic energy balance or simulation. Users then have to decide whether the calculated utilities of carbon capture system are feasible and acceptable. If the results are not acceptable, user can

proceed to Step 8 to retrofit the entire process, and proceed to Step 9 if the results are acceptable.

Step 8: Carry out retrofit on the entire process, including carbon capture. Different approaches can be done to reduce the utilities consumption of carbon capture system. For example, heat integration can be done to reduce the heating and cooling utilities, at the same time reduce operating cost.

Step 9: Finalise the entire process together with carbon capture system, when the utilities consumption are determined in Step 7 or Step 8.

## 8.4 Case Study

A case study adapted from Andiappan et al. (2015) is presented here to demonstrate the proposed approach. In this case study, the carbon capture system will be installed in an existing palm-based *biomass tri-generation system* (BTS). Biomass, which originates from plants or plant-based materials, has long been investigated as a substitute for fossil fuels (Kheshgi et al., 2000). Plant-based materials consume carbon dioxide ($CO_2$) during photosynthesis, energy production using biomass (hereinafter named bio-energy production) later releases $CO_2$ into the atmosphere (Naik et al., 2010). In other words, bio-energy production is deemed $CO_2$ neutral as it results in zero net or minimum increase of $CO_2$ in the atmosphere (Naik et al., 2010).

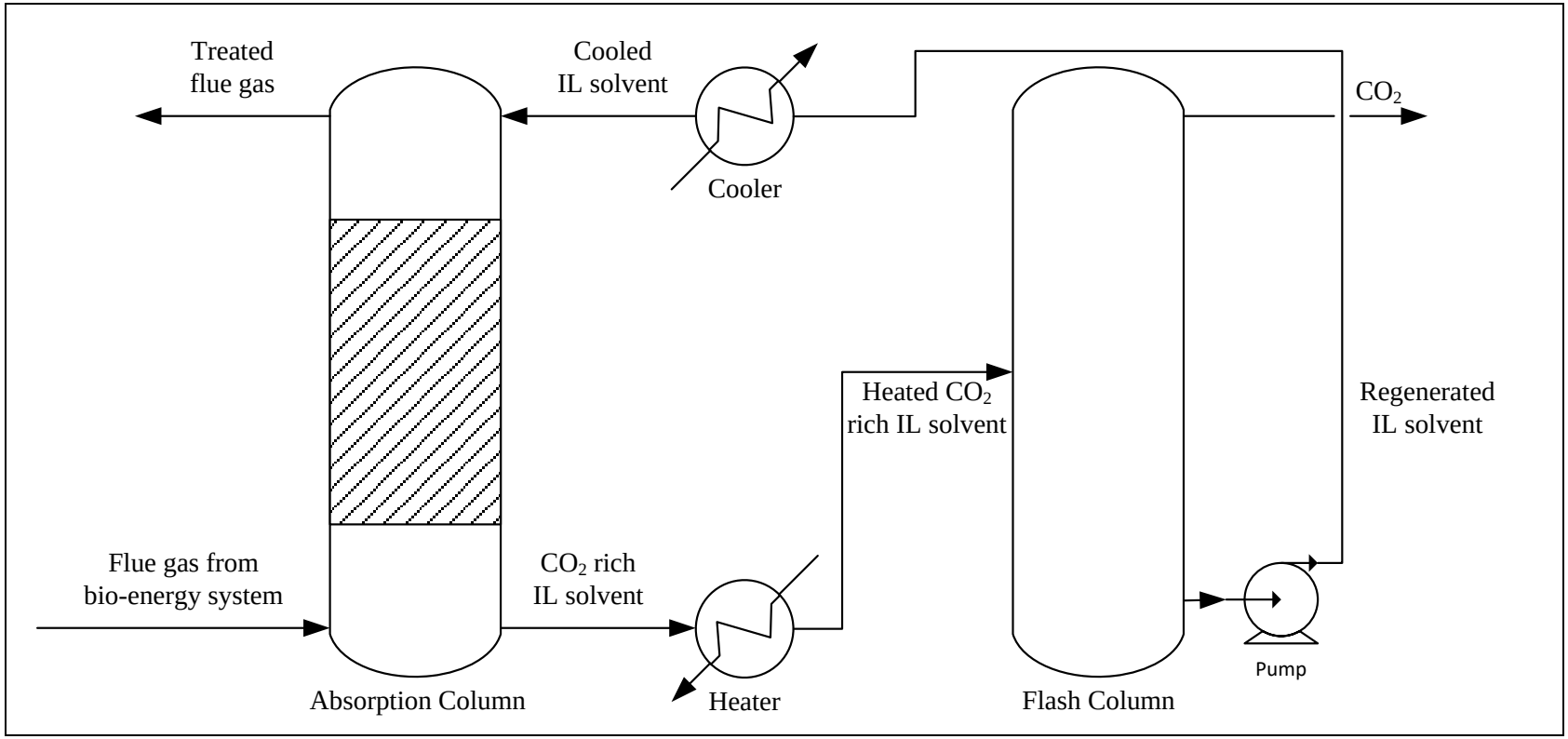


**Figure 8-3**: Process flow diagram for carbon capture system using IL solvent

Following this, several studies (Kraxner et al., 2003; Möllersten et al., 2004; Ooi et al., 2013) highlighted the potential of integrating bio-energy production with *carbon capture*, or in short *bio-energy with carbon capture* (BECC). Capturing $CO_2$ from biomass burning result in negative $CO_2$ emissions, yields zero net $CO_2$ and also removes $CO_2$ from the atmosphere (Möllersten et al., 2003). Such capability allow bio-energy systems to store more carbon than they emit, making a critical step towards a zero-carbon future (Sanders, 2015).

Figure 8-4 shows the schematic diagram of an existing palm-oil based BTS, which utilises several types of palm-based biomass as feedstock to produce cooling, heating, and power simultaneously. For instance, *palm mesocarp fibre* (PMF) and *empty fruit bunches* (EFBs) are combusted in water tube boilers to produce high pressure steam for heat and power generation. On the other hand, *palm oil mill effluent* (POME) is treated in an anaerobic digester, resulting in production of biogas. The biogas (65% methane and 35% $CO_2$) produced is then purified and sent to gas turbines for power generation. Flue gas released from BTS contains high amount of $CO_2$, and the purpose of carbon capture system installation is to separate $CO_2$ from flue gas as a by-product. In this respect, the objective of this case study is to design a suitable IL solvent for post-combustion carbon capture within BECC scheme.

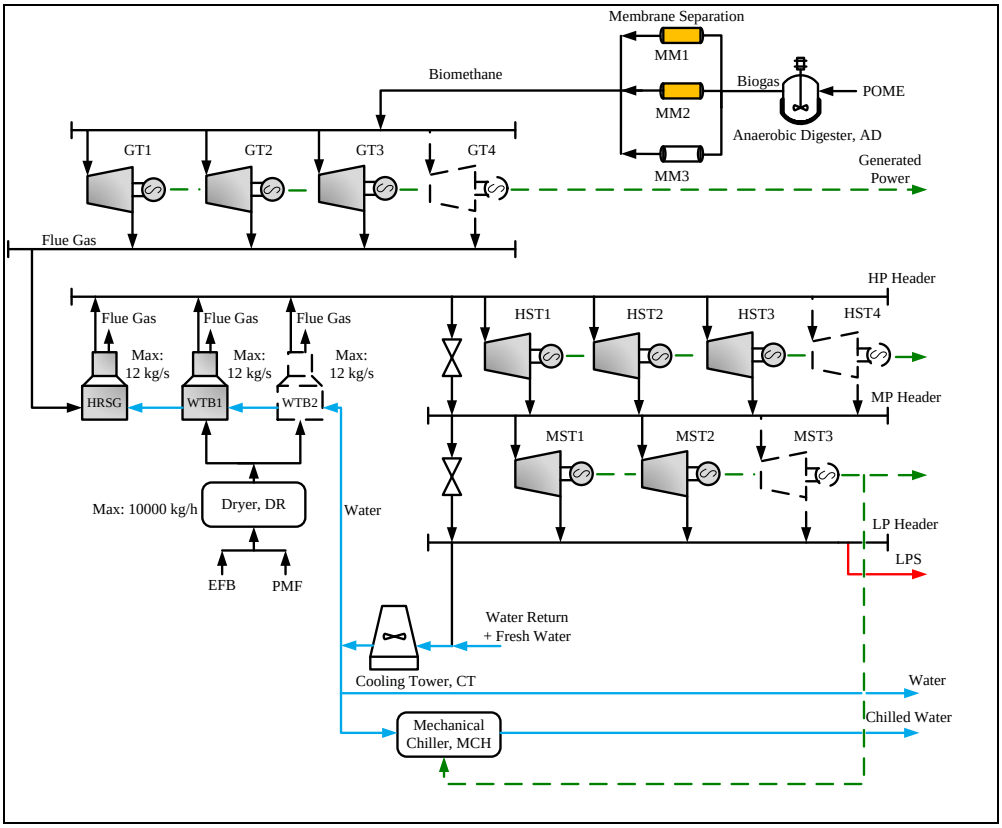


**Figure 8-4**: Existing palm oil-based BTS

### 8.4.1 Step 1: Collect related information of process which will install carbon capture system

Firstly, all related information of the palm oil-based BTS was collected. Table 8-1 shows a list of equipment in the BTS, along with the mass and energy balances of each technology within the operating BTS, where positive and negative values denote outputs and inputs respectively. These values were obtained from the design stage presented in Andiappan et al. (2015).

**Table 8-1**: Mass and energy balance data for technologies in palm-based BTS

| | AD | MM1 | MM2 | GT1 | GT2 | GT3 | HRSG | WTB1 | DR |
|---|---|---|---|---|---|---|---|---|---|
| POME (kg $h^{-1}$) | -55500.000 | | | | | | | | |
| Biogas (kg $h^{-1}$) | 319.130 | -159.565 | -159.565 | | | | | | |
| Biomethane (kg $h^{-1}$) | | 157.965 | 157.965 | -105.310 | -105.310 | -105.310 | | | |
| Power (kW) | | -47.870 | -47.870 | 416.300 | 416.300 | 416.300 | | | |
| High Temp. Flue Gas (kg $h^{-1}$) | | | | 526.570 | 526.570 | 526.570 | -1579.710 | | |
| Released Flue Gas (kg $h^{-1}$) | | | | | | | 1579.710 | 32558.010 | |
| Return Water (kg $h^{-1}$) | | | | | | | | | |
| Cooling Water (kg $h^{-1}$) | | | | | | | -1671.840 | -39268.050 | |
| Chilled Water (kg $h^{-1}$) | | | | | | | | | |
| EFB (kg $h^{-1}$) | | | | | | | | | -16875.000 |
| PMF (kg $h^{-1}$) | | | | | | | | | -9245.300 |
| Dried Biomass (kg $h^{-1}$) | | | | | | | | -11950.800 | 11950.800 |
| HPS (kg $h^{-1}$) | | | | | | | 1671.840 | 39268.050 | |
| MPS (kg $h^{-1}$) | | | | | | | | | |
| LPS (kg $h^{-1}$) | | | | | | | | | -12814.880 |

AD, anaerobic digester; MM, membrane separator; GT, gas turbine; HRSG, heat recovery steam generator; WTB, water tube boiler; DR, dryer;

**Table 8-1**: (Continued)

| | CT | MCH | HST1 | HST2 | HST3 | MST1 | MST2 | **Final Output** |
|---|---|---|---|---|---|---|---|---|
| POME (kg $h^{-1}$) | | | | | | | | -55500.000 |
| Biogas (kg $h^{-1}$) | | | | | | | | 0.000 |
| Biomethane (kg $h^{-1}$) | | | | | | | | 0.000 |
| Power (kW) | | -6.310 | 453.220 | 453.220 | 453.220 | 161.600 | 161.600 | 2781.840 |
| High Temp. Flue Gas (kg $h^{-1}$) | | | | | | | | 0.000 |
| Released Flue Gas (kg $h^{-1}$) | | | | | | | | 34137.720 |
| Return Water (kg $h^{-1}$) | -57218.000 | | | | | | | -57218.000 |
| Cooling Water (kg $h^{-1}$) | 56218.000 | -279.000 | | | | | | 14999.110 |
| Chilled Water (kg $h^{-1}$) | | 1000.000 | | | | | | 1000.000 |
| EFB (kg $h^{-1}$) | | | | | | | | -16875.000 |
| PMF (kg $h^{-1}$) | | | | | | | | -9245.300 |
| Dried Biomass (kg $h^{-1}$) | | | | | | | | 0.000 |
| HPS (kg $h^{-1}$) | | | -13646.630 | -13646.630 | -13646.630 | | | 0.000 |
| MPS (kg $h^{-1}$) | | | 13646.630 | 13646.630 | 13646.630 | -20469.945 | -20469.945 | 0.000 |
| LPS (kg $h^{-1}$) | | | | | | 20469.945 | 20469.945 | 28125.010 |

CT, cooling tower; MCH, Mechanical chiller; HST, high pressure steam turbine; MST, medium pressure steam turbine

### 8.4.2 Step 2: Identify the outputs of process and total carbon captured

As shown in Figure 8-2, the outputs from BTS and the total carbon captured were identified in this step. In this case study, the existing mass and energy balances of BTS were represented using the input-output (IO) modelling approach presented in Section 8.3.1. Based on the IO modelling approach, the process matrix **A** consists of the first 15 data rows and first 16 data columns as shown in Table 8-1, meanwhile the last column constitutes the final output vector **z**. Each column in matrix **A** is considered a process vector wherein key mass or energy balances are presented as ratios and are assumed to be scale-invariant. Following this, the final input and output for the BTS is given in Figure 8-5. The amount of flue gas produced is 34,138 kg $h^{-1}$ at an average temperature of 873.15 K. The flue gas stream consists of $CO_2$ and water vapour, their respective compositions are 72 wt% and 18 wt%. The total amount of carbon captured should be specified to fulfil $CO_2$ emission standard. However, there is no $CO_2$ emission standard for industry in Malaysia (Department of Environment, 2010), therefore a 90% of carbon captured was used in this case study for illustration purpose.

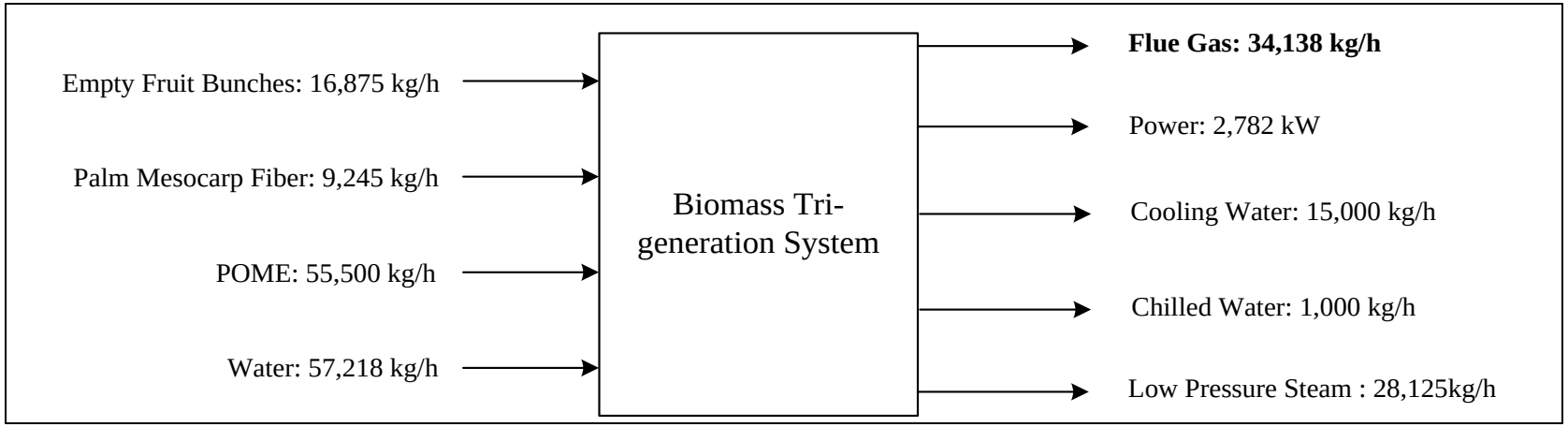


**Figure 8-5**: IO model for BTS

### 8.4.3 Step 3: Identify design objective and target properties, define related boundaries for target properties

In this step, the design objective and all influential properties related to the process was identified. Since the ionic liquid (IL) is designed for carbon capture purpose, $CO_2$ solubility ($S$) of IL is set as the design objective and it should be maximised in this case study. Two other properties were considered in this case study, namely density ($\rho$) and viscosity ($\mu$). Density is the basic transport property, viscosity affects the pumping power requirement and operating cost (Kuhlmann et al., 2007). The target ranges for these properties are included in Table 8-2. The designed IL solvent should possess similar properties as conventional carbon capture solvent, i.e. ethanolamines. Hence, the ranges of target properties are set according properties of ethanolamines (The Dow Chemical Company, 2003). Viscosity of designed IL solvent should be as low as possible to minimise pumping power required to circulate it within the process. Therefore, the target range of viscosity is set to be below 0.1 Pa.s (Bonhôte et al., 1996).

**Table 8-2**: Target property ranges to design IL solvent

| Property | Lower bound | Upper bound |
|---|---|---|
| Density, $\rho$ (g cm$^{-3}$) | 1.0 | 2.0 |
| Viscosity, $\mu$ (Pa.s) | 0 | 0.1 |

### 8.4.4 Step 4: Identify prediction models for all target properties

Appropriate prediction models were selected in this step, to predict the properties of designed IL. Equations (8.11) to (8.15) are prediction models to estimate density (Gardas and Coutinho, 2008a) and viscosity (Gardas and Coutinho, 2008b). Equation (8.16) was used to determine $CO_2$ solubility of ILs, *S* in terms of kmole $CO_2$ per kmole IL.

$$\rho = \frac{M}{NV\left(a + bT_g^{\text{chosen}} + cP_h^{\text{chosen}}\right)} \tag{8.11}$$

$$V = \sum_k v_k V_k \tag{8.12}$$

$$\ln \frac{1000\mu}{\rho M} = A_\mu + \frac{B_\mu}{T_g^{\text{chosen}}} \tag{8.13}$$

$$A_\mu = \sum_k v_k A_{\mu,k} \tag{8.14}$$

$$B_\mu = \sum_k v_k B_{\mu,k} \tag{8.15}$$

$$S = x_{CO_2} / x_{IL} \tag{8.16}$$

In Equation (8.11), $\rho$ is IL density in g $cm^{-3}$, *M* is IL molecular weight in g $mol^{-1}$, *N* is the Avogadro constant (given as 0.6022), *V* is the molecular volume of IL in $Å^3$, the coefficients *a*, *b* and *c* were estimated as 0.8005, 6.652 × $10^{-4}$ $K^{-1}$ and -5.919 × $10^{-4}$ $MPa^{-1}$ respectively. Equation (8.12) shows that molecular volume of IL is equivalent to the sum of molecular volume of each

group $k$ ($V_k$) that occurs in the structure. In Equation (8.13), $\mu$ is IL viscosity in Pa.s, $A_{\mu,k}$ and $B_{\mu,k}$ in Equations (8.14) and (8.15) are contributions of group $k$ to parameters $A_\mu$ and $B_\mu$.

### 8.4.5 Step 5: Select molecular building blocks and collect data that fulfils all target properties

Suitable molecular building blocks were chosen in this step. Table 8-3 shows the molecular fragments chosen for this design problem. These molecular fragments were chosen because they are among the most widely studied cations and anions (Zhou et al., 2009). For these selected molecular building blocks, the relevant data of each target property is given in Table 8-4, as well as the number of free bond for each functional group. These data were obtained from Gardas and Coutinho (2008a, 2008b), according to the selected prediction models in Section 8.4.4.

**Table 8-3**: Organic function groups, cation cores, and anions considered in this case study

| Type | $k$ | Groups | Type | $k$ | Groups |
|---|---|---|---|---|---|
| Organic groups | 1 | $CH_3$ | Anions | 5 | $[BF_4]$- |
| | 2 | $CH_2$ | | 6 | $[PF_6]$- |
| Cation cores | 3 | [Mim]+ | | 7 | [Cl]- |
| | 4 | [Im]+ | | | |

**Table 8-4**: Free bond number, molecular weights, and data for target properties of all molecular building blocks

| Building blocks | $k$ | $n_k$ | Molecular weight (g mol$^{-1}$) | $V_k$ | $A_{k,\mu}$ | $B_{k,\mu}$ |
|---|---|---|---|---|---|---|
| $CH_3$ | 1 | 1 | 15.03 | 35 | -0.74 | 250.0 |
| $CH_2$ | 2 | 2 | 14.03 | 28 | -0.63 | 250.4 |
| $[Mim]^+$ | 3 | 1 | 82.10 | 119 | 7.30 | 1507.1 |
| $[Im]^+$ | 4 | 2 | 67.07 | 79 | 8.04 | 1257.1 |
| $[BF_4]^-$ | 5 | 0 | 86.80 | 73 | -18.08 | 1192.4 |
| $[PF_6]^-$ | 6 | 0 | 144.96 | 107 | -20.49 | 2099.8 |
| $[Cl]^-$ | 7 | 0 | 35.45 | 47 | -27.63 | 5457.7 |

### 8.4.6 Step 6: Design optimal IL based on design objective and target properties

As presented in Section 8.4.3, the design objective in this case study is to maximise the $CO_2$ solubility of IL, and therefore it was translated into Equation (8.17).

$$\max S_g \quad \forall g \tag{8.17}$$

where $S_g$ stands for the solubility of $CO_2$ in selected IL in temperature range $g$. For illustration purpose, only the effect of temperature was included in this case study. The operating pressure was fixed at 0.7 MPa (i.e. $P_h^{\text{chosen}}$ = 0.7 MPa); while the operating temperature was modelled as variable, ranging from 323.15 to 373.15 K. The operating temperature was broken down into five ranges and each temperature range was represented by its midpoint, as illustrated in Figure 8-6. Nevertheless, this approach can be used to study the effect of pressure or both the temperature and pressure, as shown in Chapter 7.

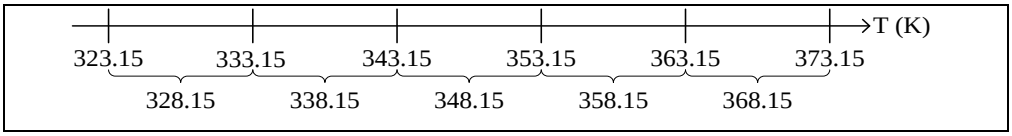


**Figure 8-6**: Midpoints for all temperature ranges considered in this case study

Using data shown in Step 2, formulation of MINLP model given in the following equations was solved to design IL solvent for this case study.

$$\max S_g = x_{\mathrm{CO_2},g} \big/ x_{\mathrm{IL},g} \tag{8.18}$$

$$T_g^{\text{chosen}} = T_{g-1}^{\text{chosen}} I_g + T_g (1 - I_g) \tag{8.19}$$

$$(T^{\mathrm{L}} - T_g^{\text{switch}}) I_g < T - T_g^{\text{switch}} \le (T^{\mathrm{U}} - T_g^{\text{switch}})(1 - I_g) \tag{8.20}$$

$$P_h^{\text{chosen}} = 0.7 \tag{8.21}$$

$$\rho = \frac{M}{0.6022(1.0151)\sum_{k=1}^{7} v_k V_k} \tag{8.22}$$

$$\mu = \frac{\rho M}{1000} \exp\left( \sum_{k=1}^{7} v_k A_{\mu,k} + \frac{\sum_{k=1}^{7} v_k B_{\mu,k}}{T_g^{\text{chosen}}} \right) \le 0.1 \tag{8.23}$$

$$x_{\mathrm{CO_2},g} = \frac{0.7 y_1 \varphi_1(T, P, y_1)}{\gamma_1 P_1^S} \tag{8.24}$$

$$\sum_i y_i = 1 \tag{8.25}$$

$$\sum_i x_i = 1 \tag{8.26}$$

$$\sum_{k=1}^{7} v_k \geq 2 \tag{8.27}$$

$$\sum_{k=1}^{7} n_k v_k - 2\left(\sum_{k=1}^{7} n_k - 1\right) = 0 \tag{8.28}$$

$$\sum_{m=3}^{4} \alpha_m = 1 \tag{8.29}$$

$$\sum_{n=5}^{7} \beta_n = 1 \tag{8.30}$$

Equation (8.18) is the objective function formulated using Equations (8.16) and (8.17). Equations (8.19) and (8.20) are included to determine operating temperature range for carbon capture process; while Equation (8.21) keeps the pressure fixed as it is not part of the objective for this example. Equations (8.22) and (8.23) estimate IL density and viscosity that are formulated based on Equations (8.11) to (8.15). Equations (8.24) are used for $CO_2$ solubility calculation, based on Equations (8.4) to (8.16). The remaining equations are structural constraints formulated from Equations (8.5) to (8.10).

The optimum IL was determined as $[C_{10}MIm][BF_4]$, i.e. 1-decyl-3-methylimidazolium tetrafluoroborate; while the optimal operating temperature range is determined as 323.15 to 333.15 K. This results means that $[C_{10}mim][BF_4]$ has the highest $CO_2$ solubility among all possible combinations of cation and anion in the identified temperature range. It has a predicted solubility of 0.1320 at 328.15 K and 0.7 MPa, and its viscosity is predicted to be 0.08627 Pa.s, which is lower than the upper limit. However, there is no solubility data for this IL in literature, and hence no comparison can be conducted at this time. This is the advantage of using the presented approach where new or novel IL solvent can be obtained, even in the absence of experimental data. Nine other alternatives were determined by doing integer cuts, along with their respective optimal operating temperature range, and the results are shown in Table 8-5. The full names of all cations and anions are given in nomenclature. As shown, the results obtained by solving this model corresponds to the best ILs that one could find from allowed combinations of anions and cations. This means that the proposed approach provides optimal structure of IL for $CO_2$ absorption, according to the given specifications or performance targets.

Predicted solubility is then compared with available experimental data, using Equation (8.31). The relative deviations between literature experimental solubility data and predicted solubility data are shown in Table 8-5. Currently, experimental data is only available for two ILs, both show very low relative

deviations (less than 10 %). The small difference occurs mainly due to the errors present in the chosen prediction models.

$$\text{Relative Deviation} = \frac{|\text{Experimental data} - \text{Predictedvalue}|}{\text{Experimental data}} \times 100 \quad (8.31)$$

### 8.4.7 Step 7: Determine utility consumption of carbon capture system

$[C_{10}MIm][BF_4]$ has the highest $CO_2$ solubility according to results in Table 8, hence it was chosen as the carbon capture solvent for the BECC scheme in this case study. In this step, the utility required by carbon capture system using $[C_{10}MIm][BF_4]$ as solvent was determined. As presented in Figure 8-3, power, heating and cooling utilities are required, they are calculated using basic energy balance equations. In Step 3, the production of BTS was identified to be 2782 kW of power, 28125 kg $h^{-1}$ of low pressure steam (LPS), and 15000 kg $h^{-1}$ of cooling water, correspond to 24579.36 kg $h^{-1}$ of $CO_2$. 90% of this generated $CO_2$ were stated to be captured in carbon capture system. A basic energy balance was carried out to determine the power consumed to circulate IL solvent within the system, using Equations (8.32) and (8.33).

**Table 8-5**: Optimal IL molecular design results

| IL chosen | Chosen system temperature, $T_g^{chosen}$ (K) | Predicted viscosity, $\mu$ (PA.s) | Predicted $CO_2$ solubility, $S_g$ | Experimental solubility | Relative deviation, RD (%) |
|---|---|---|---|---|---|
| $[C_{10}MIm][BF_4]$ | 328.15 | 0.08627 | 0.1320 | - | - |
| $[C_{12}MIm][BF_4]$ | 338.15 | 0.07121 | 0.1233 | - | - |
| $[C_9MIm][BF_4]$ | 328.15 | 0.07312 | 0.1231 | - | - |
| $[C_{11}MIm][BF_4]$ | 338.15 | 0.06182 | 0.1163 | - | - |
| $[C_8MIm][BF_4]$ | 328.15 | 0.06193 | 0.1141 | 0.1117 (Gutkowski et al., 2006) | 2.15 |
| $[C_{10}MIm][PF_6]$ | 338.15 | 0.09281 | 0.1091 | - | - |
| $[C_7MIm][BF_4]$ | 328.15 | 0.05243 | 0.1049 | - | - |
| $[C_9MIm][PF_6]$ | 338.15 | 0.08133 | 0.1022 | - | - |
| $[C_6MIm][PF_6]$ | 328.15 | 0.08747 | 0.0978 | 0.1086 (Shariati and Peters, 2004) | 9.97 |
| $[C_8MIm][PF_6]$ | 338.15 | 0.07129 | 0.0951 | - | - |

$$VF_{\mathrm{IL}} = \frac{m_{\mathrm{CO_2}}}{S_g \rho} \tag{8.32}$$

$$W = \frac{VF_{\mathrm{IL}} \Delta P}{3600} \tag{8.33}$$

$W$ is the pumping power in kW, $VF_{\mathrm{IL}}$ is IL volumetric flowrate in $m^3\ h^{-1}$, $m_{\mathrm{CO_2}}$ is the mass flowrate of $CO_2$ in kg $h^{-1}$ and $\Delta P$ is the pressure difference in kPa. Pumping power required by carbon capture system was calculated as 193.90 kW.

The heating utility was obtained through simulation using Aspen HYSYS version 8.4, which is 10567 kW. The total amount of LPS needed by carbon capture system was calculated using Equation (8.34).

$$Q^{\mathrm{H}} = \frac{m_{\mathrm{LPS}} \Delta h}{3600} \tag{8.34}$$

$Q^{\mathrm{H}}$ is the heating power in kW, $m_{\mathrm{LPS}}$ is the flowrate of LPS in kg $h^{-1}$ and $\Delta h$ is the difference in specific enthalpy in kJ $kg^{-1}$. According to calculation, 14619.56 kg $h^{-1}$ of LPS is required to heat up $CO_2$ rich solvent prior to IL solvent regeneration. The cooling utility was determined as 370.28 kW using the same simulation.

Equation (8.37) was used to determine the total amount cooling water required by carbon capture system. In Equation (8.37), $Q^C$ is the cooling power in kW and $m_{CW}$ is the cooling water flowrate in kg $h^{-1}$. The total amount of cooling water needed by carbon capture system is 14376.27 kg $h^{-1}$. From the results, it was concluded that all utilities can be provided by bio-energy system. However, the production from bio-energy system is actually for other purposes and does not consider the parasitic loads by carbon capture system initially. Hence, these extra utilities can either be supplied from external sources, or the bio-energy system can be retrofitted to cover them.

$$Q^C = \frac{m_{CW}\Delta h}{3600} \tag{8.35}$$

### 8.4.8 Step 8: Retrofit the entire process according to the requirement

Once the utilities required by carbon capture system were calculated, the integrated bio-energy system would require adjustments in output. Since bio-energy system is producing energy itself, the outputs from BTS can be increased to supply to carbon capture system. If the utilities required by the carbon capture system are more than what can be delivered by bio-energy system, the bio-energy system would require retrofitting. However, once the bio-energy system is retrofitted to produce more utilities, it will consequently produce more $CO_2$ and higher amount of utilities required by carbon capture system to maintain same total carbon removal (i.e. 90% removal in this case

study). For illustration purpose, all three utilities (i.e. power, heating and cooling) were studied, and comparisons were done between the outputs from BTS and requirements by BECC using [$C_{10}$MIm][$BF_4$] solvent. Figure 8-7 to Figure 8-9 show the difference between the outputs and requirements in entire process. It can be seen that for all three utilities, there are big gaps between the productions and requirements at the beginning. If the productions are lower than requirement, the system required utility supply from external sources. When the productions from BTS are increased, the gaps are getting narrower until productions meet requirements, this is the point where the whole system is self-sustainable and no purchasing of utilities is required from other sources. If productions are increased upon this point, productions will exceed the requirements of the system and they can be sold for profits.

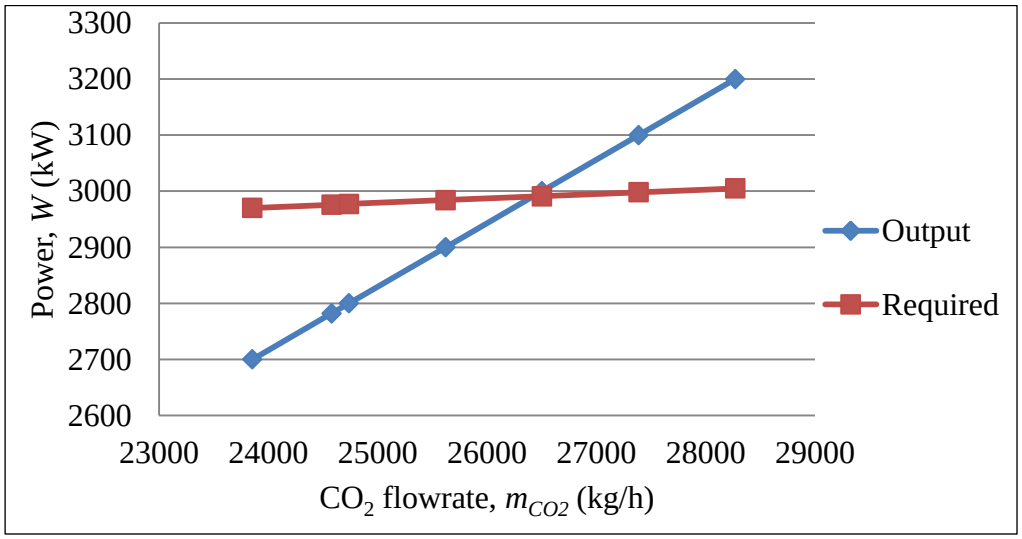


**Figure 8-7**: Comparison of power output from BTS and power consumption by BECC

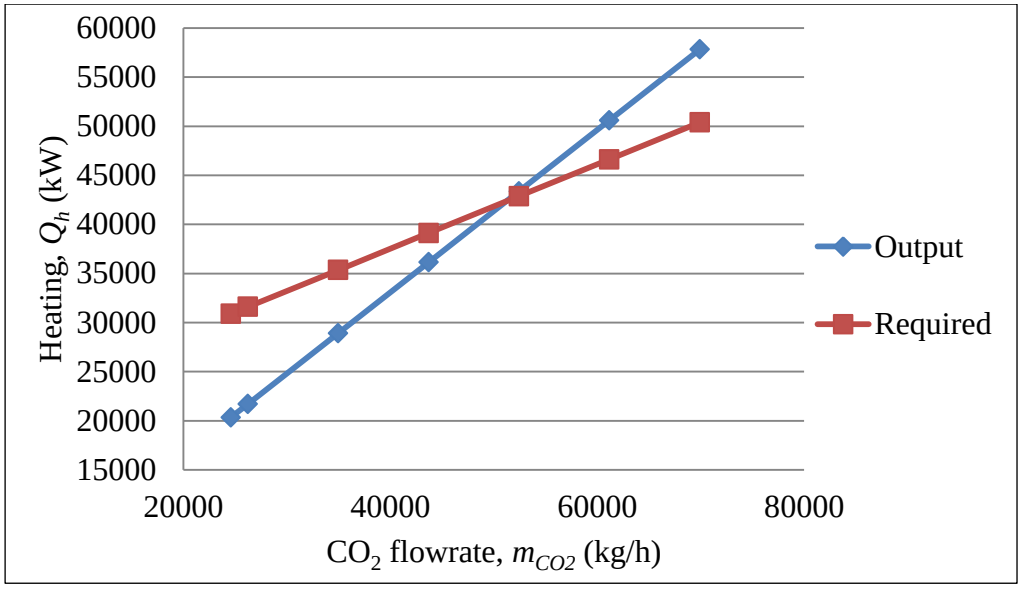


**Figure 8-8**: Comparison of heating output from BTS and heating utility consumption by entire process

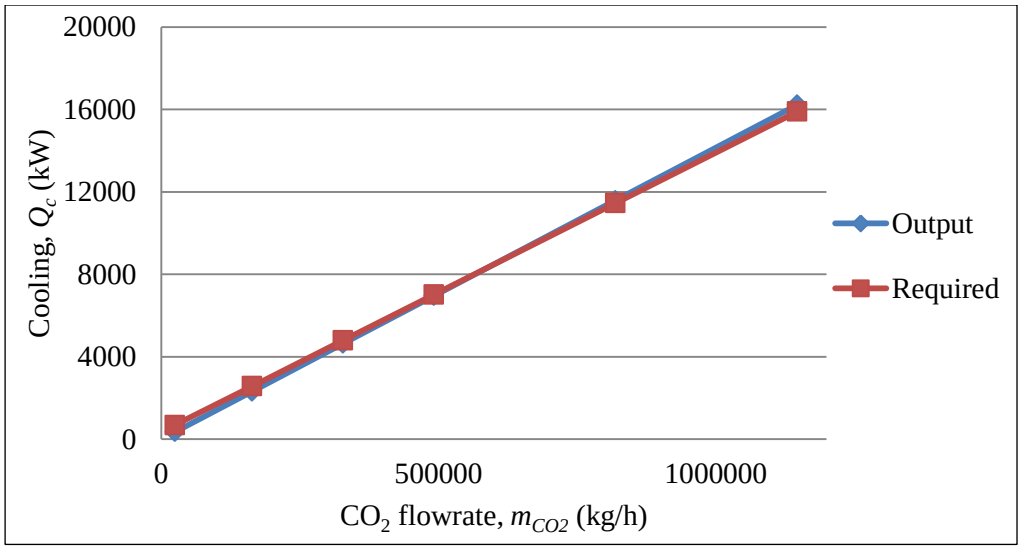


**Figure 8-9**: Comparison of cooling output from BTS and cooling utility consumption by entire process

According to Figure 8-7, power requirement of carbon capture system can be met when the total power production of BTS is 3000 kW and the corresponding $CO_2$ produced is 26500 kg $h^{-1}$. When the power production is less than 3000 kW, carbon capture system requires supply from external sources. Meanwhile, there is extra power produced from BTS and can be sold to third party, when the power production is more than 3000 kW. Similarly, heating utility requirement of carbon capture system is met when the total heating output is 43000 kW as shown in Figure 8-8, with 51000 kg $h^{-1}$. The cooling utility required by carbon capture system can be supplied completely by BTS when the output is 11500 kW and $CO_2$ generated is 815000 kg $h^{-1}$.

### 8.4.9 Step 9: Finalise the entire process

Using Figure 8-7 to Figure 8-9, user can decide how the BECC system should be retrofitted. For this case study, user can choose to fulfil power, heating utility or cooling utility required by carbon capture system. If BTS is retrofitted to fulfil power requirement only, heating and cooling utilities from external sources are required to run the carbon capture system. If decision is made to fulfil required heating utility, power requirement is fulfilled as well but cooling utility should be purchased from external source. All required utilities are fulfilled when cooling utility if fulfilled through retrofitting bio-energy system.

## 8.5 Summary

A systematic approach is presented in this chapter to integrate ionic liquid (IL) design and process design, where IL can be designed as a carbon capture solvent and applied to newly installed carbon capture system. Using the proposed approach, IL solvent for carbon capture purpose can be designed, followed by retrofitting of process to accommodate utility requirement by carbon capture system. Input-output (IO) model was applied to determine the outputs from the process that will have carbon capture system installed. Computer-aided molecular design (CAMD) was employed to solve IL design problem, identifying an optimal IL and operating conditions of carbon capture system, based on carbon capture performance and relevant constraints. The whole process can be retrofitted later according to the results from solving IL design problem. A case study was solved to demonstrate the integration between biomass tri-generation system (BTS) and carbon capture system to produce multiple energy sources and carbon dioxide ($CO_2$) as products. A simple graphical tool is also presented to assist decision making on retrofitting of process on productions and requirements within the entire system. In future work, the economic performance of entire system can be included to understand the trade-off between different aspects, including economic, environmental issue and feasibility of the process.

# CHAPTER 9

# CONCLUSIONS AND FUTURE WORKS

This chapter concludes all the works done throughout the study, with the achievements and potential future works in this area of interest. The research gaps presented in Chapter 3 have been successfully filled in through the development of different methodologies, and thus made a breakthrough in the area of designing ionic liquid (IL) solvent for carbon capture purpose. However, there are still some aspects not considered throughout this research, and can be further studied in the future.

## 9.1 Achievements

This thesis presents novel approaches that were developed to aid the design process of ionic liquid (IL) or IL mixture solvent for carbon capture purpose. The main achievement of this work is the development of different novel methodologies to design and select IL-based solvent, and integrating IL design problem with process design problem. The detailed explanation of each achievement is given below.

### 9.1.1 Development of insight-based methodology to design IL solvents for carbon capture purpose

A new insight-based visualisation tool was developed, based on visual approach for process design and molecular design, to identify potential IL solvents to capture carbon dioxide ($CO_2$) specifically. Multiple properties can be considered simultaneous to design an IL solvent. The IL design problem can be solved via multi-objective optimisation, but it can be complicated and not user-friendly. This systematic visual approach allows transformation of IL design problem onto a ternary diagram and provides useful insights to user about the problem and solutions. Design and optimisation rules were developed to aid the pure IL solvent design or selection process.

### 9.1.2 Development of a systematic approach to determine optimal IL-based carbon capture solvent

A novel systematic mathematical approach to determine optimal IL specifically for $CO_2$ absorption has been presented. This approach is based on a well-established methodology for organic solvent design, namely the computer-aided molecular design (CAMD) approach. CAMD was previously applied for organic compound design, and it is now extended to solve IL design problem as well. Using the proposed approach, IL design problem can be formulated as a mixed integer non-linear programming (MINLP) model, targeting a single design objective and all relevant properties. The presented approach utilises appropriate prediction models to predict the thermophysical

properties of ILs. The allowed combinations of cations, anions, and organic groups have been introduced as structural constraints to ensure the designed ILs are realistic and feasible structurally.

### 9.1.3 Extension of insight-based approach to identify pure IL and IL mixture solvents for carbon capture system

Pure IL solvents do not always fulfil the target properties, due to the conflicting nature of some properties. For example, ILs with higher $CO_2$ solubility have higher viscosities, high $CO_2$ solubility is desired for carbon capture purpose but high viscosity increase operating cost. To overcome such situations, IL mixture can be used instead. An original systematic visual approach, which is an extension of approach discussed in Section 9.1.1, is presented to solve IL and IL mixture design problem. This developed approach is also based on property clustering technique. Currently, there is very little study on properties of IL mixtures, and limited property prediction models for IL mixtures. This was considered as well during the development of the presented approach, where the approach can utilise both the prediction models and experimental data to estimate properties of mixtures. The presented approach is useful as it can guide user to determine potential mixture prior to exhaustive experimental works, and hence save time and reduce cost.

### 9.1.4 Development of an mathematical approach to determine optimal IL solvent and the corresponding optimal operating conditions for carbon capture purpose

As a first step to integrate IL design and process design, the developed mathematical approach was further improved to simultaneously determine the optimal operating conditions of the designed IL in carbon capture process. The operating conditions of carbon capture process have been introduced as part of the optimisation objective. They can be modelled to be variables, which will be targeted by the approach simultaneously during IL design stage. Using this approach, wide range of temperatures and pressures can be included into the model, and they will be broken down into smaller ranges. Each range is represented by the midpoint, the temperatures and pressures are then modelled as discrete variables via disjunctive programming. This reduces the complexity of the model and the search space for optimal result, which ease the process of solving this model.

### 9.1.5 Integration of IL design and process design, considering the effects of IL solvent selection on whole process

Following the consideration of operating conditions in IL design, the integration of IL design and process design has been presented in this thesis as well. This proposed approach allows the design of IL solvent and retrofitting of overall process to accommodate utility requirement by carbon capture system. Input-output (IO) model was applied to identify the outputs from the

process that will be installing carbon capture system; CAMD was employed to identify optimal IL and operating conditions of carbon capture system similar to previously developed mathematical approaches. The effect of IL-based solvent choice on the whole process can be seen clearly using this presented approach, and designers can study and retrofit the whole process accordingly.

## 9.2 Future Works

During the development of presented approaches, there were some factors not taken into consideration. There are still opportunities to further improve and extend these approaches or advance the study in this research area of ionic liquid (IL) design.

### 9.2.1 Consideration of economic, environmental, safety, and health performances in integration of IL design and process design

As demonstrated in the thesis, the economic, environmental, safety and health performances of process are not considered in all the methodologies. The developed approaches are not taking these performances into consideration, but they are very important to the industry and surroundings. To have a better overview on the process, these can be considered in the future during development of approaches for integrated IL and process design. Proposed approach in Chapter 8 can be further improved to inclusion of total annualised cost, environmental impact, safety and health factors during the

retrofitting of process. With these additions, designers can understand the process in a more comprehensive way regarding performance of IL solvent, economic, environmental, safety and health aspects of the overall process.

### 9.2.2 Integration of models with new experimental data to further improve the accuracy of developed approach

The importance and possibility of integrating new experimental data into visualisation approach to design IL mixture were discussed in Chapter 6. Apart from the presented visualisation tool, the mathematical approaches can consider this aspect as well. Since IL and IL mixture design is relative new area, there is a need to consider newly available experimental data in the model to widen the applications and improve the accuracy of model. It will be more convenient for designers with experimental background to solve the IL design problem, with the combination of computer-aided molecular design (CAMD) and real time integration with experimental data.

### 9.2.3 Extension of developed approaches into different research areas

As discussed in Section 2.2.1, ILs have been reported for various industrial applications, such as heat transfer fluids, biotechnological process, and pre-treatment of lignocellulosic biomass. Similar to the problems presented in this thesis, selection of ILs specifically for one task can be time

consuming and costly due to huge number of ILs available. Hence, to overcome such problems, the developed approaches can be extended to design ILs or IL mixtures for different purposes. Other than that, the proposed approach in Chapter 6 can be useful to biorefinery design and research as well, where the experimental data can be integrated into modelling. Biorefinery design and research involves biomass, which is a mixture of different compounds. Its properties are not predictable, and this makes the property prediction process difficult. When the model can accommodate experimental data to predict the properties of biomass, the modelling work for biomass-based research or design will be more convenient. Apart from that, the presented approach in Chapter 7 can be applied to selection of solvent from organic compounds by considering operating conditions simultaneously, as performance of solvent is generally affected by the conditions.

### 9.2.4 Further improvement on property prediction models for IL and IL mixture

The study of ILs is considered scarce as there are too many possible IL systems to be studied. The currently available property prediction models for IL were developed based on commonly studied IL only. It is necessary to experiment and study different cations and anions, to obtain new data and improve currently available prediction models. Besides that, some properties cannot be estimated directly using simple prediction models. These properties include carbon dioxide ($CO_2$) solubility and selectivity of gases in IL. It would

be beneficial if simple prediction models can be developed for such properties and ease the model solving process. In addition, it is necessary to study and develop predictive models for properties of IL mixture. This is always necessary because a reliable prediction model is required to solve product design problem. The properties that will be useful for carbon capture solvent design are heat of vaporisation, heat capacity, and $CO_2$ solubility. These models can be generated through regression after collecting enough data points from laboratory. The major challenge is the existence of $10^{18}$ possible IL (binary and ternary) mixtures. It is difficult to study all mixtures and relate them in prediction models. This can possibly be overcome by estimating the properties of mixtures based on functional groups instead of IL constituents.

### 9.2.5 Inclusion of Design of Experiments as proof of concept

A Design of Experiments (DoE) approach is a structured methodology that can be applied to identify critical and non-critical parameters, as well as the interactions between these parameters within a process. This systematic tool can be used to solve different engineering problem, including studying the effect of a parameter in a process, ranking the effects of parameters to a process, modelling and optimising a process. The approaches presented in this thesis are new and should be proven to be feasible. DoE approach can be applied, in order to confirm the developed models have high predictive power and high accuracy. It can also be used to study the effect of different IL properties to carbon capture process and overall process.

# REFERENCE


Abbott, A.P., 2004. Application of hole theory to the viscosity of ionic and molecular liquids. Chemphyschem 5, 1242–1246.

Abu-Zahra, M.R.M., Abbas, Z., Singh, P., Feron, P.H.M., 2013. Carbon Dioxide Post-Combustion Capture: Solvent Technologies Overview, Status and Future Directions. In: Mendez-Vilas, A. (Ed.), Materials and Processes for Energy: Communicating Current Research and Technological Developments. Formatex Research Center, pp. 923–934.

Ali, E., AlNashef, I.M., Ajbar, A., HadjKali, M., Mulyono, S., 2013a. On the use of Ionic Liquids for CO2 Capturing. World Academy of Science, Engineering and Technology 7, 28–33.

Ali, E., AlNashef, I.M., Ajbar, A., Mulyono, S., Hizaddin, H.F., Hadj-Kali, M.K., 2013b. Determination of cost-effective operating condition for CO2 capturing using 1-butyl-3-methylimidazolium tetrafluoroborate ionic liquid. Korean Journal of Chemical Engineering 30, 2068–2077.

Alvira, P., Tomás-Pejó, E., Ballesteros, M., Negro, M.J., 2010. Pretreatment technologies for an efficient bioethanol production process based on enzymatic hydrolysis: A review. Bioresource technology 101, 4851–4861.

Andiappan, V., Tan, R.R., Aviso, K.B., Ng, D.K.S., 2015. Synthesis and optimisation of biomass-based tri-generation systems with reliability aspects. Energy 89, 803–818.

Anthony, J.L., Aki, S.N.V.K., Maginn, E.J., Brennecke, J.F., 2004. Feasibility of using ionic liquids for carbon dioxide capture. International Journal of Environmental Technology and Management 4, 105–115.

Anthony, J.L., Anderson, J.L., Maginn, E.J., Brennecke, J.F., 2005. Anion effects on gas solubility in ionic liquids. The Journal of Physical Chemistry B 109, 6366–6374.

Anthony, J.L., Maginn, E.J., Brennecke, J.F., 2001. Solution thermodynamics of imidazolium-based ionic liquids and water. The Journal of Physical Chemistry B 105, 10942–10949.

Argoub, K., Benkouider, A.M., Yahiaoui, A., Kessas, R., Guella, S., Bagui, F., 2014. Prediction of standard enthalpy of formation in the solid state by a third-order group contribution method. Fluid Phase Equilibria 380, 121–127.

Asif, M., Muneer, T., 2007. Energy supply, its demand and security issues for developed and emerging economies. Renewable and Sustainable Energy Reviews 11, 1388–1413.

Baltus, R.E., Culbertson, B.H., Dai, S., Luo, H., DePaoli, D.W., 2004. Low-Pressure Solubility of Carbon Dioxide in Room-Temperature Ionic Liquids Measured with a Quartz Crystal Microbalance. The Journal of Physical Chemistry B 108, 721–727.

Bandrés, I., Alcalde, R., Lafuente, C., Atilhan, M., Aparicio, S., 2011. On the viscosity of pyridinium based ionic liquids: an experimental and computational study. The Journal of Physical Chemistry B 115, 12499–513.

Bardow, A., Steur, K., Gross, J., 2010. Continuous-Molecular Targeting for Integrated Solvent and Process Design. Industrial & Engineering Chemistry Research 49, 2834–2840.

Bates, E.D., Mayton, R.D., Ntai, I., Davis, J.H., 2002. CO2 Capture by a Task-Specific Ionic Liquid. Journal of the American Chemical Society 124, 926–927.

Bhattacharjee, A., Luís, A., Santos, J.H., Lopes-da-Silva, J. a., Freire, M.G., Carvalho, P.J., Coutinho, J.A.P., 2014. Thermophysical properties of sulfonium- and ammonium-based ionic liquids. Fluid Phase Equilibria 381, 36–45.

Billard, I., Marcou, G., Ouadi, A., Varnek, A., 2011. In Silico Design of New Ionic Liquids Based on Quantitative Structure-Property Relationship Models of Ionic Liquid Viscosity. The Journal of Physical Chemistry B 115, 93–98.

Blanchard, L.A., Hancu, D., Beckman, E.J., Brennecke, J.F., 1999. Green processing using ionic liquids and CO2. Nature 399, 28–29.

Bommareddy, S., Chemmangattuvalappil, N.G., Eden, M.R., 2012. An Integrated Framework for Flowsheet Synthesis and Molecular Design. In: Bogle, I.D.L., Fairweather, M. (Eds.), Proceedings of the 22nd European Symposium on Computer Aided Process Engineering. Elsevier B.V., London, pp. 662–666.

Bonhôte, P., Dias, A.-P., Armand, M., Papageorgiou, N., Kalyanasundaram, K., Grätzel, M., 1996. Hydrophobic, Highly Conductive Ambient-Temperature Molten Salts. Inorganic chemistry 35, 1168–1178.

Brennecke, J.F., Maginn, E.J., 2001. Ionic liquids: Innovative fluids for chemical processing. AIChE Journal 47, 2384–2389.

Buzzeo, M.C., Hardacre, C., Compton, R.G., 2004. Use of room temperature ionic liquids in gas sensor design. Analytical Chemistry 76, 4583–4588.

Cabezas, H., Harten, P.F., Green, M.R., 2000. Designing Greener Solvents. Chemical Engineering 107, 107–109.

Cadena, C., Anthony, J.L., Shah, J.K., Morrow, T.I., Brennecke, J.F., Maginn, E.J., 2004. Why Is CO2 so soluble in imidazolium-based ionic liquids? Journal of the American Chemical Society 126, 5300–5308.

Camarda, K. V., Maranas, C.D., 1999. Optimization in Polymer Design Using Connectivity Indices. Industrial & Engineering Chemistry Research 38, 1884–1892.

Camper, D., Scovazzo, P., Koval, C., Noble, R., 2004. Gas solubilities in room-temperature ionic liquids. Industrial & Engineering Chemistry Research 43, 3049–3054.

Chavali, S., Lin, B., Miller, D.C., Camarda, K. V., 2004. Environmentally-benign transition metal catalyst design using optimization techniques. Computers and Chemical Engineering 28, 605–611.

Chávez-Islas, L.M., Vasquez-medrano, R., Flores-tlacuahuac, A., 2011. Optimal Molecular Design of Ionic Liquids for High-Purity Bioethanol Production. Industrial & Engineering Chemistry Research 50, 5153–5168.

Chemmangattuvalappil, N.G., Eljack, F.T., Solvason, C.C., Eden, M.R., 2009. A novel algorithm for molecular synthesis using enhanced property operators. Computers and Chemical Engineering 33, 636–643.

Chemmangattuvalappil, N.G., Solvason, C.C., Bommareddy, S., Eden, M.R., 2010a. Reverse problem formulation approach to molecular design using property operators based on signature descriptors. Computers and Chemical Engineering 34, 2062–2071.

Chemmangattuvalappil, N.G., Solvason, C.C., Bommareddy, S., Eden, M.R., 2010b. Combined property clustering and GC+ techniques for process and product design. Computers and Chemical Engineering 34, 582–591.

Chen, Y., Mutelet, F., Jaubert, J.-N., 2012. Modeling the solubility of carbon dioxide in imidazolium-based ionic liquids with the PC-SAFT equation of state. The Journal of Physical Chemistry B 116, 14375–14388.

Constantinou, L., Gani, R., 1994. New group contribution method for estimating properties of pure compounds. AIChE Journal 40, 1697–1710.

Constantinou, L., Prickett, S.E., Mavrovouniotis, M.L., 1993. Estimation of thermodynamic and physical properties of acyclic hydrocarbons using the ABC approach and conjugation operators. Industrial & Engineering Chemistry Research 32, 1734–1746.

Conte, E., Gani, R., Ng, K.M., 2011. Design of formulated products: a systematic methodology. AIChE Journal 57, 2431–2449.

Coutinho, J.A.P., Carvalho, P.J., Oliveira, N.M.C., 2012. Predictive methods for the estimation of thermophysical properties of ionic liquids. RSC Advances 2, 7322–7346.

Cuéllar-Franca, R.M., Azapagic, A., 2015. Carbon capture, storage and utilisation technologies: A critical analysis and comparison of their life cycle environmental impacts. Journal of CO2 Utilization 9, 82–102.

D'Alessandro, D.M., Smit, B., Long, J.R., 2010. Carbon dioxide capture: prospects for new materials. Angewandte Chemie (International ed. in English) 49, 6058–6082.

Da Silva, M.V., Barbosa, D., 2004. Prediction of the solubility of aromatic components of wine in carbon dioxide. The Journal of Supercritical Fluids 31, 9–25.

De Souza, R.F., Padilha, J.C., Gonçalves, R.S., Dupont, J., 2003. Room temperature dialkylimidazolium ionic liquid-based fuel cells. Electrochemistry Communications 5, 728–731.

Department of Environment, 2010. Environmental Requirements: A Guide For Investors. Putrajaya, Malaysia.

Dlugokencky, E., Tans, P., 2016. Trends in Atmospheric Carbon Dioxide [WWW Document]. NOAA/ESRL. URL www.esrl.noaa.gov/gmd/ccgg/trends/ (accessed 11.30.16).

Duchin, F., 1992. Industrial input-output analysis: implications for industrial ecology. Proceedings of the National Academy of Sciences of the United States of America 89, 851–855.

Dutt, N.V.K., Ravikumar, Y.V.L., 2008. A viscosity temperature relationship in reduced form for ionic liquids. In: 3rd National Conference on Thermodynamics of Chemical and Biological Systems. The Indian Thermodynamics Society, Nagpur, India.

Dutt, N.V.K., Ravikumar, Y.V.L., Yamuna Rani, K., 2013. Representation of Ionic Liquid Viscosity-Temperature Data By Generalized Correlations and an Artificial Neural Network (Ann) Model. Chemical Engineering Communications 200, 1600–1622.

Duvedi, A.P., Achenie, L.E.K., 1997. On the design of environmentally benign refrigerant mixtures: a mathematical programming approach. Computers and Chemical Engineering 21, 915–923.

Eden, M.R., Jørgensen, S.B., Gani, R., El-Halwagi, M.M., 2004. A novel framework for simultaneous separation process and product design. Chemical Engineering and Processing 43, 595–608.

El-Halwagi, M.M., 2012. Overview of Optimization. In: Sustainable Design Through Process Integration: Fundamentals and Applications to Industrial Pollution Prevention, Resource Conservation, and Profitability Enhancement. Elsevier Inc., Oxford, U.K., pp. 255–286.

El-Halwagi, M.M., Glasgow, I.M., Qin, X., Eden, M.R., 2004. Property integration: Componentless design techniques and visualization tools. AIChE Journal 50, 1854–1869.

Eljack, F.T., 2007. A Property Based Approach to Integrated Process and Molecular Design. Auburn University.

Eljack, F.T., Abdelhady, A.F., Eden, M.R., Gabriel, F.B., Qin, X., El-Halwagi, M.M., 2005. Targeting optimum resource allocation using reverse

problem formulations and property clustering techniques. Computers and Chemical Engineering 29, 2304–2317.

Eljack, F.T., Eden, M.R., 2008. A systematic visual approach to molecular design via property clusters and group contribution methods. Computers and Chemical Engineering 32, 3002–3010.

Eljack, F.T., Eden, M.R., Kazantzi, V., El-Halwagi, M.M., 2006. Property Clustering and Group Contribution for Process and Molecular Design. In: Marquardt, W., Pantelides, C. (Eds.), 16th European Symposium on Computer Aided Process Engineering and 9th International Symposium on Process Systems Engineering. Elsevier B.V., Garmisch-Partenkirchen, Germany, pp. 907–912.

Eljack, F.T., Eden, M.R., Kazantzi, V., Qin, X., El-Halwagi, M.M., 2007. Simultaneous process and molecular design—A property based approach. AIChE Journal 53, 1232–1239.

Eljack, F.T., Solvason, C.C., Chemmangattuvalappil, N.G., Eden, M.R., 2008. A Property Based Approach for Simultaneous Process and Molecular Design. Chinese Journal of Chemical Engineering 16, 424–434.

Eslick, J.C., Shulda, S.M., Spencer, P., Camarda, K. V., 2010. Optimization-Based Approaches to Computational Molecular Design. In: Adjiman, C.S., Galindo, A. (Eds.), Molecular Systems Engineering. Wiley-VCH, Weinheim, Germany, pp. 173–194.

Fadeev, A.G., Meagher, M.M., 2001. Opportunities for ionic liquids in recovery of biofuels. Chemical Communications 295–296.

Figueroa, J.D., Fout, T., Plasynski, S., McIlvried, H., Srivastava, R.D., 2008. Advances in CO2 capture technology—The U.S. Department of Energy's Carbon Sequestration Program. International Journal of Greenhouse Gas Control 2, 9–20.

Folger, P., 2013. Carbon Capture: A Technology Assessment. University of Nebraska-Lincoln.

Fouskakis, D., Draper, D., 2002. Stochastic Optimization: a Review. International Statistical Review 70, 315.

Freemantle, M., 1998. Designer Solvents: Ionic liquids may boost clean technology development. Chemical & Engineering News 76, 32–37.

Fröba, A.P., Kremer, H., Leipertz, A., 2008. Density, refractive index, interfacial tension, and viscosity of ionic liquids [EMIM][EtSO4], [EMIM][NTf2], [EMIM][N(CN)2], and [OMA][NTf2] in dependence on temperature at atmospheric pressure. The Journal of Physical Chemistry B 112, 12420–12430.

Gani, R., 2002. ProCAMD Manual. Lyngby, Denmark.

Gani, R., 2004a. Chemical product design: challenges and opportunities. Computers and Chemical Engineering 28, 2441–2457.

Gani, R., 2004b. Computer-aided methods and tools for chemical product design. Chemical Engineering Research and Design 82, 1494–1504.

Gani, R., Achenie, L.E.K., Venkatasubramanian, V., 2003. Introduction to CAMD. In: Achenie, L.E.K., Gani, R., Venkatasubramanian, V. (Eds.), Computer Aided Molecular Design: Theory and Practice. Elsevier Science B.V., Amsterdam, pp. 3–22.

Gani, R., Brignole, E.A., 1983. Molecular design of solvents for liquid extraction based on UNIFAC. Fluid Phase Equilibria 13, 331–340.

Gani, R., Nielsen, B., Fredenslund, A., 1991. A Group Contribution Approach to Computer-Aided Molecular Design. AIChE Journal 37, 1318–1332.

Gardas, R.L., Coutinho, J.A.P., 2008a. Extension of the Ye and Shreeve group contribution method for density estimation of ionic liquids in a wide range of temperatures and pressures. Fluid Phase Equilibria 263, 26–32.

Gardas, R.L., Coutinho, J.A.P., 2008b. A group contribution method for viscosity estimation of ionic liquids. Fluid Phase Equilibria 266, 195–201.

Gardas, R.L., Coutinho, J.A.P., 2008c. A Group Contribution Method for Heat Capacity Estimation of Ionic Liquids. Industrial & Engineering Chemistry Research 47, 5751–5757.

Gardas, R.L., Coutinho, J.A.P., 2009. Group contribution methods for the prediction of thermophysical and transport properties of ionic liquids. AIChE journal 55, 1274–1290.

Gjernes, E., Helgesen, L.I., Maree, Y., 2013. Health and environmental impact of amine based post combustion CO2 capture. Energy Procedia 37, 735–742.

Global CCS Institute, 2012. CO2 capture technologies: Post-Combustion Capture (PCC). Global Carbon Capture and Storage Institute, Canberra, Australia.

Gmehling, J., Rasmussen, P., Fredenslund, A., 1982. Vapor-liquid equilibria by UNIFAC group contribution. 2. Revision and extension. Industrial & Engineering Chemistry Process Design and Development 21, 118–127.

Gonzalez-Miquel, M., Talreja, M., Ethier, A.L., Flack, K., Switzer, J.R., Biddinger, E.J., Pollet, P., Palomar, J., Rodríguez, F., Eckert, C.A., Liotta, C.L., 2012. COSMO-RS Studies: Structure–Property Relationships for CO2 Capture by Reversible Ionic Liquids. Industrial & Engineering Chemistry Research 51, 16066–16073.

Gutkowski, K., Shariati, A., Peters, C.J., 2006. High-pressure phase behavior of the binary ionic liquid system 1-octyl-3-methylimidazolium tetrafluoroborate+carbon dioxide. The Journal of Supercritical Fluids 39, 187–191.

Han, C., Yu, G., Wen, L., Zhao, D., Asumana, C., Chen, X., 2011. Data and QSPR study for viscosity of imidazolium-based ionic liquids. Fluid Phase Equilibria 300, 95–104.

Harini, M., Adhikari, J., Rani, K.Y., 2013. A Review on Property Estimation Methods and Computational Schemes for Rational Solvent Design: A Focus on Pharmaceuticals. Industrial & Engineering Chemistry Research 52, 6869–6893.

Harini, M., Jain, S., Adhikari, J., Noronha, S.B., Rani, K.Y., 2015. Design of an ionic liquid as a solvent for the extraction of a pharmaceutical intermediate. Separation and Purification Technology 155, 45–57.

Harper, P.M., Gani, R., 2000. A multi-step and multi-level approach for computer aided molecular design. Computers and Chemical Engineering 24, 677–683.

Hasib-ur-Rahman, M., Siaj, M., Larachi, F., 2010. Ionic liquids for CO2 capture—Development and progress. Chemical Engineering and Processing: Process Intensification 49, 313–322.

Herzog, H., Meldon, J., Hatton, A., 2009. Advanced Post-Combustion CO2 Capture. Cambridge.

Hoeven, M., 2013. CO2 Emissions from Fuel Combustion Highlights.

Holbrey, J.D., Seddon, K.R., 1999. Ionic Liquids. Clean Products and Processes 1, 223–236.

Hosseini, S.E., Wahid, M.A., Aghili, N., 2013. The scenario of greenhouse gases reduction in Malaysia. Renewable and Sustainable Energy Reviews 28, 400–409.

Houghton, J.T., Ding, Y., Griggs, D.J., 2001. Climate change 2001: the scientific basis. Cambridge University Press, Cambridge, United Kingdom.

IPCC, 2007. Climate Change 2007: Mitigation. Contribution of Working Group III to the Fourth Assessment Report of the Intergovernmental Panel on Climate Change. In: Metz, B., Davidson, O.R., Bosch, P.R., Dave, R., Meyer, L.A. (Eds.), . Cambridge University Press, Cambridge, United Kingdom and New York, NY, USA.

Isard, W., Schooler, E.W., 1959. Industrial Complex Analysis, Agglomeration Economies, and Regional Development. Journal of Regional Science 1, 19–33.

Jacquemin, J., Ge, R., Nancarrow, P., Rooney, D.W., Costa Gomes, M.F., Pádua, A.A.H., Hardacre, C., 2008a. Prediction of Ionic Liquid Properties. I. Volumetric Properties as a Function of Temperature at 0.1 MPa. Journal of Chemical & Engineering Data 53, 716–726.

Jacquemin, J., Nancarrow, P., Rooney, D.W., Costa Gomes, M.F., Husson, P., Majer, V., Pádua, A.A.H., Hardacre, C., 2008b. Prediction of Ionic Liquid Properties. II. Volumetric Properties as a Function of Temperature and Pressure. Journal of Chemical & Engineering Data 53, 2133–2143.

Jenkins, H.D.B., Roobottom, H.K., Passmore, J., Glasser, L., 1999. Relationships among Ionic Lattice Energies, Molecular (Formula Unit) Volumes, and Thermochemical Radii. Inorganic Chemistry 38, 3609–3620.

Ji, X., Adidharma, H., 2010. Thermodynamic modeling of CO2 solubility in ionic liquid with heterosegmented statistical associating fluid theory. Fluid Phase Equilibria 293, 141–150.

Joback, K.G., Reid, R.C., 1987. Estimation of Pure-Component Properties from Group-Contributions. Chemical Engineering Communications 57, 233–243.

Joback, K.G., Stephanopoulos, G., 1989. Designing molecules possessing desired physical property values. In: Proceedings FOCAPD 1989. CACHE Corporation, Austin, Texas, pp. 631–636.

Jork, C., Seiler, M., Beste, Y., Arlt, W., 2004. Influence of ionic liquids on the phase behavior of aqueous azeotropic systems. Journal of Chemical & Engineering Data 49, 852–857.

Karadas, F., Köz, B., Jacquemin, J., Deniz, E., Rooney, D.W., Thompson, J., Yavuz, C.T., Khraisheh, M., Aparicio, S., Atilhan, M., 2013. High pressure CO2 absorption studies on imidazolium-based ionic liquids: Experimental and simulation approaches. Fluid Phase Equilibria 351, 74–86.

Karakatsani, E.K., Economou, I.G., Kroon, M.C., Peters, C.J., Witkamp, G.-J., 2007. tPC-PSAFT Modeling of Gas Solubility in Imidazolium-Based Ionic Liquids. The Journal of Physical Chemistry C 111, 15487–15492.

Karunanithi, A.T., Achenie, L.E.K., Gani, R., 2005. A New Decomposition-Based Computer-Aided Molecular/Mixture Design Methodology for the Design of Optimal Solvents and Solvent Mixtures. Industrial & Engineering Chemistry Research 44, 4785–4797.

Karunanithi, A.T., Achenie, L.E.K., Gani, R., 2006. A computer-aided molecular design framework for crystallization solvent design. Chemical Engineering Science 61, 1247–1260.

Karunanithi, A.T., Mehrkesh, A., 2013. Computer-Aided Design of Tailor-Made Ionic Liquids. AIChE Journal 59, 4627–4640.

Kazantzi, V., Qin, X., El-Halwagi, M.M., Eljack, F.T., Eden, M.R., 2007. Simultaneous process and molecular design through property clustering techniques: A visualization tool. Industrial & Engineering Chemistry Research 46, 3400–3409.

Kenarsari, S.D., Yang, D., Jiang, G., Zhang, S., Wang, J., Russell, A.G., Wei, Q., Fan, M., 2013. Review of recent advances in carbon dioxide separation and capture. RSC Advances 3, 22739–22773.

Khanna, V., Bakshi, B.R., 2009. Modeling the risks to complex industrial networks due to loss of natural capital. In: 2009 IEEE International Symposium on Sustainable Systems and Technology. IEEE, pp. 1–6.

Kheireddine, H.A., El-Halwagi, M.M., Elbashir, N.O., 2013. A property-integration approach to solvent screening and conceptual design of solvent-extraction systems for recycling used lubricating oils. Clean Technologies and Environmental Policy 15, 35–44.

Kheshgi, H.S., Prince, R.C., Marland, G., 2000. The Potential of Biomass Fuels in the Context of Global Climate Change: Focus on Transportation Fuels. Annual Review of Energy and the Environment 25, 199–244.

Klein, J.A., Wu, D.T., Gani, R., 1992. Computer aided mixture design with specified property constraints. Computers and Chemical Engineering 16, S229–S236.

Koo, Y.K., Kim, B.H., Park, D.H., Joo, J., 2004. Electrochemical Polymerization of Polypyrrole Nanotubes and Nanowires in Ionic Liquid. Molecular Crystals and Liquid Crystals 425, 333–338.

Kraxner, F., Nilsson, S., Obersteiner, M., 2003. Negative emissions from BioEnergy use, carbon capture and sequestration (BECS)—the case of biomass production by sustainable forest management from semi-natural temperate forests. Biomass and Bioenergy 24, 285–296.

Kuhlmann, E., Himmler, S., Giebelhaus, H., Wasserscheid, P., 2007. Imidazolium dialkylphosphates - a class of versatile, halogen-free and hydrolytically stable ionic liquids. Green Chemistry 9, 233–242.

Kulajanpeng, K., Suriyapraphadilok, U., Gani, R., 2014. Ionic-liquid Based Separation of Azeotropic Mixtures. Chemical Engineering Transactions 39, 517–522.

Lazzús, J.A., 2010. A Group Contribution Method to Predict ρ-T-P of Ionic Liquids. Chemical Engineering Communications 197, 974–1015.

Lee, B.-S., Lin, S.-T., 2015. Screening of ionic liquids for CO2 capture using the COSMO-SAC model. Chemical Engineering Science 121, 157–168.

Lee, G.C., Smith, R., Zhu, X.X., 2002. Optimal Synthesis of Mixed-Refrigerant Systems for Low-Temperature Processes. Industrial & Engineering Chemistry Research 41, 5016–5028.

Lei, Z., Dai, C., Chen, B., 2014. Gas solubility in ionic liquids. Chemical Reviews 114, 1289–1326.

Lei, Z., Dai, C., Song, W., 2015. Adsorptive absorption: A preliminary experimental and modeling study on CO2 solubility. Chemical Engineering Science 127, 260–268.

Lei, Z., Dai, C., Wang, W., Chen, B., 2013. UNIFAC model for ionic liquid-CO2 systems. AIChE Journal 60, 716–729.

Lei, Z., Zhang, J., Li, Q., Chen, B., 2009. UNIFAC Model for Ionic Liquids. Industrial & Engineering Chemistry Research 48, 2697–2704.

Leontief, W.W., 1936. Quantitative Input and Output Relations in the Economic Systems of the United States. The Review of Economics and Statistics 18, 105–125.

Leung, M., Haimes, Y.Y., Santos, J.R., 2007. Supply- and Output-Side Extensions to the Inoperability Input-Output Model for Interdependent Infrastructures. Journal of Infrastructure Systems 13, 299–310.

Li, X., Wang, S., Chen, C., 2013. Experimental Study of Energy Requirement of CO2 Desorption from Rich Solvent. Energy Procedia 37, 1836–1843.

Liebmann, B., Friedl, A., Carvalho Rodrigues, J.F., 2012. Lignocellulosic Biomass Dissolution and Fractioning Using Ionic Liquids as a Solvent. Chemical Engineering Transactions 29, 553–558.

Macchietto, S., Odele, O., Omatsone, O., 1990. Design of Optimal Solvents for Liquid-Liquid Extraction and Gas-Absorption Processes. Chemical Engineering Research and Design 68, 429–433.

MacFarlane, D.R., Tachikawa, N., Forsyth, M., Pringle, J.M., Howlett, P.C., Elliott, G.D., Davis, J.H., Watanabe, M., Simon, P., Angell, C.A., 2014. Energy applications of ionic liquids. Energy & Environmental Science 7, 232–250.

Maginn, E.J., 2007. Design and Evaluation of Ionic Liquids as Novel CO2 Absorbents. Notre Dame.

Manan, N.A., Hardacre, C., Jacquemin, J., Rooney, D.W., Youngs, T.G.A., 2009. Evaluation of Gas Solubility Prediction in Ionic Liquids using COSMOthermX. Journal of Chemical & Engineering Data 54, 2005–2022.

Maples, R.E., 2000. Blending. In: Petroleum Refining Process Economics. PennWell Corporation, Oklahoma, pp. 359–382.

Marrero, J., Gani, R., 2001. Group-contribution based estimation of pure component properties. Fluid Phase Equilibria 183-184, 183–208.

Marsh, K.N., Boxall, J.A., Lichtenthaler, R., 2004. Room temperature ionic liquids and their mixtures—a review. Fluid Phase Equilibria 219, 93–98.

Matsuda, H., Yamamoto, H., Kurihara, K., Tochigi, K., 2007. Computer-aided reverse design for ionic liquids by QSPR using descriptors of group contribution type for ionic conductivities and viscosities. Fluid Phase Equilibria 261, 434–443.

McLeese, S.E., Eslick, J.C., Hoffmann, N.J., Scurto, A.M., Camarda, K. V., 2010. Design of ionic liquids via computational molecular design. Computers and Chemical Engineering 34, 1476–1480.

Miller, R.E., Blair, P.D., 1985. Input-Output Analysis: Foundations and Extensions. Cambridge University Press.

Mirkhani, S., Gharagheizi, F., 2012. Predictive quantitative structure–property relationship model for the estimation of ionic liquid viscosity. Industrial & Engineering Chemistry Research 51, 2470–2477.

Miyafuji, H., 2013. Liquefaction of Wood by Ionic Liquid Treatment. In: Kadokawa, J. (Ed.), Ionic Liquids - New Aspects for the Future. InTech, pp. 299–314.

Möllersten, K., Gao, L., Yan, J., Obersteiner, M., 2004. Efficient energy systems with CO2 capture and storage from renewable biomass in pulp and paper mills. Renewable Energy 29, 1583–1598.

Möllersten, K., Yan, J., R. Moreira, J., 2003. Potential market niches for biomass energy with CO2 capture and storage—Opportunities for energy supply with negative CO2 emissions. Biomass and Bioenergy 25, 273–285.

Mood, S.H., Golfeshan, A.H., Tabatabaei, M., Jouzani, G.S., Najafi, G.H., Gholami, M., Ardjmand, M., 2013. Lignocellulosic biomass to bioethanol, a comprehensive review with a focus on pretreatment. Renewable and Sustainable Energy Reviews 27, 77–93.

Naik, S.N., Goud, V. V., Rout, P.K., Dalai, A.K., 2010. Production of first and second generation biofuels: A comprehensive review. Renewable and Sustainable Energy Reviews 14, 578–597.

Ng, L.Y., Andiappan, V., Chemmangattuvalappil, N.G., Ng, D.K.S., 2015a. Novel Methodology for the Synthesis of Optimal Biochemicals in

Integrated Biorefineries via Inverse Design Techniques. Industrial & Engineering Chemistry Research 54, 5722–5735.

Ng, L.Y., Andiappan, V., Chemmangattuvalappil, N.G., Ng, D.K.S., 2015b. A systematic methodology for optimal mixture design in an integrated biorefinery. Computers and Chemical Engineering.

Nonthanasin, T., Henni, A., Saiwan, C., 2014. Densities and low pressure solubilities of carbon dioxide in five promising ionic liquids. RSC Advances 4, 7566–7578.

Olajire, A.A., 2010. CO2 capture and separation technologies for end-of-pipe applications – A review. Energy 35, 2610–2628.

Ooi, R.E.H., Foo, D.C.Y., Tan, R.R., Ng, D.K.S., Smith, R., 2013. Carbon Constrained Energy Planning (CCEP) for Sustainable Power Generation Sector with Automated Targeting Model. Industrial & Engineering Chemistry Research 52, 9889–9896.

Paduszyński, K., Domańska, U., 2012. A new group contribution method for prediction of density of pure ionic liquids over a wide range of temperature and pressure. Industrial & Engineering Chemistry Research 51, 591–604.

Paduszyński, K., Domańska, U., 2014. Viscosity of Ionic Liquids: An Extensive Database and a New Group Contribution Model Based on Feed-forward Artificial Neural Network. Journal of Chemical Information and Modeling 54, 1311–1324.

Palomar, J., Gonzalez-Miquel, M., Polo, A., Rodríguez, F., 2011. Understanding the Physical Absorption of CO2 in Ionic Liquids Using the COSMO-RS Method. Industrial & Engineering Chemistry Research 50, 3452–3463.

Papadopoulos, A.I., Linke, P., 2005. A Unified Framework for Integrated Process and Molecular Design. Chemical Engineering Research and Design 83, 674–678.

Papadopoulos, A.I., Linke, P., 2006. Efficient integration of optimal solvent and process design using molecular clustering. Chemical Engineering Science 61, 6316–6336.

Pires, J.C.M., Martins, F.G., Alvim-Ferraz, M.C.M., Simões, M., 2011. Recent developments on carbon capture and storage: An overview. Chemical Engineering Research and Design 89, 1446–1460.

Plechkova, N. V, Seddon, K.R., 2008. Applications of ionic liquids in the chemical industry. Chemical Society Reviews 37, 123–150.

Poling, B.E., Prausnitz, J.M., O'Connell, J.P., 2001. Viscosity. In: The Properties of Gases and Liquids. McGraw-Hill, New York.

Qiao, Y., Ma, Y., Huo, Y., Ma, P., Xia, S., 2010. A group contribution method to estimate the densities of ionic liquids. The Journal of Chemical Thermodynamics 42, 852–855.

Quadrelli, R., Peterson, S., 2007. The energy–climate challenge: Recent trends in CO2 emissions from fuel combustion. Energy Policy 35, 5938–5952.

Quijano, G., Couvert, A., Amrane, A., 2010. Ionic liquids: applications and future trends in bioreactor technology. Bioresource technology 101, 8923–8930.

Ramdin, M., de Loos, T.W., Vlugt, T.J.H., 2012. State-of-the-art of CO2 capture with ionic liquids. Industrial & Engineering Chemistry Research 51, 8149–8177.

Rochelle, G.T., 2009. Amine scrubbing for CO2 capture. Science 325, 1652–1654.

Rockström, J., Steffen, W., Noone, K., Persson, A., Chapin, F.S., Lambin, E.F., Lenton, T.M., Scheffer, M., Folke, C., Schellnhuber, H.J., Nykvist, B., de Wit, C.A., Hughes, T., van der Leeuw, S., Rodhe, H., Sörlin, S., Snyder, P.K., Costanza, R., Svedin, U., Falkenmark, M., Karlberg, L., Corell, R.W., Fabry, V.J., Hansen, J., Walker, B., Liverman, D., Richardson, K., Crutzen, P., Foley, J.A., 2009. A safe operating space for humanity. Nature 461, 472–475.

Rogers, R.D., Seddon, K.R., 2003. Ionic Liquids - Solvents of the Future? Science 302, 792–793.

Rohr, A.C., McDonald, J.D., Kracko, D., Doyle-Eisele, M., Shaw, S.L., Knipping, E.M., 2013. Potential toxicological effects of amines used for carbon capture and storage and their degradation products. Energy Procedia 37, 759–768.

Roughton, B.C., Christian, B., White, J., Camarda, K. V., Gani, R., 2012. Simultaneous design of ionic liquid entrainers and energy efficient azeotropic separation processes. Computers and Chemical Engineering 42, 248–262.

Sahinidis, N. V., 1996. BARON: A general purpose global optimization software package. Journal of Global Optimization 8, 201–205.

Sahinidis, N. V., Tawarmalani, M., Yu, M., 2003. Design of Alternative Refrigerants via Global Optimization. AIChE Journal 49, 1761–1775.

Sanders, R., 2015. Electricity from biomass with carbon capture could make western U.S. carbon-negative [WWW Document]. Berkeley News.

Sato, T., Masuda, G., Takagi, K., 2004. Electrochemical properties of novel ionic liquids for electric double layer capacitor applications. Electrochimica Acta 49, 3603–3611.

Scovazzo, P., Camper, D., Kieft, J., Poshusta, J., Koval, C., Noble, R., 2004. Regular solution theory and CO2 gas solubility in room-temperature

ionic liquids. Industrial & Engineering Chemistry Research 43, 6855–6860.

Seddon, K.R., 1997. Ionic Liquids for Clean Technology. Journal of Chemical Technology and Biotechnology 68, 351–356.

Seddon, K.R., 2003. Ionic Liquids: A taste of the future 6, 363–365.

Seiler, M., Jork, C., Kavarnou, A., Arlt, W., Hirsch, R., 2004. Separation of azeotropic mixtures using hyperbranched polymers or ionic liquids. AIChE Journal 50, 2439–2454.

Shariati, A., Peters, C.J., 2004. High-pressure phase behavior of systems with ionic liquids. The Journal of Supercritical Fluids 30, 139–144.

Shelley, M.D., El-Halwagi, M.M., 2000. Component-less design of recovery and allocation systems: a functionality-based clustering approach. Computers and Chemical Engineering 24, 2081–2091.

Shiflett, M.B., Yokozeki, A., 2005. Solubilities and Diffusivities of Carbon Dioxide in Ionic Liquids: [bmim][PF6 ] and [bmim][BF4 ]. Industrial & Engineering Chemistry Research 44, 4453–4464.

Shiflett, M.B., Yokozeki, A., 2006. Solubility and diffusivity of hydrofluorocarbons in room-temperature ionic liquids. AIChE Journal 52, 1205–1219.

Sinha, M., Achenie, L.E.K., Gani, R., 2003. Blanket wash solvent blend design using interval analysis. Industrial & Engineering Chemistry Research 42, 516–527.

Sittler, L., Ajikutira, D., 2013. Jump Start: Aspen HYSYS V8.

Skjold-Jørgensen, S., Kolbe, B., Gmehling, J., Rasmussen, P., 1979. Vapor-Liquid Equilibria by UNIFAC Group Contribution. Revision and Extension. Industrial & Engineering Chemistry Process Design and Development 18, 714–722.

Solvason, C.C., Chemmangattuvalappil, N.G., Eljack, F.T., Eden, M.R., 2009. Efficient Visual Mixture Design of Experiments using Property Clustering Techniques. Industrial & Engineering Chemistry Research 48, 2245–2256.

Span, R., Wagner, W., 1996. A New Equation of State for Carbon Dioxide Covering the Fluid Region from the Triple Point Temperature to 1100K at Pressures up to 800MPa. Journal of Physical And Chemical Reference Data 25, 1509–1596.

Spigarelli, B.P., Kawatra, S.K., 2013. Opportunities and challenges in carbon dioxide capture. Journal of CO2 Utilization 1, 69–87.

Tan, R.R., Lam, H.L., Kasivisvanathan, H., Ng, D.K.S., Foo, D.C.Y., Kamal, M., Hallaler, N., Klemeš, J.J., 2012. An algebraic approach to identifying bottlenecks in linear process models of multifunctional energy systems. Theoretical Foundations of Chemical Engineering 46, 642–650.

The Dow Chemical Company, 2003. Ethanolamines.

Tobishima, S., 2002. Electrochemistry using ionic liquid (2) 7. Application of ionic liquids as electrolytes in rechargeable cells. ELECTROCHEMISTRY 70, 198–202.

U.S. Energy Information Administration, 2016. International Energy Outlook 2016. Washington, DC, USA.

Vaidyanathan, R., El-Halwagi, M.M., 1994. Global optimization of nonconvex nonlinear programs via interval analysis. Computers and Chemical Engineering 18, 889–897.

Valderrama, J.O., Muñoz, J.M., Rojas, R.E., 2011. Viscosity of ionic liquids using the concept of mass connectivity and artificial neural networks. Korean Journal of Chemical Engineering 28, 1451–1457.

Valencia-marquez, D., Flores-tlacuahuac, A., Vasquez-medrano, R., 2012. Simultaneous Optimal Design of an Extractive Column and Ionic Liquid for the Separation of Bioethanol-Water Mixtures. Industrial & Engineering Chemistry Research 51, 5866–5880.

Varun, Bhat, I.K., Prakash, R., 2009. LCA of renewable energy for electricity generation systems—A review. Renewable and Sustainable Energy Reviews 13, 1067–1073.

Venkatasubramanian, V., Chan, K., Caruthers, J.M., 1994. Computer-aided molecular design using genetic algorithms. Computers and Chemical Engineering 18, 833–844.

Verevkin, S.P., 2008. Predicting enthalpy of vaporization of ionic liquids: a simple rule for a complex property. Angewandte Chemie (International ed. in English) 47, 5071–5074.

Wang, L.-S., Wang, X.-X., Li, Y., Jiang, K., Shao, X.-Z., Du, C.-J., 2013. Ionic liquids: Solubility parameters and selectivities for organic solutes. AIChE Journal 59, 3034–3041.

Wappel, D., Gronald, G., Kalb, R., Draxler, J., 2010. Ionic liquids for post-combustion CO2 absorption. International Journal of Greenhouse Gas Control 4, 486–494.

Weisser, D., 2007. A guide to life-cycle greenhouse gas (GHG) emissions from electric supply technologies. Energy 32, 1543–1559.

Welton, T., 1999. Room-Temperature Ionic Liquids. Solvents for Synthesis and Catalysis. Chemical Reviews 99, 2071–2084.

Wu, H.S., Sandler, S.I., 1989. Proximity effects on the predictions of the UNIFAC model: I. Ethers. AIChE journal 35, 168–172.

Xue, B., Wang, H., Hu, Y., Li, H., Wang, Z., Meng, Q., Huang, X., Sato, O., Chen, L., Fujishima, A., 2004. An alternative ionic liquid based

electrolyte for dye-sensitized solar cells. Photochemical & photobiological sciences : Official journal of the European Photochemistry Association and the European Society for Photobiology 3, 918–919.

Yamamoto, H., 2006. Structure Properties Relationship of Ionic Liquid. Journal of Computer Aided Chemistry 7, 18–30.

Yang, X., Song, H., 2006. Computer Aided Molecular Design of Solvents for Separation Processes. Chemical Engineering & Technology 29, 33–43.

Ye, C., Liu, W., Chen, Y., Yu, L., 2001. Room-temperature ionic liquids: a novel versatile lubricant. Chemical Communications 2244–2245.

Ye, C., Shreeve, J.M., 2007. Rapid and accurate estimation of densities of room-temperature ionic liquids and salts. The Journal of Physical Chemistry A 111, 1456–1461.

Yu, C.-H., Huang, C.-H., Tan, C.-S., 2012. A Review of CO2 Capture by Absorption and Adsorption. Aerosol and Air Quality Research 12, 745–769.

Yunus, N.A., Gernaey, K. V., Woodley, J.M., Gani, R., 2012. An Integrated Methodology for Design of Tailor-Made Blended Products. In: Bogle, I.D.L., Fairweather, M. (Eds.), Proceedings of the 22nd European Symposium on Computer Aided Process Engineering. Elsevier B.V., London, pp. 752–756.

Zaman, M., Lee, J.H., 2013. Carbon capture from stationary power generation sources: A review of the current status of the technologies. Korean Journal of Chemical Engineering 30, 1497–1526.

Zhang, X., Zhang, X., Dong, H., Zhao, Z., Zhang, S., Huang, Y., 2012. Carbon capture with ionic liquids: overview and progress. Energy & Environmental Science 5, 6668–6681.

Zhang, Y., Chen, C.-C., 2013. Modeling CO2 Absorption and Desorption by Aqueous Monoethanolamine Solution with Aspen Rate-based Model. Energy Procedia 37, 1584–1596.

Zhao, H., 2006. Innovative Applications of Ionic Liquids As “Green” Engineering Liquids. Chemical Engineering Communications 193, 1660–1677.

Zhao, H., Jones, C.L., Baker, G.A., Xia, S., Olubajo, O., Person, V.N., 2009. Regenerating cellulose from ionic liquids for an accelerated enzymatic hydrolysis. Journal of Biotechnology 139, 47–54.

Zhou, D., Spinks, G.M., Wallace, G.G., Tiyapiboonchaiya, C., MacFarlane, D.R., Forsyth, M., Sun, J., 2003. Solid state actuators based on polypyrrole and polymer-in-ionic liquid electrolytes. Electrochimica Acta 48, 2355–2359.

Zhou, F., Liang, Y., Liu, W., 2009. Ionic liquid lubricants: designed chemistry for engineering applications. Chemical Society Reviews 38, 2590–2599.

# APPENDIX

## A.1 Data

**Table A-1**: Coefficients and exponents for Span-Wagner equation of state

| $i$ | $n_i$ | $d_i$ | $t_i$ |
|---|---|---|---|
| 1 | 0.38857 | 1 | 0.00 |
| 2 | 2.93855 | 1 | 0.75 |
| 3 | -5.5867 | 1 | 1.00 |
| 4 | -0.7675 | 1 | 2.00 |
| 5 | 0.31729 | 2 | 0.75 |
| 6 | 0.54803 | 2 | 2.00 |
| 7 | 0.12279 | 3 | 0.75 |

| $i$ | $n_i$ | $d_i$ | $t_i$ | $c_i$ |
|---|---|---|---|---|
| 8 | 2.1659 | 1 | 1.5 | 1 |
| 9 | 1.58417 | 2 | 1.5 | 1 |
| 10 | -0.2313 | 4 | 2.5 | 1 |
| 11 | 0.05812 | 5 | 0.0 | 1 |
| 12 | -0.5537 | 5 | 1.5 | 1 |
| 13 | 0.48947 | 5 | 2.0 | 1 |
| 14 | -0.0243 | 6 | 0.0 | 1 |
| 15 | 0.06249 | 6 | 1.0 | 1 |
| 16 | -0.1218 | 6 | 2.0 | 1 |
| 17 | -0.3706 | 1 | 3.0 | 2 |
| 18 | -0.0168 | 1 | 6.0 | 2 |
| 19 | -0.1196 | 4 | 3.0 | 2 |
| 20 | -0.0456 | 4 | 6.0 | 2 |
| 21 | 0.03561 | 4 | 8.0 | 2 |
| 22 | -0.0074 | 7 | 6.0 | 2 |
| 23 | -0.0017 | 8 | 0.0 | 2 |
| 24 | -0.0218 | 2 | 7.0 | 3 |
| 25 | 0.02433 | 3 | 12.0 | 3 |
| 26 | -0.0374 | 3 | 16.0 | 3 |
| 27 | 0.14339 | 5 | 22.0 | 4 |
| 28 | -0.1349 | 5 | 24.0 | 4 |
| 29 | -0.0232 | 6 | 16.0 | 4 |

**Table A-1** continued

| $i$ | $n_i$ | $d_i$ | $t_i$ | $c_i$ |
|---|---|---|---|---|
| 30 | 0.01236 | 7 | 24.0 | 4 |
| 31 | 0.00211 | 8 | 8.0 | 4 |
| 32 | -0.0003 | 10 | 2.0 | 4 |
| 33 | 0.0056 | 4 | 28.0 | 5 |
| 34 | -0.0003 | 8 | 14.04 | 6 |

| $i$ | $n_i$ | $d_i$ | $t_i$ | $\alpha_i$ | $\beta_i$ | $\gamma_i$ | $\varepsilon_i$ |
|---|---|---|---|---|---|---|---|
| 35 | -213.65 | 2 | 1 | 25 | 325 | 1.16 | 1 |
| 36 | 26641.6 | 2 | 0 | 25 | 300 | 1.19 | 1 |
| 37 | -24027 | 2 | 1 | 25 | 300 | 1.19 | 1 |
| 38 | -283.42 | 3 | 3 | 15 | 275 | 1.25 | 1 |
| 39 | 212.473 | 3 | 3 | 20 | 275 | 1.22 | 1 |

| $i$ | $n_i$ | $a_i$ | $b_i$ | $\beta_i$ | $A_i$ | $B_i$ | $C_i$ | $D_i$ |
|---|---|---|---|---|---|---|---|---|
| 40 | -0.6664 | 3.5 | 0.875 | 0.3 | 0.7 | 0.3 | 10 | 275 |
| 41 | 0.72609 | 3.5 | 0.925 | 0.3 | 0.7 | 0.3 | 10 | 275 |
| 42 | 0.05507 | 3.5 | 0.875 | 0.3 | 0.7 | 1 | 12.5 | 275 |

## A.2 Equations

### A.2.1 UNIFAC Model

UNIFAC model is a well-established method to estimate activity coefficient and it is expressed as a function of composition and temperature, as shown in Equations (A.1) to (A.9). The model consists of a combinatorial contribution, ln $\gamma_i^C$, which is essentially due to the differences in size and shape of the molecules, and a residual contribution, ln $\gamma_i^R$, which is due to energetic interactions (Skjold-Jørgensen et al., 1979).

$$\ln \gamma_i = \ln \gamma_i^C + \ln \gamma_i^R \tag{A.1}$$

The combinatorial contribution can be determined using Equations (A.2) to (A.3).

$$\ln \gamma_i^C = 1 - V_i + \ln V_i - 5q_i\left[1 + \frac{V_i}{F_i} + \ln\left(\frac{V_i}{F_i}\right)\right] \tag{A.2}$$

$$F_i = \frac{q_i}{\sum_j q_j x_j}; \qquad \mathrm{V}_i = \frac{r_i}{\sum_j r_j x_j} \tag{A.3}$$

where $x_j$ is the mole fraction of group $j$.

Pure component parameters $r_i$ is relative to molecular van der Waals volumes; while $q_i$ is relative to molecular surface areas. They are calculated

as the total of the group volume and group area parameters, $R_k$ and $Q_k$, as shown in Equation (A.4).

$$r_i = \sum_k v_k^{(i)} R_k; \qquad q_i = \sum_k v_k^{(i)} Q_k \tag{A.4}$$

Residual contribution of the component can be determined as follows:

$$\ln \gamma_i^R = \sum_k v_k^{(i)} [\ln \Gamma_k - \ln \Gamma_k^{(i)}] \tag{A.5}$$

where $\Gamma_K$ is the residual activity coefficient of group $k$, and $\Gamma_K^{(i)}$ is the residual activity of group $k$ in reference solution containing only molecules of type $i$. These can be determined using Equations (A.6) and (A.7).

$$\ln \Gamma_k = Q_k \left[ 1 - \ln\left( \sum_m \theta_m \psi_{mk} \right) - \sum_m \left( \theta_m \psi_{km} \Big/ \sum_n \theta_n \psi_{nm} \right) \right] \tag{A.6}$$

$$\theta_m = \frac{Q_m X_m}{\sum_n Q_n X_n}; \qquad X_m = \frac{\sum_i v_m^{(i)} x_i}{\sum_i \sum_k v_k^{(i)} x_i} \tag{A.7}$$

where $X_m$ is the fraction of group $m$ in the mixture. The group interaction parameter $\psi_{mk}$ is defined by Equation (A.8).

$$\psi_{nm} = \exp\left[ -\left( a_{nm} / T \right) \right] \tag{A.8}$$

Parameter $a_{nm}$ characterises the interaction between groups *n* and *m*. For each group-group interaction, there are two parameters $a_{nm}$ and $a_{mn}$, which are not the same.

$CH_3$ groups present in the cation of the selected IL should be quantified and added to the UNIFAC model calculation. Therefore, the equation below was included.

$$g_{CH3} = \sum_m G_{CH3,m} \nu_m \alpha_m \tag{A.9}$$

where $g_{CH3}$ is the number of $CH_3$ groups in the selected cation, $G_{CH3,m}$ is the number of $CH_3$ group in the individual cation structure.

### A.2.2 Gas-Phase Fugacity Coefficient

Gas-phase fugacity coefficient for $CO_2$ is determined using equation of state for $CO_2$ proposed by Span & Wagner (1996).

$$\ln \varphi_i = \phi^r + \delta \phi_\delta^r - \ln\left(1 + \delta \phi_\delta^r\right) \tag{A.10}$$

where $\varphi_i$ is the gas-phase fugacity coefficient of component *i*, $\delta = \rho/\rho_c$ is the reduced density, and the other variables are determined using the following equations:

$$\phi^r = \sum_{i=1}^{7} n_i \delta^{d_i} \tau^{t_i} + \sum_{i=8}^{34} n_i \delta^{d_i} \tau^{t_i} e^{-\delta^{c_i}} + \sum_{i=35}^{39} n_i \delta^{d_i} \tau^{t_i} e^{-\alpha_i (\delta-\varepsilon_i)^2 - \beta_i (\tau-\gamma_i)^2} + \sum_{i=40}^{42} n_i \Delta^{b_i} \delta \Psi \tag{A.11}$$

$$\Delta = \theta^2 + B_i \left[ (\delta - 1)^2 \right]^{a_i} \tag{A.12}$$

$$\theta = (1-\tau) + A_i \left[ (\delta - 1)^2 \right]^{1/2\beta_i} \tag{A.13}$$

$$\Psi = e^{-C_i (\delta-1)^2 - D_i (\tau-1)^2} \tag{A.14}$$

In these equations, $\tau = T_c/T$ is the inverse reduced temperature, while other coefficients are given in Table A-1 (Span & Wagner, 1996).

$$\phi_\delta^r = \sum_{i=1}^{7} n_i d_i \delta^{d_i - 1} \tau^{t_i} + \sum_{i=8}^{34} n_i e^{-\delta^{c_i}} \left[ \delta^{d_i - 1} \tau^{t_i} \left( d_i - c_i \delta^{c_i} \right) \right] + \sum_{i=35}^{39} n_i \delta^{d_i} \tau^{t_i} e^{-\alpha_i (\delta-\varepsilon_i)^2 - \beta_i (\tau-\gamma_i)^2} \left[ \frac{d_i}{\delta} - 2\alpha_i (\delta - \varepsilon_i) \right] + \sum_{i=40}^{42} n_i \left[ \Delta^{b_i} \left( \Psi + \delta \frac{\partial \Psi}{\partial \delta} \right) + \frac{\partial \Delta^{b_i}}{\partial \delta} \delta \Psi \right] \tag{A.15}$$

The derivatives of the distance function $\Delta^{b_i}$ and exponential function $\Psi$ are given as follows:

$$\frac{\partial \Delta^{b_i}}{\partial \delta} = b_i \Delta^{b_i - 1} \frac{\partial \Delta}{\partial \delta} \tag{A.16}$$

$$\frac{\partial \Psi}{\partial \delta} = -2C_i(\delta - 1)\Psi \qquad \text{(A.17)}$$

where Critical density, $\rho_c$ and critical temperature, $T_c$ of $CO_2$ are given as 0.4676 g $cm^{-3}$ and 304.1282 K respectively.